

Title Page

**RESERVOIR CHARACTERISATION AND SIMULATION
STUDY OF THE X RESERVOIR IN THE OGBO FIELD OF THE
NIGER DELTA**

M.Sc (Applied Geophysics)

BY

ONWUKA, OGBONNA JULIUS

PG/MSc/13/64800

DEPARTMENT OF GEOLOGY

FACULTY OF PHYSICAL SCIENCES

UNIVERSITY OF NIGERIA NSUKKA

SUPERVISOR:

PROF. K.M. ONUOHA

OCTOBER, 2016

CERTIFICATION

ONWUKA, OGBONNA JULIUS, a postgraduate student in the Department of Geology with registration, PG/M.Sc/13/64800 has satisfactorily completed the requirements for the Course and Research work for the Degree of Master of Science (M.Sc.) in Applied Geophysics.

This work embodied in this thesis is original and has not been submitted in part or full for any other degree or diploma of this or any other university.

Prof. K.M. Onuoha

(Supervisor)

Date

Dr. S.C. Obiora

(Head of Department)

Date

DEDICATION

This work is dedicated

With love:

To my parents, my siblings, my sweet heart and relations

With affection:

To my Mentor and Friends

In all:

To God

ACKNOWLEDGEMENTS

This work could never have been possible without the support and encouragement of my parents, and siblings, friends and Family, Dr. Ogonnaya Igwe, Dr. S.O Onwuka and Dr. A.C Ekwe; the assistance and understanding of my mentor and supervisor Prof. K.M Onuoha; the collaboration of my lecturers in Geology Department; and the guidance and support of Mabon Ltd, Elder Dr. K.U. Kalu and family, Prof C. O. Nebo and family, Prof. C. A. Nwadinigwe and family, Prof. C. Chukwuali, Prof. A. A. Ubachukwu, Prof Mrs .O. Nzewunwa, Prof. Mrs. Nkadi Onyegegbu and family , Mrs Patricia Maseli, Prof Mrs Uju Umeji, Prof Victor Ndirika, Dr. Mrs Ruth Ajiobiewe, Dr. Julius Fatoba, Dr. O. A. Anyiam, Dr. Ifeanyichukwu . S Obi, Dr. D.K. Amogu, Mr. Chukwuma Atuanya and family, Mr. Ugochukwu Nwachukwu, Mr Uchenna Ndianefo, Mr. Nonso Udeh Azor, Dr. Peter Obiakor, Mr. Chukwudike Okeugo and family, Mr. Otuka Umahi and family, Mr. Chidozie Dim, Mrs. Precious Orji, Mrs. Ngozi Okoye, Mr. Chidiebere Oji-Nwosu, Dr. K. C. Ndukaba and family, Dr. Collins .C. Adumah and family, Engr. Edward Kalu and family, Dr. Emeka Onyedike, Engr. Olisaemeka Osadebe, Mr. Imo. O. Imo and family and all those who in one way or the other played a part in the carrying out of this work. My thanks to SPDC for providing the data set which I used for this study.

In all, the greatest possible thanks and glory goes to God in whom we move, live and have our being and for whose reason I am here.

ABSTRACT

This study involves the understanding of the stratigraphic distribution of the area by integrating well logs, biostratigraphic data and seismic data to better define hydrocarbon reservoir distributions within the Middle to Late Miocene sediments in the OGBO Field Coastal swamp Depobelt of Niger Delta Basin. Sequence stratigraphic, geostatistical and structural analytical tool have been incorporated in this study, in order to achieve this. Based on the sequence stratigraphic studies, stratigraphic bounding surface such as Maximum Flooding Surfaces (MFS), Sequence Boundaries (SB) and Transgressive Surface of Erosion (TSEs), were delineated and dated. The surfaces were correlated across various wells and mapped along dip and strikes lines on seismic sections, thus providing a good understanding of the stratigraphic distribution. In addition, genetic system tracts which include Lowstand System Tract (LST), Transgressive System Tract- TST and Highstand System Tract (HST), were recognized with the aid of sediment stacking patterns (progradational, retrogradational and aggradational stacks). This gave insight into reservoir, source, and seal rock distributions across the study area. Geostatistical analysis and petrophysical studies were carried out across reservoir tops of interest to determine variation in parameters such as porosity, permeability, water saturation, net to gross, etc. Structural analysis indicates the occurrence down to basin faults, deep seated rollovers, anticlinal structures, and dip fault closures at deeper intervals. These studies unraveled the existence of by-passed opportunities (B5000AB, C4000, D4100A and D4100AA prospects) which in no small measure led to an upward (about 3, 766, 750 MMBOE and 47, 376,962 MMSCF) review of the hydrocarbon reserves in the field. This study led to the generation of a better and more reliable geological model for use in the reservoir studies of the OGBO field.

TABLE OF CONTENTS

TITLE PAGE	i
CERTIFICATION	ii
DEDICATION	iii
ACKNOWLEDGMENT	iv
ABSTRACT	v
TABLE OF CONTENTS	vi
LIST OF FIGURES	xi
LIST OF TABLES	viii
CHAPTER ONE	
INTRODUCTION	1
1.1 STATEMENT OF PROBLEM	1
1.2 BACKGROUND STATEMENT AND STUDY LOCATION	5
1.3 AIM/OBJECTIVES AND WORK SCOPE	6
1.4 REVIEW OF PREVIOUS WORKS	7
CHAPTER TWO	
NIGER DELTA GEOLOGIC SETTING	12
2.1 TECTONIC AND STRUCTURAL SETTING	12
2.2 DEPOBELT AND ENVIRONMENT OF DEPOSITION	19
2.3 STRATIGRAPHIC SETTING	22

CHAPTER THREE

METHODOLOGY	28
3.1 METHOD	28
3.2 DATA SET	30
3.2.1 DATA QUALITY AND SOFTWARE APPLICATION	31
3.3 WELL CORRELATION	38
3.4 RESERVOIR PETROPHYSICAL ANALYSIS	39
3.4.1 PETROPHYSICAL ANALYSIS	39
3.4.1.1 VOLUME OF SHALE	39
3.4.1.2 NET-TO-GROSS RATIO (NTG)	39
3.4.1.3 TOTAL POROSITY (ϕ)	40
3.4.1.4 EFFECTIVE POROSITY	40
3.4.1.5 WATER AND HYDROCARBON SATURATION	40
3.4.1.6 IRREDUCIBLE WATER SATURATION	40
3.4.1.7 BULK VOLUME OF WATER (BVW)	41
3.4.1.8 PERMEABILITY	41
3.4.1.9 FLUID TYPE	41

3.4.1.10 VOLUMETRIC EQUATION	41
3.4.1.11 OOIP	42
3.4.1.12 STOOIP	42
3.4.1.13 RESERVE (oil)	42
3.4.1.14 OGIP	42
3.4.1.15 STOGIP	42
3.4.1.16 RESERVE (gas)	42
3.5 SEISMIC SECTION	43
CHAPTER FOUR	
RESULTS, DATA ANALYSIS AND INTERPRETATIONS	44
4.1 LITHOFACIES AND DEPOSITIONAL ENVIRONMENTS	44
4.1.1 COARSE GRAINED BASAL SANDSTONE FACIES (FACIES 1)	44
4.1.2 MUDROCK FACIES (FACIES 2)	46
4.1.3 HETEROLITHICS FACIES (FACIES 3)	47
4.1.4 SANDSTONE/SHALY FACIES (FACIES 4)	50
4.2 ENVIRONMENT OF DEPOSITION (EOD) DELINEATION AND INTERPRETATION	53
4.2.1 ENVIRONMENT OF DEPOSITION DELINEATION BY INTEGRATION APPROACH	53

4.3 SEQUENCE STRATIGRAPHIC ANALYSIS	68
4.3.1 MAXIMUM FLOODING SURFACES (MFS)	68
4.3.2 SEQUENCE BOUNDARY (SB) AND TRANSGRESSIVE SURFACE OF EROSION (TSE)	72
4.3.3 DEPOSITIONAL SEQUENCES AND SYSTEMS TRACTS	73
4.3.3.1 STRATIGRAPHIC SEQUENCES AND SYSTEMS TRACTS	74
4.3.4 WELL CORRELATION	75
4.4 SEISMIC DATA INTERPRETATION	76
4.4.1 SYNTHETIC SEISMOGRAM AND WELL-TO -SEISMIC TIE	79
4.4.2.1 HORIZON AND FAULT INTERPRETATIONS	88
4.4.2.3 STRUCTURAL INTERPRETATION	93
4.4.2.3.1 GENERATION OF MAPS	94
4.4.2.3.2 STRUCTURAL DISCUSSION	96
4.5 OGBO FIELD PETROLEUM SYSTEM POTENTIAL AND EVALUATION	104
4.6 FORMATION EVALUATION	110
4.6.1 PETROPHYSICAL ANALYSIS SUMMARY	110
4.7 PROSPECT EVALUATION	113
4.8 VOLUMETRICS, PROSPECT RANKING, RISK AND UNCERTAINTY ASSESSMENT	120

4.8.1 VOLUMETRICS	120
4.8.2 PROSPECT RANKING	124
4.8.3 RISK ASSESSMENT	124
4.8.4 UNCERTAINTY	130
CHAPTER FIVE	
SUMMARY AND CONCLUSION	131
5.1 SUMMARY AND CONCLUSION	131
5.2 RECOMMENDATION	134
REFERENCE	

LIST OF FIGURES

1.	1.1: Niger Delta: Location Map of Study area showing Topographic and Fields (SPDC, 2011)	4
2.	1. 2: Base Map of the Studied Field showing the location of the studied wells	4
3.	1.3: Base Map of the Studied Field showing the location of the studied wells in strike and dip direction	5
4.	2.1: Tectonic Map showing the Niger Delta (Modified after Kogbe, 1989)	13
5.	2.2: Regional structural provinces map of the Niger Delta showing the Fracture Zones (Wiener et al., 2010)	16
6.	2.3: Margin evolution included phases of break-up and continental separation from Late Aptian rifting through to passive margin development. Tectonic episodes resulting in uplift are recognized in the Santonian and Mid and Late Tertiary (Steve et al., 2002)	17
7.	2.3b: Paleogeography showing the opening of the South Atlantic, and development of the region around Niger Delta. A. Cretaceous paleogeography (130.0 to 69.4 Ma). B. Cenozoic paleogeography (50.3Ma to present). Plots generated with PGIS software (Tuttle et al., 1999)	18
8.	2.4: Structural Features of the Tertiary Niger Delta showing Growth Faults and Rollover Anticlines. After Doust and Omatsola, (1990) and Stacher (1995)	18
9.	2.5: Depobelts with their relative ages (after Doust and Omotsola, 1990)	20
10.	2.5b: Depobelt map with the structural play segments, onshore and offshore Niger Delta Basin showing the study area (SPDC,2011)	21
11.	2.6 Schematic Dip Section of the Niger Delta (Modified after P. Kamerling, from Weber and Daukoru, 1975)	22
12.	2.7: Diagrammatic representation of the stratigraphic evolution of the Niger Delta (After Reijers, 2011)	24
13.	2.7b: Regional Tectonostratigraphy. Regional stratigraphy is broken down into megasequences representing phases of basin development. Tectonic episodes are marked by regionally significant unconformities in the Santonian and Mid and Late Tertiary (Steve et al., 2002)	25

14.	2.8: Stratigraphic column showing the three formations of the Niger Delta (modified from Lawrence et al, 2002)	26
15.	2.9: Schematic diagram of the regional stratigraphy of the Niger Delta and seismic display of the main stratigraphic units in the outer fold and thrust belt and main reflectors (Corredor et al, 2005)	27
16.	3.1: Work Flow Chart of the study	29
17.	3.2: The well log section for OGBO field	29
18.	3.2b: The well log section for OGBO field	30
19.	3.3: Paleobathymetry and Depositional Environment Chart (Modified After Allen, 1965)	32
20.	3.3b: Foraminifera biofacies model for the Niger Delta adapted from SPDC in-house Report	33
21.	3.4: Stratigraphic data sheet (west and east halves combined) of the Niger Delta (Reijers, 2011)	34-35
22.	3.5: Niger Delta Chronostratigraphic Chart (SPDC, 2010)	36
23.	3.5b: Parasequence stacking pattern model (After Van Wagoner et al., 1990)	37
24.	3.5c: Sequence stratigraphic model showing key stratigraphic surfaces and various systems tracts (Kendall, 2008, After Van Wagoner et al., 1988)	37
25.	3.5d: Ideal clastic sequence stacking pattern (Kendall, 2004)	38
26.	4: Coarse grained basal sandstone facies represented by blocky gamma ray log in well OGBO 019STI	45
27.	5: Course grained basal sandstone facies represented by blocky gamma ray logs enlarged	45
28.	6: Mudrock facies represented by high gamma ray log signature enlarged (high frequency and forams diversity)	46
29.	7: Mudrock facies represented by high gamma ray log signature in well OGBO 019STI (high frequency and forams diversity)	42
30.	8: Heterolithic facies encountered in OGBO 056 well	48
31.	9: Heterolithic facies encountered in well in OGBO 038 well	48
32.	10: Heterolithic facies encountered in OGBO 005 well	49
33.	11: Heterolithic facies encountered in OGBO 005 well with biofacies data	49

34.	12: Crescent or bow trend expressed in OGBO 056, 036 and 038 wells	50
35.	13: Sandstone/ shaly facies defined by funnel-shaped gamma ray logs	51
36.	14: Sandstone/shaly facies defined by funnel-shaped gamma ray logs	52
37.	15: Integrated workflow for environment of deposition delineation	53
38.	16: Conceptual sedimentary depositional model, Bevis (2014)	54
39.	17: Net to Gross plot at 4000ft interval from six well location and inferred Environment of Deposition Trend	58
40.	18: Net to Gross plot at 5000ft interval from six well location and inferred Environment of Deposition Trend	58
41.	19: Net to Gross plot at 6000ft interval from six well location and inferred Environment of Deposition Trend	59
42.	20: Well location representation of the well log motif interpretation and NTG map Environment of Deposition Trend and the inferred field environment	60
43.	21: RMS Amplitude map for horizon B5000 surface interval with well log motif and amplitude analysis	61
44.	22: RMS Amplitude map for horizon B5000 surface interval	62
45.	23: RMS amplitude map for horizon B5000 surface interval- (for amplitude extraction at 4500ft depth gamma ray log motif)	62
46.	24: RMS Amplitude map for horizon C4000 surface interval	63
47.	25: RMS amplitude map for horizon C4000 surface interval- (for amplitude extraction at 5500ft depth gamma ray log motif)	63
48.	26: RMS Amplitude map for horizon D4100 surface interval	64
49.	27: RMS amplitude map for horizon D4100 surface interval- (for amplitude extraction at 5500ft depth gamma ray log motif)	64
50.	28: Map pattern of B5000 surface interval amplitude extraction in yellow and black colour background	65
51.	29: Environment of deposition delineation by integrated model approach	67
52.	30: Well Log Sequence Stratigraphic Interpretation and Correlation across Strike within the Field and wells	71
53.	31: Well Log Sequence Stratigraphic Interpretation and Correlation across Dip within the Field and wells	71

54.	32: Well log sequence stratigraphic interpretation and correlation across Dip with surfaces interval within the field and wells	73
55.	33: Cross section of the studied wells showing sequences and correlated surfaces	76
56.	34: Seismic interpretation well OGBO 046 (vertical) inline 11677 showing the SB ϕ , MFS ϕ and the faults	77
57.	35: OGBO field seismic section showing fault sticks	78
58.	36: 3D seismic map showing the faults with hydrocarbon trap configuration and some wells in the OGBO Field	78
59.	37: Seismic section showing the horizons, faults and well position between faults	79
60.	38: Synthetic seismogram showing high correlation between seismic and stratigraphy	81
61.	39: Synthetic seismogram showing well OGBO 019STI and OGBO 038 correlation between seismic and stratigraphy	81
62.	40: Wavelet Extraction window showing variables and settings	84
63.	41: Wavelet Extraction workflow	85
64.	42: The Petrel wavelet extraction summary	85
65.	43: The spectrum for a Ricker wavelet	86
66.	44: (a) Zero phase wavelet time response at an interval of -0.025 to +0.025ms, (b) (Wavelet frequency window) Wavelet frequency and amplitude band response at 5Hz to 75Hz. (c) Wavelet amplitude spectrum	86
67.	45: Well to Seismic tie showing the good character match	87
68.	46: Structural/Trapping styles - Upper extensional zone of listric faults and simple-rollover anticlines	89
69.	47: Gridded fault and event on cube Volume view showing Structural and stratigraphic Framework of study area on Plan and Dip section	89
70.	48: 3D seismic map showing the faults with hydrocarbon trap configuration and some wells in the studied field	90
71.	49: Gridded fault and event on cube Volume view showing Structural and stratigraphic framework of study area on Plan from Dip section to strike section	90
72.	50: Seismic section of OGBO field	91
73.	51: Depth structure map for horizon B5000 surface with well log motif	95

74.	52: Depth structure map for horizon B5000 surface	95
75.	53: Depth structure map for horizon C4000 surface	95
76.	54: Depth structure map for horizon D4100 surface	95
77.	55: Time Structural map for horizon B5000 surface	95
78.	56: Time Structural map for horizon C4000 surface	95
79.	57: Time Structural map for horizon D4100 surface	95
80.	58: B5000 AB Prospect	97
81.	59: D4100 AA Prospect	97
82.	60: D4100 Prospect A (in white indication) Nameless	98
83.	61: D4100 Prospect A (in white indication) Named A	99
84.	62: RMS amplitude map for B5000 prospect (stratigraphic trap prospect indication) 100	
85.	63: RMS amplitude map for C4000 prospect (stratigraphic trap prospect indication) 100	
86.	64: RMS amplitude map for D4100 prospects (stratigraphic trap prospect indication) 102	
87.	65: C4000 Prospect	102
88.	66: C4000 Prospect (blue blanket highlights the saddle structure)	103
89.	67: Seismic section and the sand surfaces studied	103
90.	68: Low Gamma Ray and high resistivity values of potential reservoirs for wells in Strike direction	104
91.	69: Low Gamma Ray and high resistivity values of potential reservoirs for wells in Dip direction	105
92.	70: Low Gamma Ray and high resistivity values of potential reservoirs for wells in both Strike and Dip direction	105
93.	71: Low Gamma Ray and high resistivity values of potential reservoirs for wells in both strike and Dip direction from OGBO 019STI, 038,046,005,036 and 056	106
94.	72: Depositional sequence analysis across the six OGBO wells in both strike and dip direction	106
95.	73: Delineated reservoir from OGBO 005 well	107
96.	74: Delineated reservoir from OGBO 036 well	107

97.	75: Depth Structural map for horizon B5000 surface with B5000AB prospect	115
98.	76: D4100 horizon surface interval depth map with prospect AA	116
99.	77: D4100 surface Maximum Amplitude map	117
100.	78: C4000 Surface Maximum Amplitude map	118
101.	79: Maastricht Template (Shell, 2004)	128

LIST OF TABLES

Table 1: Stratigraphic units of Niger Delta area, Nigeria. (Modified from Short and Stauble (1967))	26
Table 2: Represents the summary of the depositional environments from well log motifs of various electrofacies analysis from Cant (1992) as shown in Gonzales (2003) and Kendall (2008)	55- 57
Table 3: Different log motifs for the six correlated wells in OGBO Field	57
Table 4: Table showing the delineated MFS, marker fauna and biozone studied summary for six wells studied	69
Table 4: Table showing the delineated MFS, marker fauna and biozone studied summary for six wells studied continued	70
Table 5: Table showing summary of the delineated system tracts and inferred depth studied for six wells	73
Table 6: Table showing the delineated Sequence Boundary with depth penetrated	75
Table 7: Formation Evaluation (Petrophysical analysis summary)	111
Table 8: Reservoir Delineation and petrophysical parameters summary	112
Table 9: Prospects Volumetric analytical studies	123
Table 10: Summary of Prospects Volumetric analytical studies	125
Table 11a: Risk analysis for Prospect B5000 AB	129
Table 11b: Risk analysis for Prospect C4000	129

Table 11c: Risk analysis for Prospect D4100 A	129
Table 11d: Risk analysis for Prospect D4100 AA	129

CHAPTER ONE

INTRODUCTION

1.1 STATEMENT OF PROBLEM

Indices from recent researches indicate that our planet's growing population and the industrialization of emerging economies will lead to an exponential increase in energy demand by year 2025. Finding and developing all the fuel we need, in a sustainable environment, could be one of the greatest challenges our generation will face. With a population of about 167million, Nigeria is the largest country in Africa and seventh largest in the world. According to the UN projections, Nigeria could have the world's fourth largest population by 2030. This burgeoning population is the country's most important and also the most powerful incentive to make the most of its huge energy potential. Today oil and gas are produced from land, swamp, shallow water fields in the Niger Delta and deep water reserves in the Gulf of Guinea. Despite challenges of crude oil theft, sabotage, illegal refining that affect oil and gas companies, hydrocarbon reservoirs distributions problems have become increasingly exploration challenges with long term impacts. The complex exploration challenges associated with Nigeria's Niger Delta Basin exploration and zeal by the Federal Government of Nigeria to increase its hydrocarbon reserves has necessitated this study. Nigeria has a reserve target of 40 billion barrels of oil and 4 million barrels of production per day, and it is projected that by year 2014 Nigeria's offshore (deepwater) production will account for 2.5 million barrels of oil per day beside gas production (www.dpr.gov.ng). These national target poses two major challenges to Geoscientists; -huntingø for old by-passed pay zones and high risk, deepwater (offshore) exploration, hydrocarbon reserves is underpinned by the availability of technology and skilled personnel. The Niger Delta basin has assumed the status of a mature petroleum province in terms of exploration and production. Exploration and production activities have been active in the basin for over five decades now and this has resulted in reduced volume of crude oil from several fields. With the renewed call for increased reserves, there is need to boost reserves of old producing oil fields in the basin using newer approaches equipped with the relevant skills to contribute to developing Nigeria's hydrocarbon reserves, especially in unraveling the complex geology of the area. Newer exploration techniques have been adopted to improve and understand the stratigraphic distribution by integrating well logs, biostratigraphic data and seismic data to better define hydrocarbon reservoir distributions within the Middle to Late Miocene sediments in "OGBO"

field Coastal swamp Depobelt of Niger Delta Basin. These techniques involve the use of sequence stratigraphic, geostatistical and structural analytical tools in order to achieve this. Based on sequence stratigraphic studies, stratigraphic bounding surface such as Maximum Flooding Surfaces - MFSs, Sequence Boundaries -SBs and Transgressive Surface of Erosion ó TSEs, would be delineated and dated. The surfaces correlation investigation across various wells and mapped along dip and strikes lines on seismic sections, thus providing a good understanding of the stratigraphic distribution. In addition, genetic system tracts which include Lowstand System Tract ó LST, Transgressive System Tract ó TST and Highstand System Tract ó HST, have been found with the aid of sediment stacking patterns (progradational, retrogradational and aggradational stacks). This gave insight into reservoir, source, and seal rock distributions across the study area. Geostatistical analysis and petrophysical studies were carried out across reservoir tops of interest to determine variation in parameters such as porosity, permeability, water saturation, net to gross, etc. These studies, would have unraveled the existence of by-passed prospects which in no small measure led to an upward review of hydrocarbon reserves in the field. This study has led to the generation of a better and more reliable geological model for use in the reservoir modeling studies of "OGBO" field. Improved exploitation of Nigeria's resources, with the latest technologies available, will strengthen the Gross Domestic Product (GDP) of Nigeria. Presently, Nigeria holds the ninth largest proven natural gas reserves in the world. The Federal Government has made it a priority to unlock this resource potential to increase domestic and industrial power supply, raise living standards and support sustainable economic growth.

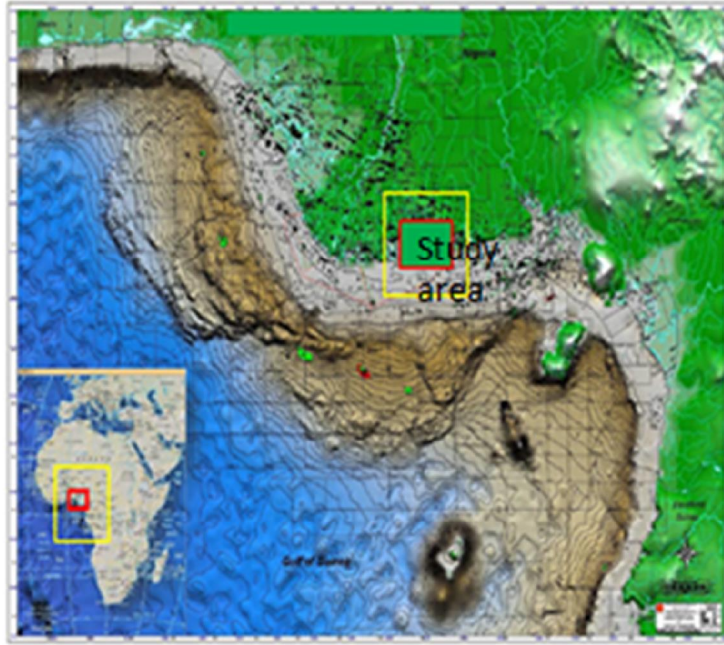


Figure 1.1: Niger Delta: Location Map of Study area showing Topographic and Fields (SPDC, 2011)

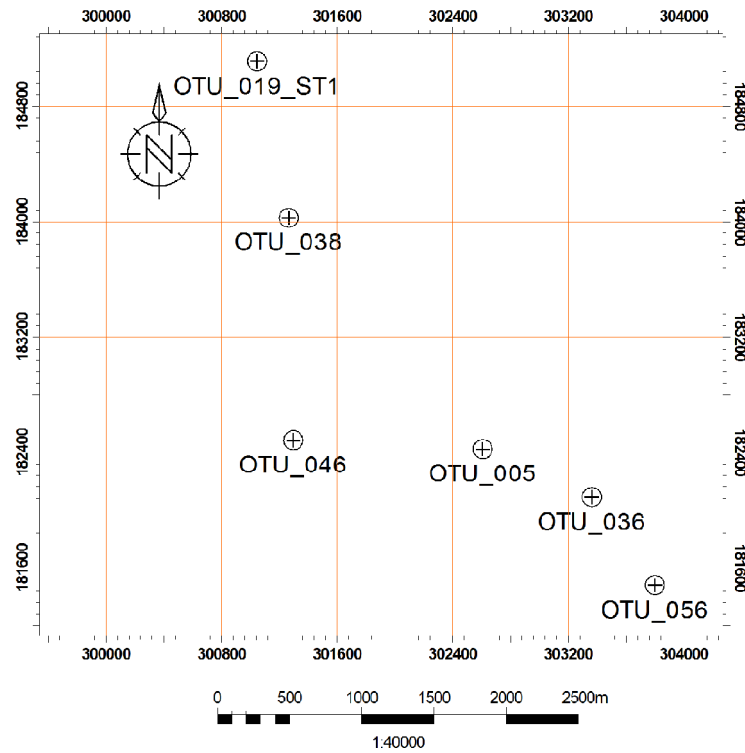


Figure 1.2: Base Map of the Studied Field showing the location of the studied wells

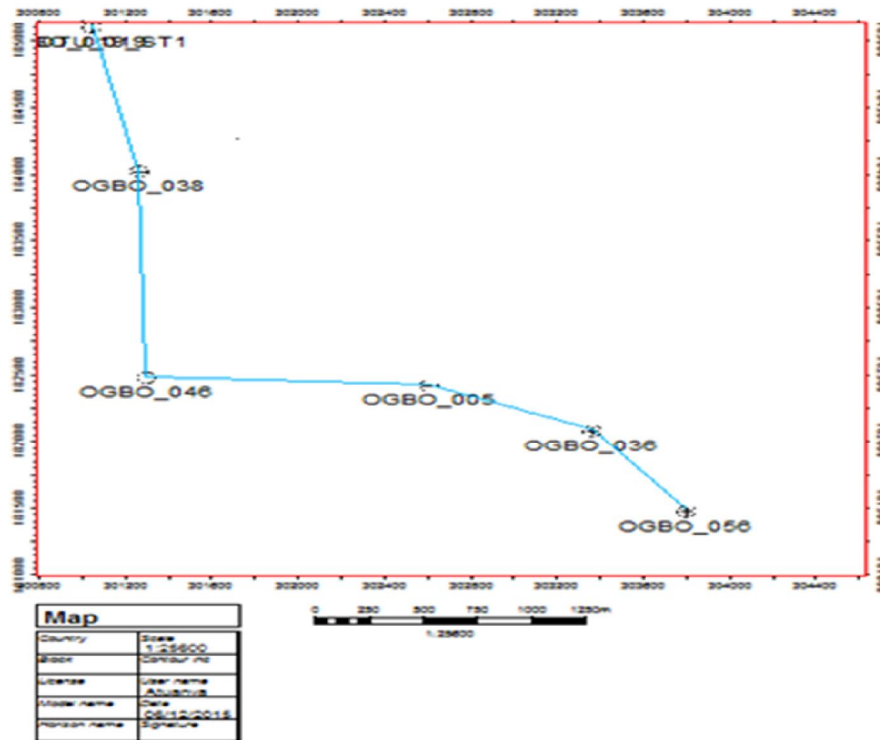


Figure 1.3: Base Map of the Studied Field showing the location of the studied wells in strike and dip direction

1.2 BACKGROUND STATEMENT AND STUDY LOCATION

Nigeria's entire petroleum production as of today is from the Tertiary Niger Delta (Figure. 1.1, 1.2, and 1.3) which has gradually developed into a matured drilling province, it is a very prolific and economically important sedimentary basin in terms of hydrocarbon exploration and production. This hydrocarbon province situated in the Gulf of Guinea, between longitudes 5° E to 8° E and latitude 3° N to 5° N is ranked as one of the largest regressive deltas in the world with an area of some $300,000\text{km}^2$ Kulke (1995). It is bounded by the Cretaceous Anambra Basin to the northeast of the delta and Benue Trough in the North and lies South of the West African shield, and West of the Oban Massif and the Tertiary Cameroon Volcanic Trend (Haack et al. 1997). It consists of three important depobelts which include the onshore, shallow offshore and deep/ultra offshore. The study area is a matured field situated in the Coastal swamp region of the Niger Delta in Nigeria belonging to Shell Development Company of Nigeria. The OGBO field structure is a large collapsed crest rollover anticline trending east-west and it is bounded to the north by the major bounding fault. The field is operated by shell petroleum Development Company and was first discovered in 1975. However, with exploration and production activities currently at

downward trend mainly due to international politics and economics dynamics and its effect in oil and gas price demand and supply, emergence of new oil producing nations also socio-political activities locally are not friendly to the stakeholders in making key long term business decisions. One challenge currently facing exploration and international oil companies is, a very strong possibility of recovering a lot of bypassed hydrocarbons from subtle traps in some old producing field by the application of newer technologies, since the technologies originally employed for exploration of most producing fields in the basin were such that could not reliably discriminate between lithologies, thereby resulting in bypassed hydrocarbon zones. These bypassed zones can improve hydrocarbon recovery in the basin, through the use of modern technique. Also, the stratigraphic distribution can be better understood through the integration of well logs, biostratigraphic data and seismic data in the study.

1.3 AIM/OBJECTIVE AND WORK SCOPE

The aim and objective of this research study is to build a sequence stratigraphic interpretation using well logs and seismic data sets covering an area in the coastal swamp field using petrel 2010 software to delineate and identify between lithologies, system tracts, stacking pattern with F, P zones and surfaces correlation across various wells. Map along dip and strikes on seismic sections and predict fluid types in subtle traps and to aid further exploration activities within the producing field. Create high resolution geological model and build structural analysis for reservoir simulation. Determination of petrophysical parameters at inter-well locations across the reservoir tops of interest. Deduce Formation evaluation, risk and economic analysis for the reservoir model. Predict prospects identification and ranking, also increase hydrocarbon reserve in the field.

The scope of this project includes the following:

- Integration of the available data sets namely, 3D seismic data along with well log data from the wells data, so as to get a detailed vertical resolution of the sedimentary section, determine the continuity of the stratigraphic frame work and age of sediments
- Identification and interpretation of various facies using lithology sensitive logs such as gamma ray.
- Recognition of well logs responses that characterize sequence boundaries and the maximum flooding surfaces as well as the different system tracts.

- Identification of seismic facies pattern, faults and mappable horizons identified in the well log.
- Petroleum system analysis, Formation and prospect evaluation, volumetric and risk assessment.

1.4 REVIEW OF PREVIOUS WORKS

The last 40 million years have been important in shaping the geology of the Niger Delta. The petroleum potential of the area has been studied with a variety of geophysical approaches. However, few researchers have used Poisson and other elastic impedances to discriminate and predict lithofacies and fluids in mature fields of the basin. Stoneley (1966) and Burke et al (1970 and 1972) analyzed and discussed the mega tectonic setting of the Niger Delta. Short and Stauble (1967) and Weber and Daukoru (1975) described roughly the three major depositional cycles in the coastal sedimentary basins of Nigeria. Firstly, they started with an Albian marine incursion and terminated during the Santonian time; the proto-Niger Delta set in motion during the second cycle, the growth of Niger Delta exist over a prolonged period of time from Eocene to Recent time. In agreement to Short and Stauble (1967) and Doust and Omatsola (1990), the Niger delta comprises of a regressive sequence of deltaic and marine clastics, decided upon by three major lithofacies at the base of marine shale, made up of Akata formation, be next by paralic sequence of Agbada Formation and topmost non-marine alluvial (continental) sands of Benin formation. Weber (1971) accounted the cyclic nature of sedimentation of the Tertiary paralic deposits. He showed a complete cycle consists of thin, fossiliferous transgressive marine sands followed by an offlap sequence which commences with marine sediments and another transgressive may terminate the cycle. Burke et al (1972) brought into a reciprocal relation these late Quaternary canyons to the drowing of river mouths, which were incised on the continental shelf during the Wisconsin fall in sea level, which probably resulted in the formation of the Afam Canyon and the Qua Iboe clay fill, during the Miocene, in the south-east Niger Delta. The syn-sedimentary tectonics of the Tertiary delta was outlined by Merki (1972) and Evamy et al (1978). Oomken (1974) observed the sediments in the terrestrial and submarine parts of the modern delta and arranged them into five major lithofacies (sandstone, heteroliths and mudstone), using lithological characteristics and other sedimentary features. At several stages during the late Quaternary, sedimentation was terminated by uplift and erosion, where by several cycles of channels were cut and filled which happened afterwards as a consequence to submarine

canyons, Evamy et al, (1978). Sequence stratigraphy, thus make easier the subdivision of the Niger Delta into packages of sediments that are essentially bounded together by chronostratigraphically significant surfaces. Various sequence stratigraphy study have been carried out, in different parts of Niger Delta. These include Poston et al., (1983) showed the geology and reservoir characteristics at Meren field. They noted evidence for syn - depositional displacement on growth faults across the field. They expressed clearly combining well -log interpretations and laboratory analyses of sidewall cores in the determination of the spatial variation of porosity and permeability within particular reservoir intervals. Doust and Omatsola (1990) showed approval of six depobelts in the Niger Delta, which are distinguished primarily by their age. They are : Northern delta (Late Eocene-early Miocene), Great Ughelli (Oligocene-Early Miocene), Central swamp I (Early-Middle Miocene), Central swamp II (Middle Miocene), Coastal swamp I and II (Middle Miocene) and Offshore mega structures (Late Miocene). Stacher (1994) released a delta wide framework of Cretaceous chronostratigraphic surfaces, and a sequence stratigraphic chart for the Niger Delta, using digitally stored biostratigraphic data obtained from wells. Ozumba (1999) worked out a sequence stratigraphic framework of the western Niger Delta, using foraminifera and wire line log data obtained from four wells drilled in the coastal and central swamp depobelts. He finalised that the late Miocene sequences were thicker than the middle Miocene sequences. Balogun (2003) accounted that the Middle Miocene strata of Western Coastal Swamp Depobelt of Niger Delta were deposited by interaction of subsidence, eustatic changes in sea level and varying sediment supply. Also, He noted that the development of excellent reservoir sands and the shales of the upper transgressive system tract form seals that are good at least on the outer shelf and characterize the highstand systems tract. The alternation of highstand systems tracts and transgressive system tracts sands and shales respectively provides a union of reservoir and seal rocks that is essential for hydrocarbon accumulation and stratigraphic trapping. The sand within the prograding wedge has good reservoir properties which on being sealed by the transgressive shales creates potential stratigraphic traps. Posamentier and Kolla (2003) considered in detail 3D seismic data in predominantly basin floor settings offshore Niger Delta. These make visible the extensive presence of gravity - flow depositional elements. Five key elements were observed and are; turbidity - flow levees channel, frontal splays and distributaries channel complexes, channel - over bank sediment waves and levees, crevasse - splay complexes, debris flow channels, lobes and sheets. The reservoir architecture of each of these depositional elements

is a function of the interaction between seafloor morphology, sediment grain - size distribution and processes. Owoyemi (2004) worked out a sequence stratigraphic model for Agbada Formation in Niger Delta Basin based on the work he did in Delta Field, and concluded that in the first place, five sequence boundaries that divide the Agbada Formation, each formed during an episode of structural collapse of the basin-prograding clastic wedge along basinward dipping listric normal faults. Additionally, that sequence boundaries were cut by submarine mass flows across basin gradient steepened over a succession of down-dropped fault blocks. Depositional patterns within sequences manifest diversion of sediment transport pathways along irregular basin floor topography produced by faulting. In most locations deposits within sequences abruptly fine above a basal layer of submarine channel deposits, and then gradually coarsen as deposits filled topography above down-dropped fault blocks. Furthermore, although sequence boundaries do not appear to have formed by lowstand fluvial incision, there does appear to be some relationship between periods of eustatic sea levels and sequence development. Sea level fall may be associated with increased rates of sediment progradation, sediment loading onto shales of the underlying Akata Formation and accelerated structural collapse of the clastic wedge into the basin. Adeogba et al (2005) have interpreted a near surface, 3D seismic data set from the Niger Delta continental slope, offshore Nigeria and make visible important stratigraphy and architectural features. Sequence stratigraphic concepts are finding new and without equal applications in the regressive siliciclastic deposits of Niger Delta. The lithostratigraphic interpretation of the Niger Delta sediments, cut across time lines and their lateral associations make an indirect suggestion that the sedimentary deposits were strongly influenced by eustacy and tectonics. Porebski and Steel (2006) accounted that Niger Delta depositional systems are more supply driven than accommodation driven. Anyiam and Mode (2008) viewed that the primary seal rocks in the Niger Delta are the inter-bedded shale within the Agbada Formation, the juxtaposition of reservoir sands against shale beds due to faulting creates good seal integrity. The shale provides seals in the form of clay smears along these synsedimentary faults and vertical fault seals in a compressive stress setting. Onyekuru et al (2012) came up with the analysis of the vertical succession of depositional facies revealing four third order depositional sequences of mid-Miocene in age as He carried out sequence stratigraphic analysis of depositional systems in a field in the Central Swamp Depobelt, Niger Delta Basin.

CHAPTER TWO

NIGER DELTA GEOLOGIC SETTING

2.1 TECTONIC AND STRUCTURAL SETTING

The Niger Delta is in the Gulf of Guinea and extends through the Niger Delta province as defined by Klett et al (1997). It covers a 70,000 square kilometer area within the Gulf of Guinea, West Africa. Although the modern Niger Delta formed in the Early Tertiary, sediments began to accumulate in this region during the Mesozoic rifting associated with the separation of the Africa and South American continents, Weber and Daukoru (1975); Evamy et al (1978); Doust and Omatsola (1990). According to Selley (1985), the Niger Delta is a terrigenous epicratonic embayment which lies on the edge of the continental crust. It is by chance the most important sedimentary basin in Sub-Saharan Africa with respect to oil production. In (Figure 2.1), Niger Delta is shown to be located within the peri-oceanic section of the Abakaliki-Benue suture zone of the Southern Nigerian Basin. On the West, it is separated from the Dahomey Basin by the Okitipupa Basement High, and on the east it is bounded by the Cameroon volcanic line. Its northern margin transects several older (Cretaceous) tectonic elements such as the Anambra basin, Afikpo Syncline, Abakaliki Anticlinorium, and the Calabar Flank. Synrift marine clastics and carbonates accumulated during a series of transgressive and regressive phases between the Cretaceous to Early Tertiary; the oldest dated sediments are Albian age, Doust and Omatsola (1989). These synrift phases put an end with basin inversion in the Late Cretaceous (Santonian). Proto-Niger Delta regression continued as continental margin subsidence resumed at the end of the Cretaceous (Maastrichtian). Niger Delta progradation into the Gulf of Guinea accelerated from the Miocene onward in response to evolving drainages of the River Niger, River Benue and Cross River and continued continental margin subsidence.

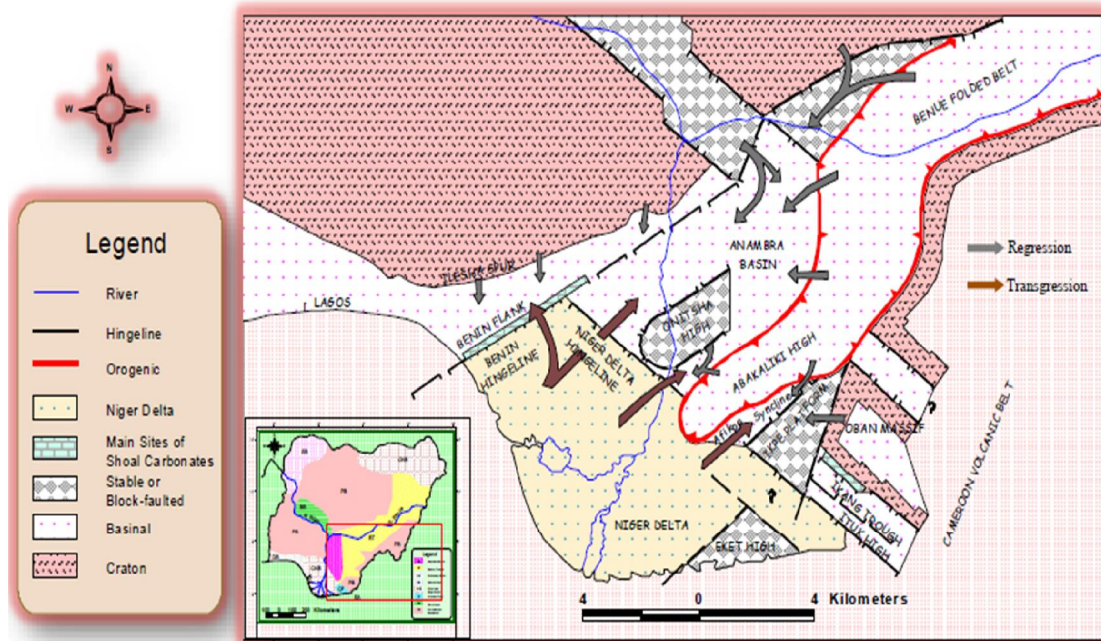


Figure 2.1: Tectonic Map showing the Niger Delta (Modified after Kogbe, 1989)

It is believed that the modern Niger Delta was formed in the early Tertiary, and that sediments began to accumulate in this region during the Mesozoic rifting associated with the separation of the African and South American continents, Weber et al (1975). From the Eocene to the present, the delta has prograded southwestward, forming depobelts that represent the most active portion of the delta at each stage of its development, Doust et al (1990). These depobelts form one of the largest regressive deltas in the world with an area of some 300,000 km², Kulke, (1995), with sediment volume of about 500,000 km³, Hospers (1965), and sediment thickness of over 10 km in the basin depocenter, Kaplan et al (1994). The province contains only one identified petroleum system known as the Akata-Agbada petroleum system Kulke (1995); Ekweozor et al (1994). Tertiary Niger Delta deposits are characterized by a series of depobelts that strike northwest- southeast, sub- parallel to the present day shoreline. Depobelts become successively younger basinward, ranging in age from Eocene in the north to Pliocene offshore of the present shoreline. Depobelts, tens of kilometers wide, are bounded by a growth fault to the north and a counter regional fault seaward. Each sub-basin contains a distinct shallowing upward depositional cycle with its own tripartite assemblage of marine, paralic, and continental deposits. Depobelts define a series of punctuations in the progradation of this deltaic system. As deltaic sediment loads

increase, underlying delta front and prodelta marine shale begin to move upward and basinward. Mobilization of basal shale caused structural collapse along normal faults, and created accommodation for additional deltaic sediment accumulation. As shale withdrawal nears completion, subsidence slows dramatically, leaving little room for further sedimentation. As declining accommodation forces a basinward progradation of sediment, a new depocenter develops basinward. Most Niger Delta faulting is due to extensional deformation. The exception is in the distal section, where overthrust faults form in the toe of the proto-Niger Delta. These extensional faults are normal and generally listric, comprising syn-depositional growth faults and crustal tensional relief faults. These faults are synthetic or antithetic, running sub-parallel to the strike of the sub-basins. These syn-sedimentary faults exhibit growth strata above the down thrown block, as well as anticlinal (rollover) closures. Most hydrocarbon bearing structures in Niger Delta deposits are close to these structure-building faults, in complexly collapsed crest and faulted anticlinal structures. The growth faults and antithetic faults play an essential role in trap configuration. The growth faults show an attribute of significant throw (up to several hundred meters), are arcuate in plain view, concave basinward and may be several tens of kilometers in length. Antithetic faults have less throw (generally less than a hundred meters). It can be linear or arcuate in plain view and they rarely exceed ten kilometers in length, Cathles et al, (2003).

Furthermore, studies have extensively relate the tectonic framework of the Niger Delta to the forces that produced strain that accompanied the separation of African and South American plates, which led to the opening of the South Atlantic and was later controlled by cretaceous fracture zones expressed as trenches and ridges in the deep Atlantic. These fracture zone ridges are subdivided into individual basins which, in Nigeria, form the boundary faults of the Cretaceous Benue-Abakaliki Trough, which cuts far into the West African shield. This trough represents a failed arm of a rift triple junction associated with the opening of the South Atlantic. The fracture zone ridges subdivide the margin into individual basins (Figure 2.2) and in Nigeria, form the boundary faults of the Cretaceous Benue-Abakaliki Trough, which cuts far into the West African Shield. The trough represents a failed arm of a rift triple junction associated with the opening of the South Atlantic. In this region, rifting started in the Late Jurassic and persisted into the Middle Cretaceous. In the region of the Niger Delta, rifting diminished altogether in the Late Cretaceous. It is believed that rifting started in the Late Jurassic and persisted into the Middle Cretaceous (Lehner et al (1977); Steve et al (2002)) Margin evolution included phases of break-up and continental separation

from Late Aptian rifting through to passive margin development. Tectonic episodes resulting in uplift are recognized in the Santonian and mid and Late Tertiary (figure 2.3).

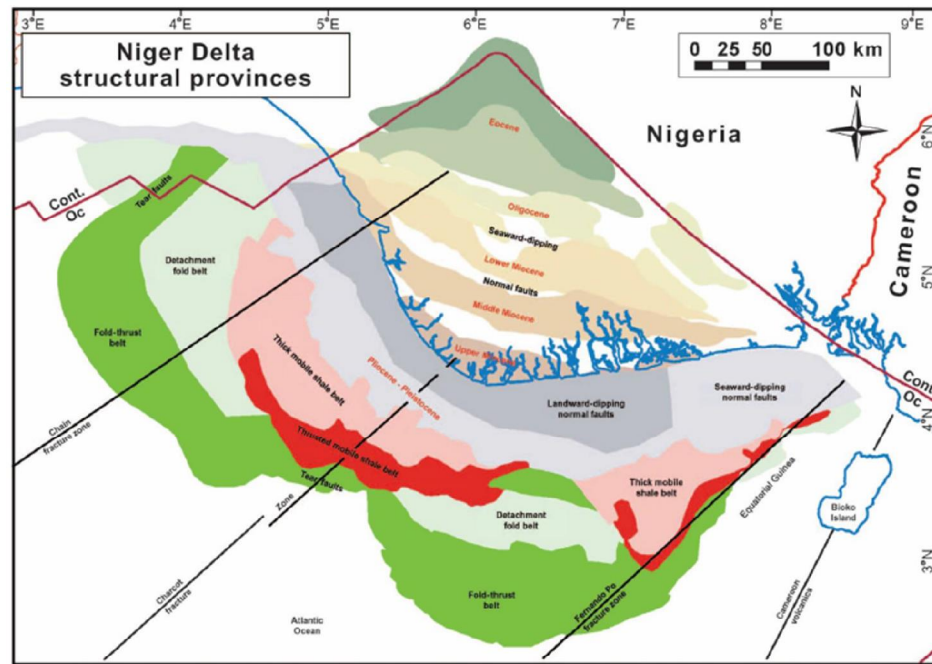


Figure 2.2: Regional structural provinces map of the Niger Delta showing the Fracture Zones.(Wiener et al., 2010)

The gross paleogeography of the region as well as the relative position of the African and South American plates since rifting began is shown in (Figure 2.33). After rifting ended temporarily, gravity tectonics became the primary deformational process. For any given depobelt, gravity tectonics were completed before deposition of the Benin Formation and are expressed in complex structures, including closely spaced flank faults, shale diapirs, collapsed growth fault crests, roll-over anticlines, back-to-back features, and steeply dipping, Evamy et al (1978); Xiao and Suppe (1992).

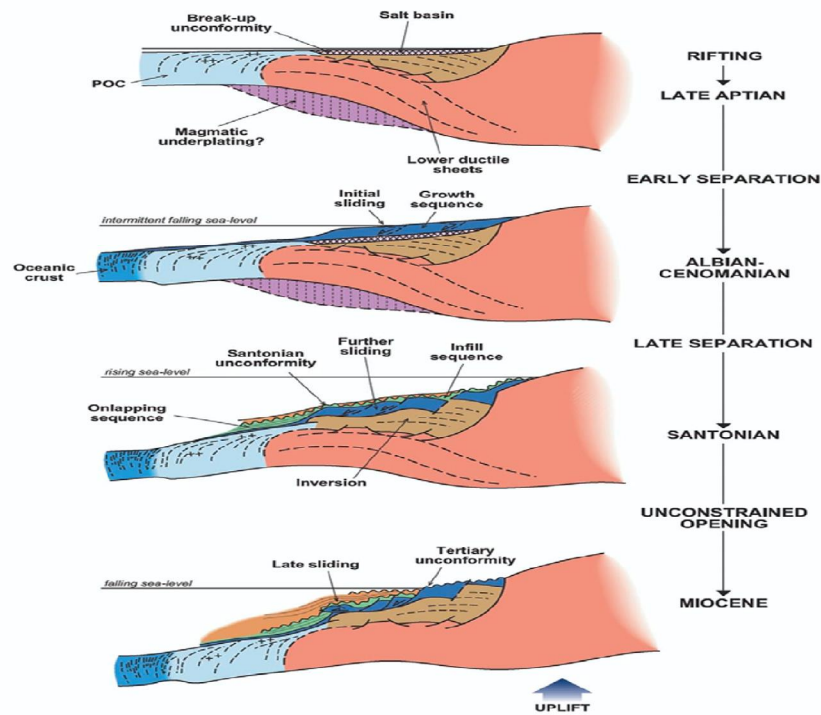


Figure 2.3: Margin evolution included phases of break-up and continental separation from Late Aptian rifting through to passive margin development. Tectonic episodes resulting in uplift are recognized in the Santonian and Mid and Late Tertiary (Steve et al., 2002).

These faults mostly offset different parts of the Agbada Formation and flatten into detachment planes near the top of the Akata Formation (Figure 2.4). Shale mobility induced internal deformation and occurred in response to two processes Kulke (1995). At first, diapiric shale structure formed from loading of poorly compacted, over-pressured, pro-delta and delta-slope clays (Akata Fm.) by the higher density delta-front sands (Agbada Fm.). Moreover, slope instability came to pass due to a lack of lateral, basinward, and support for under-compacted delta-slope clays (Akata Fm.); these resulted to development of depo-belts in some areas.

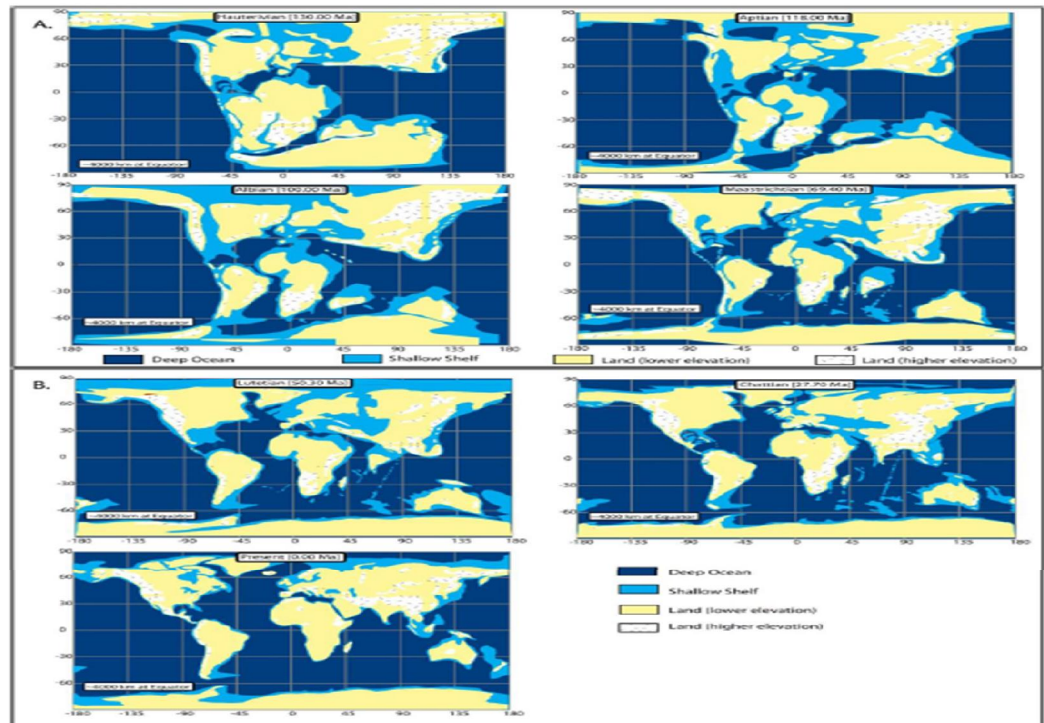


Figure 2.33: Paleogeography showing the opening of the South Atlantic, and development of the region around Niger Delta. A. Cretaceous paleogeography (130.0 to 69.4 Ma). B. Cenozoic paleogeography (50.3Ma to present). Plots generated with PGIS software. (Tuttle et al., 1999)

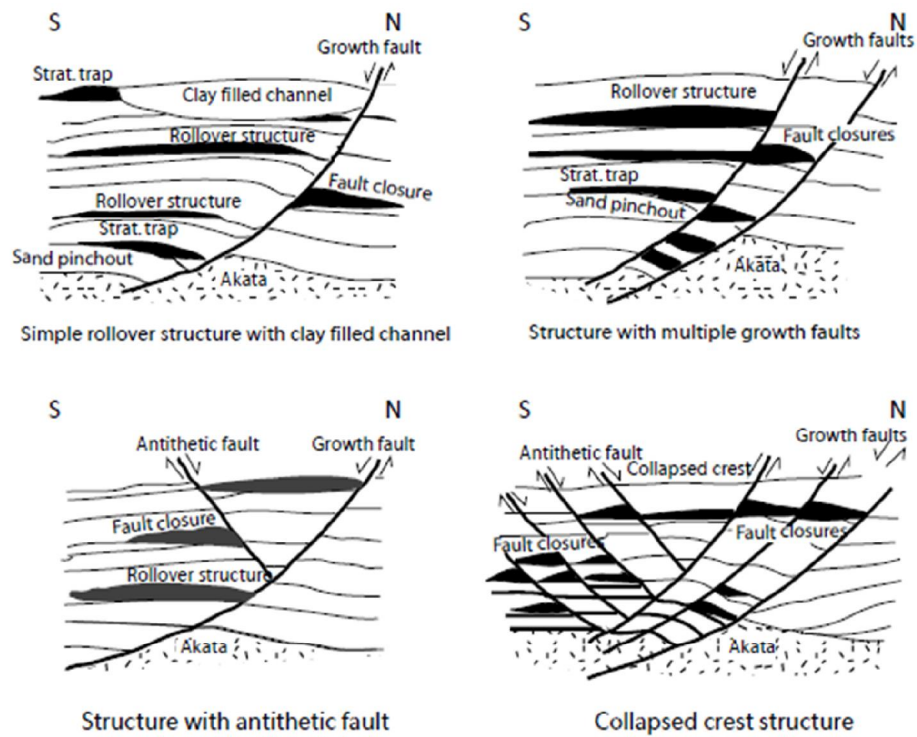


Figure 2.4: Structural Features of the Tertiary Niger Delta showing Growth Faults and Roll-over Anticlines. After Doust and Omatsola, (1990) and Stacher (1995)

2.2 DEPOBELT AND ENVIRONMENT OF DEPOSITION

The growth of the Niger Delta started in the Eocene in response to the positive epeirogenic movements along the Benin and Calabar Flanks. In the mid-Eocene, a major regression commenced which accelerated the expansion of the Niger Delta, leading to regression that gave rise to the formation of the present Niger Delta in mid-Eocene times. It began with the deposition of the Ameki Formation west and east of the Niger River. This regressive phase has continued until the present, although it has been interrupted by not too significant minor regressions. Sediment supply into the delta was developed from two main drainage systems, the Niger-Benue system through the Anambra Basin north of Onitsha and the Cross River system through the Afikpo Basin. This resulted in 3 depocenters (1) the Afikpo Ikang Depocenter fed by the Cross River system (2) the Anambra Depocenters fed by the proto-Niger-Benue system, and (3) the Onitsha Depocenter fed by rivers draining the basin, Onitsha high and Abakaliki fold belt. Whiteman (1982); Etu-Efeotor (1997) These depocenters are 30-60 kilometers wide, prograde southwestward 250 kilometers over oceanic crust into the Gulf of Guinea, Stacher (1995), and defined by syn-sedimentary faulting that occurred in response to variable rates of subsidence and sediment supply Doust and Omatsola (1990). The reciprocal action and reaction of subsidence and supply rates resulted in deposition of discrete depobelts-when further crustal subsidence of the basin could no longer be accommodated, the focus of sediment deposition shifted seaward, forming a new depobelt, Doust et al (1990). Each depobelt is a separate unit that corresponds to a break in regional dip of the delta and is bounded landward by growth faults and seaward by large counter-regional faults or the growth fault of the next seaward belt Evamy et al (1978); Doust et al (1990). The depobelts are generally recognized in Tertiary Niger Delta, each with its own sedimentation, deformation, and petroleum history. They include the Northern Delta Depo-belt, Central Swamp I and II Depo-belts, Greater Ughelli Depo-belt, Coastal Swamp I and II Depo-belts and offshore Depo-belt as shown in (Figure 2.5). Whereas five major depobelts are generally recognized by SPDC, each with its own sedimentation, deformation, and petroleum history (Figure 2.55). Doust and Omatsola (1990) described three depobelt provinces based on structure. The northern delta province, which overlies relatively shallow basement, has the oldest growth faults that are generally rotational, evenly spaced, and increases their steepness seaward. The central delta province has depobelts with well-defined structures such as successively deeper rollover crests that shift seaward for any given growth fault. Last, the distal delta province which is the most structurally complex due to internal gravity tectonics

on the modern continental slope. The study area lies within the coastal swamp depobelts (Figures 2.7 and 2.77).

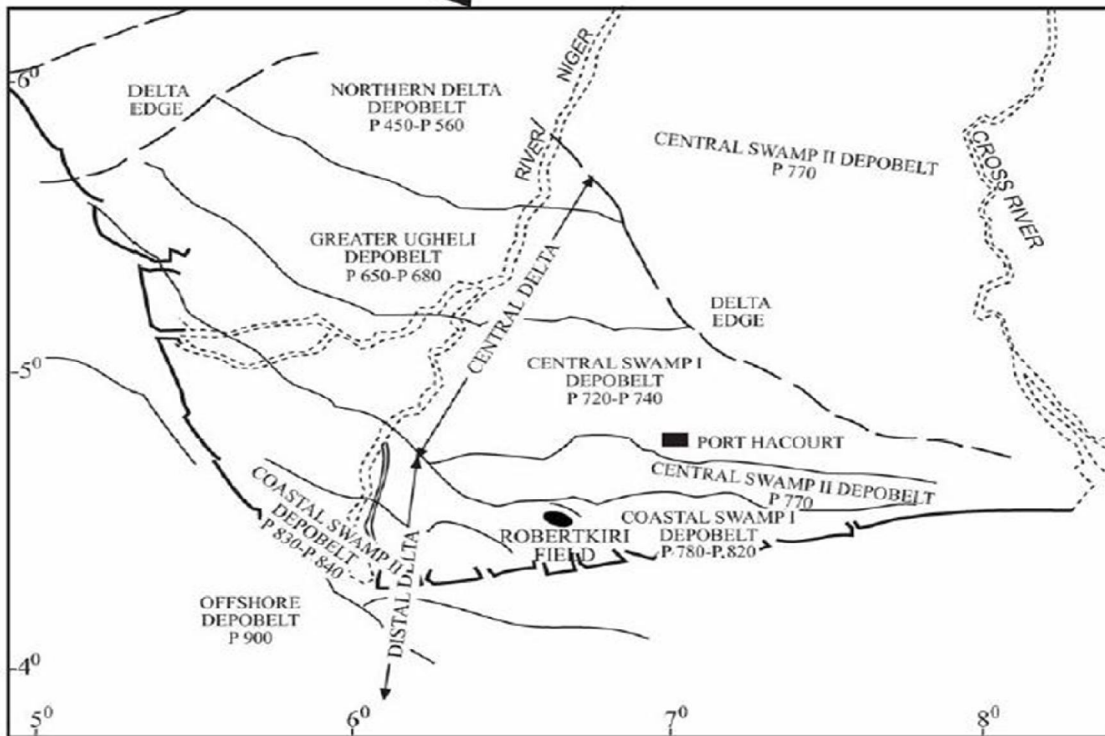


Figure 2.5: Depobelts with their relative ages (after Doust and Omotsola, 1990)

The modern Niger Delta is a mixed wave, tide and fluvial deltaic system. The delta is reworked by wave action along an arcuate coast with barrier islands, back-barrier lagoons, and channel ridges. Thick mangroves border the coastline of the lower Niger Delta plain. Incised into this coastline are numerous tide-dominated coastal estuaries, that have gradually been filled with sediment following the Holocene sea level highstand. The modern delta front and continental slope is characterized by localized slumps and canyons that bypass sediments into deeper waters. Although details of deltaic features are difficult to decipher within reservoir intervals of Niger Delta deposits, the modern distribution of distributary channels, estuary fills, shoreface, back barrier lagoonal sediments, and delta plain deposits are assumed to be a good analog.

2.3 STRATIGRAPHIC SETTING

The Niger Delta stratigraphic sequence comprises an upward-coarsening regressive association of Tertiary clastics up to 12 km thick (Figure 2.6).

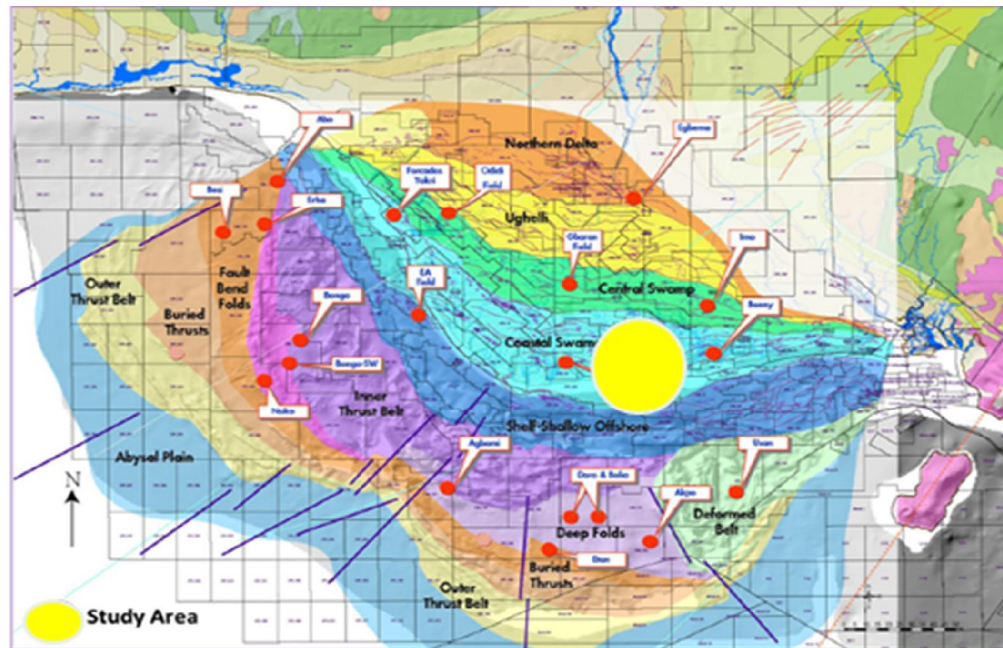


Figure 2.55: Depobelt map with the structural play segments, onshore and offshore Niger Delta Basin showing the study area (SPDC, 2011)

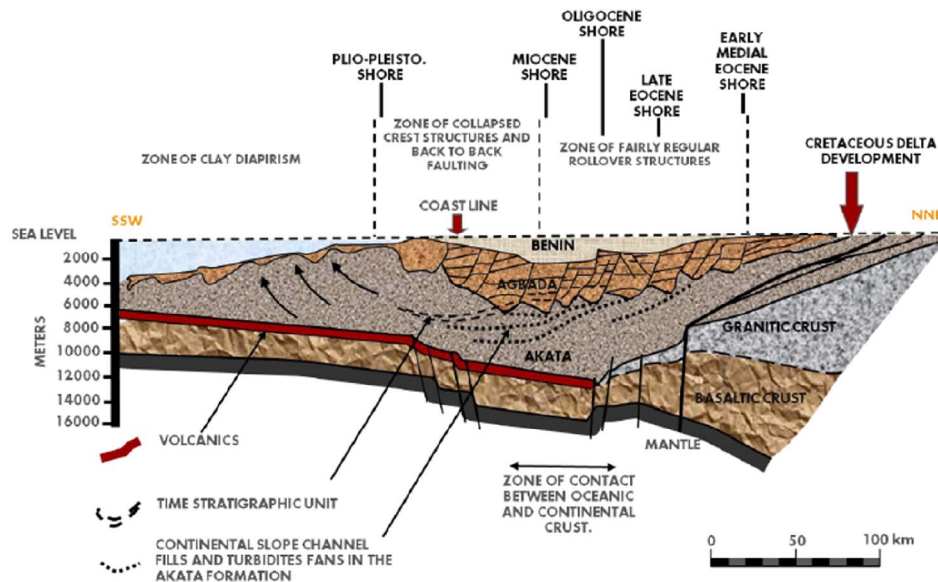


Figure 2.6: Schematic Dip Section of the Niger Delta (Modified after P. Kamerling, from Weber and Daukoru, 1975)

It is informally divided into three gross lithofacies: (i) alternation of sandstones, siltstones and claystones, in which the sand percentage increases upwards; (ii) alluvial sands, at the top; (iii) marine claystones and shales of unknown thickness, at the base; Doust (1990). The Tertiary Niger Delta is a sedimentary structure formed as a complex regressive offlap sequence of clastic sediments ranging in thickness from 9,000-12,000m, Etu-Efeotor (1997). Starting as separate depocenters, the Niger delta has coalesced to form a single united system since Miocene.

In Niger Delta, as in many delta areas, it is extremely difficult to define a stratigraphic nomenclature. The occurrences of small number of differing lithologies make it almost impossible to define units and boundaries succinctly to constitute separate formations in a formal sense. However, evidence from all the deep wells in the Niger Delta shows three lithostratigraphic successions in which a regressive sequence is properly defined. Short et al (1967) divided the Tertiary deltaic complex into three major facies units based on the dominant environmental influences. These main sedimentary environments are the continental environment, the transitional environment and the marine environment. In an advancing delta, such as the Niger Delta, sediments of the three environments become stratigraphically superimposed. The base of the stratigraphic sequence is represented by marine shales. The middle part of the sequence is represented by interbedded shallow marine and fluvial sands, silts and clays which are typically of a paralic setting. The sequence is

capped by a section of massive continental sands. Because of the history or relative unbroken progradation throughout the Tertiary, the three depositional lithofacies are readily identified despite local facies variation, as three regional and diachronous formations, ranging from Eocene to Recent age. (Figure 2.7) displays the diagrammatic representation of the stratigraphic evolution of the Niger Delta, Reijers (2011). Moreover, (Figure 2.77) shows the regional tectonostratigraphy, the Niger Delta's regional stratigraphy is broken down into megasequences representing phases of basin development. tectonic episodes are marked by regionally significant unconformities in the Santonian and Mid and Late Tertiary, Steve et al (2002).The three formations are locally designated (from the bottom) as Akata Formation, Agbada Formation and Benin Formation respectively (Table 1, Figure 2.8), whereas (Figure 2.9) shows the schematic diagram of the regional stratigraphy of the Niger Delta and seismic display of the main stratigraphic units in the outer fold and thrust belt and main reflectors, Corredor et al (2005).

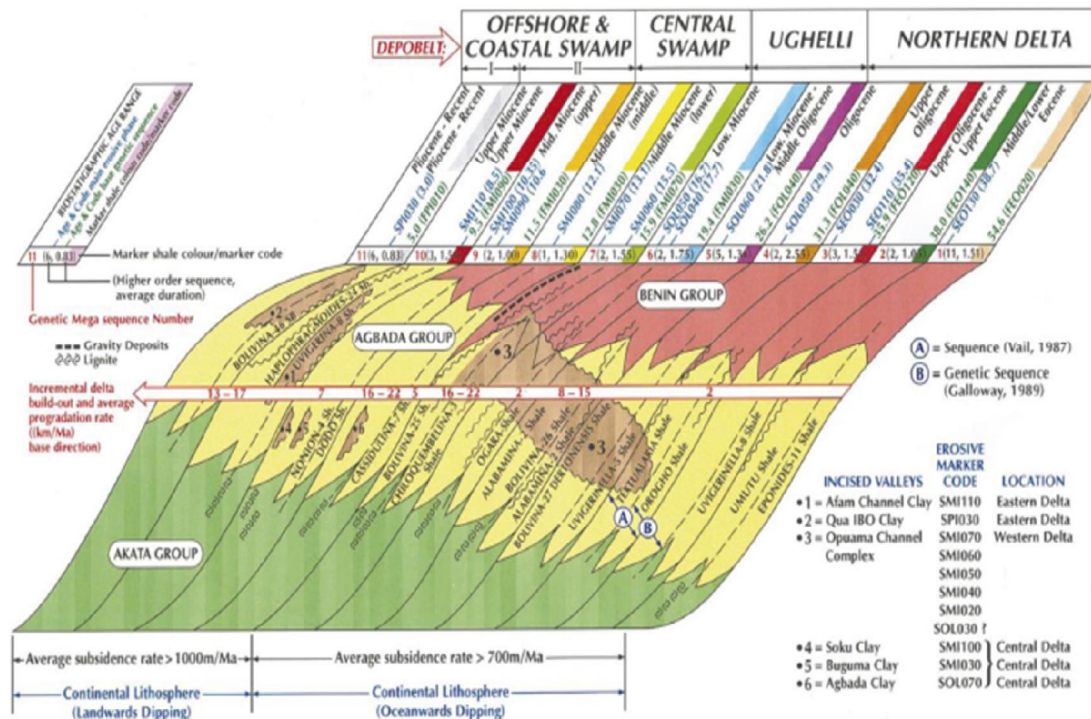


Figure 2.7: Diagrammatic representation of the stratigraphic evolution of the Niger Delta (After Reijers, 2011)

THE BENIN FORMATION

The Benin Formation comprises the top part of the Niger Delta clastic wedge, from the Benin-Onitsha area in the north to beyond the coast line, Short and Stauble (1967). The top of the formation is recent, and its base extends to a depth of 4600 feet. The base is defined by the youngest marine shale. Shallow parts of the formation are composed entirely of non-marine sand deposited in alluvial or upper coastal plain environments during progradation of the delta, Doust and Omatsola (1989). Although lack of preserved fauna inhibits accurate age dating, the formation is estimated to range from Oligocene to Recent, Short and Stauble (1967).

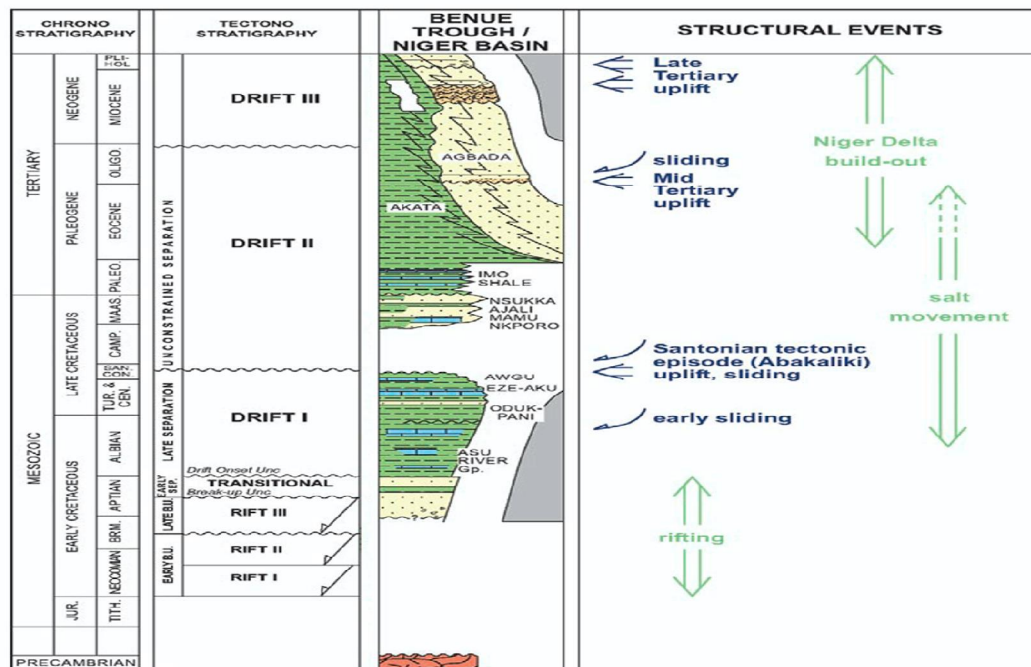


Figure 2.77. Regional Tectonostratigraphy. Regional stratigraphy is broken down into megasequences representing phases of basin development. Tectonic episodes are marked by regionally significant unconformities in the Santonian and Mid and Late Tertiary (Steve et al., 2002)

THE AGBADA FORMATION

Of the three lithostratigraphic formations of the Niger Delta listed above, the Agbada Formation constitutes the main reservoir for hydrocarbons in the Niger Delta. The age of the formation ranges from Eocene to Pleistocene. The formation occurs throughout the Niger Delta clastic wedge and has a maximum thickness of about 13,000 feet. It cuts short in southern Nigeria (between Ogwashi and Asaba). The lithologies consist of alternating sands,

silts and shales arranged within ten to hundred feet successions defined by progressive upward change in grain size and bed thickness. The strata are generally resitated to have formed in fluvial-deltaic environments.

Table 1: Stratigraphic units of Niger Delta area, Nigeria. (Modified from Short and Stauble (1967))

Subsurface			Surface Outcrops		
Youngest known Age		Oldest known Age	Youngest Known Age		Oldest Known Age
Recent	Benin Formation (Afam clay member)	Oligocene	Plio/Pleistocene	Benin Formation	
Recent	Agbada Formation	Eocene	Miocene Eocene	Ogwashi-Asaba Formation Ameki Formation	Oligocene Eocene
Recent	Akata Formation	Eocene	lower Eocene	Imo shale Formation	Paleocene
	Unknown		Paleocene Maestrichtian Campanian Campanian/Maestrichtian Coniacian/Santonian Turonian Albian	Nsukka Formation Ajali Formation Mamu Formation Nkporo Shale Awgu Shale Eze Aku Shale Asu River Group	Maestrichtian Maestrichtian Campanian Santonian Turonian Turonian Albian

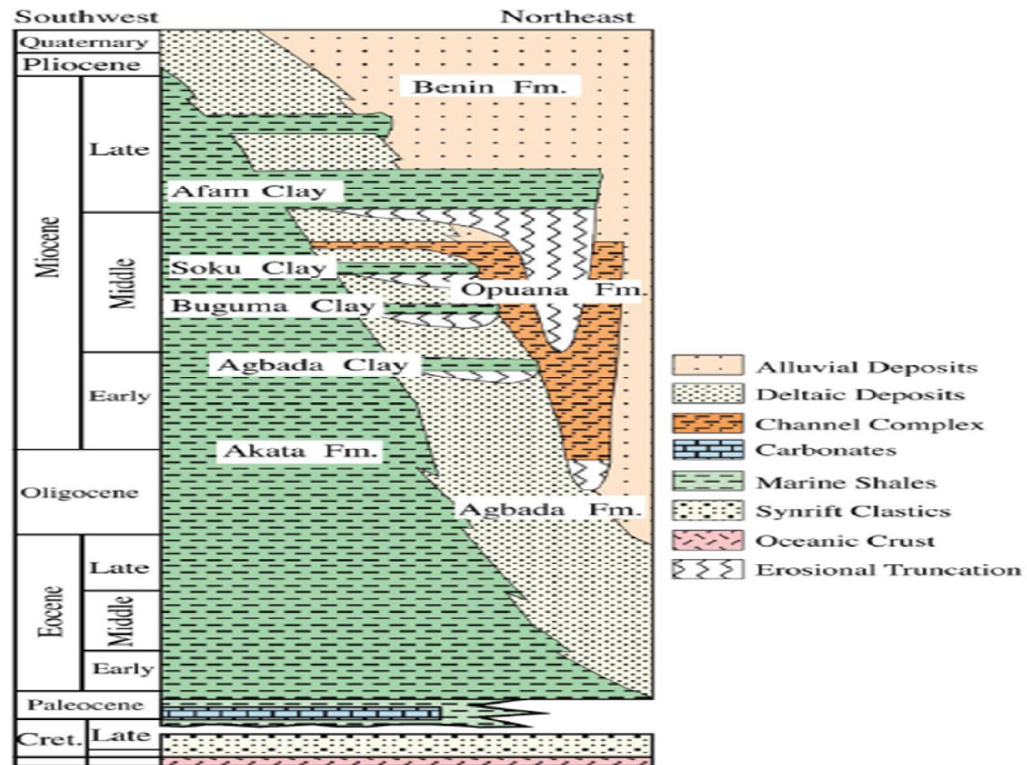


Figure 2.8: Stratigraphic column showing the three formations of the Niger Delta (modified from Lawrence et al, 2002)

THE AKATA FORMATION

The Akata Formation is of old duration of the three major lithostratigraphic units in Tertiary Niger Delta. The age of the Akata Formations ranges from Paleocene to Recent Doust and Omatsola, (1989). Stacher (1995) and Doust and Omatsola, (1989) interpreted Akata Formation as to be deep lowstand deposit that has estimated thickness of about 21,000 feet in the central part of the clastic wedge. It includes Marine planktonic foraminifera making up to 50% of the microfauna assemblage and suggest shallow marine shelf deposition. The Akata shales formed during the early development stages of Niger Delta progradation are thickest along the axis of the Benue and Bida Troughs. It is uncovered onshore in the north-eastern part of Nigeria, and the Formation is called the Imo shale. The formation also crops offshore in diapirs along the continental slope where deeply buried marine shales are typically over pressured. The Formation grades vertically into the Agbada Formation with abundant plant remains and micas in the transition zone Doust and Omatsola (1989).

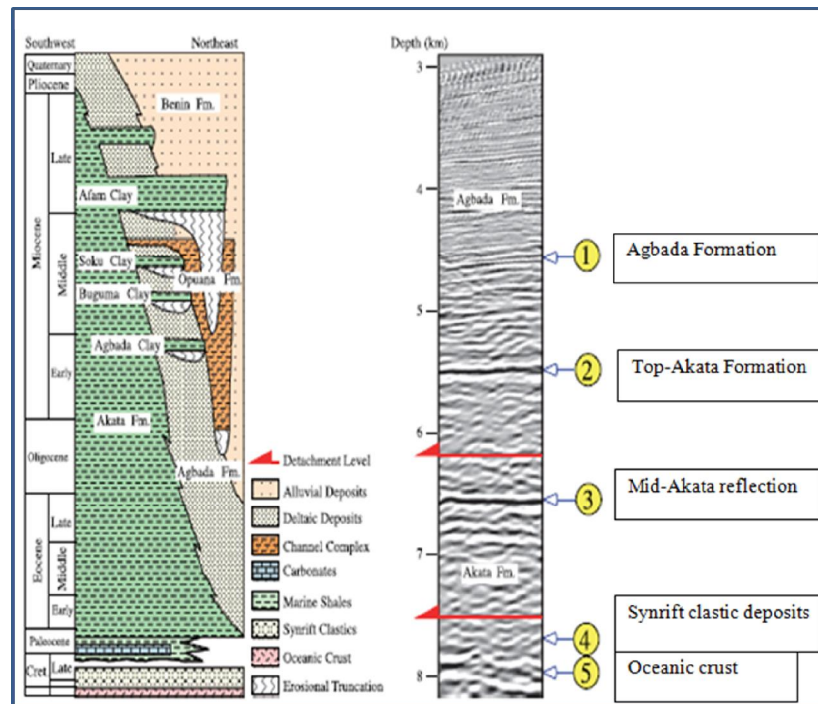


Figure 2.9: Schematic diagram of the regional stratigraphy of the Niger Delta and seismic display of the main stratigraphic units in the outer fold and thrust belt and main reflectors (Corredor et al, 2005)

CHAPTER THREE

METHODOLOGY

3.1 METHOD

This study focuses on integrating biofacies, well logs and seismic tools to reconstruct the sequence stratigraphy interpret the structural and stratigraphic framework of the OGBO field in the Coastal Swamp Depo-belt of the Niger Delta Basin. The summary of the workflow chart employed in this analysis is given in (Figure 3.1). This approach consists of developing a detailed work plan to accomplish study objective, define limitations with no provision of field documentation report, analogue data, historic and recent production data, pressure data, core data and only well OGBO 046 biostatigraphic data was provided. Integration of well logs, seismic data and biofacies data in petrel software application platform aid the sequence stratigraphy delineation and dating using laid down procedures (Figures 3.3 and 3.33, 3.4 , 3.5, 3.55, 3.555 and 3.5555).

A general quality control assessment was done on the 3-D prestack seismic volume and well logs suites in the given software. Developing the list of six wells used in the study and their available data well log correlation. Delineation of lithologies and fluid type prediction in the producing field from the available stratigraphic data. Stratigraphic indicators and the nature of the gamma ray curves that characterize the surface interval. The lithologies penetrated by the studied wells were determined by setting the cutoff point at 65 API on the gamma ray logs, Interpretation of environment of deposition is based on the combination of the gamma ray log with resistivity log signatures which were corroborated by Schlumberger (1985), Cant (1992), Emery and Myers (1996) and Kendall (2003) charts (well log motif) with the conceptual model, Net to Gross (NTG) map, and attribute extraction. Three horizons sand bodies were defined from the gamma ray and resistivity log sections (Figure 3.2 and 3.22).

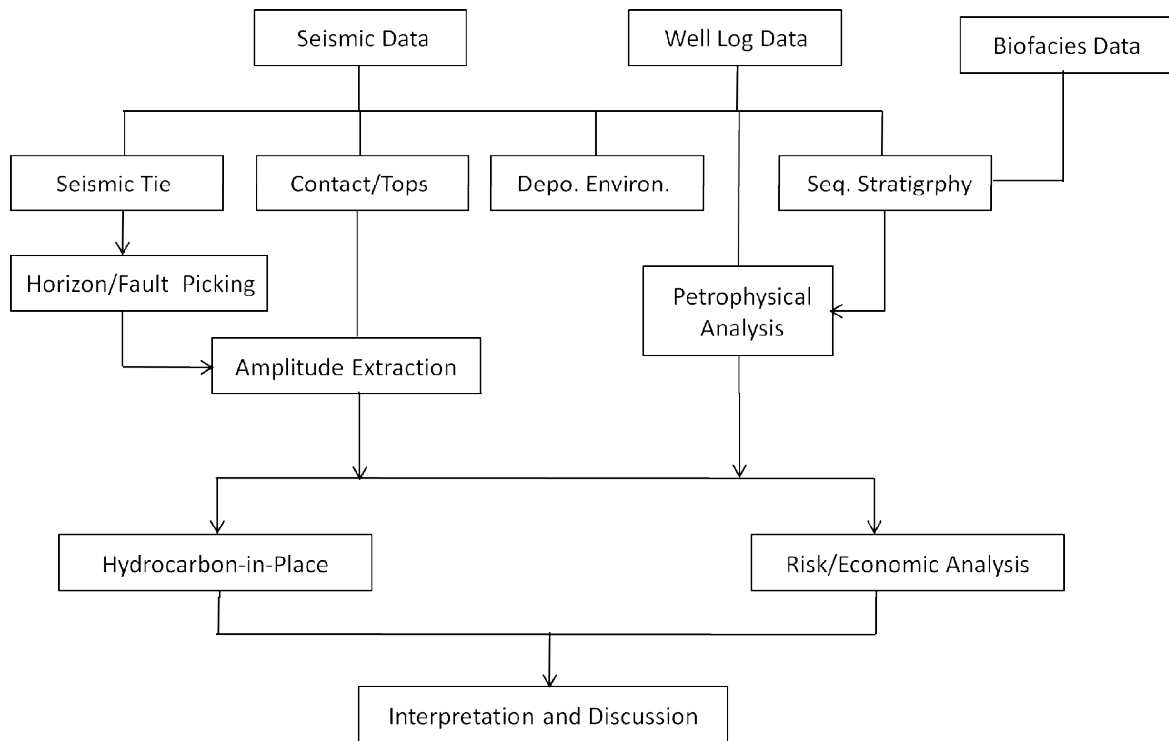


Figure 3.1 : Work Flow Chart of the Study

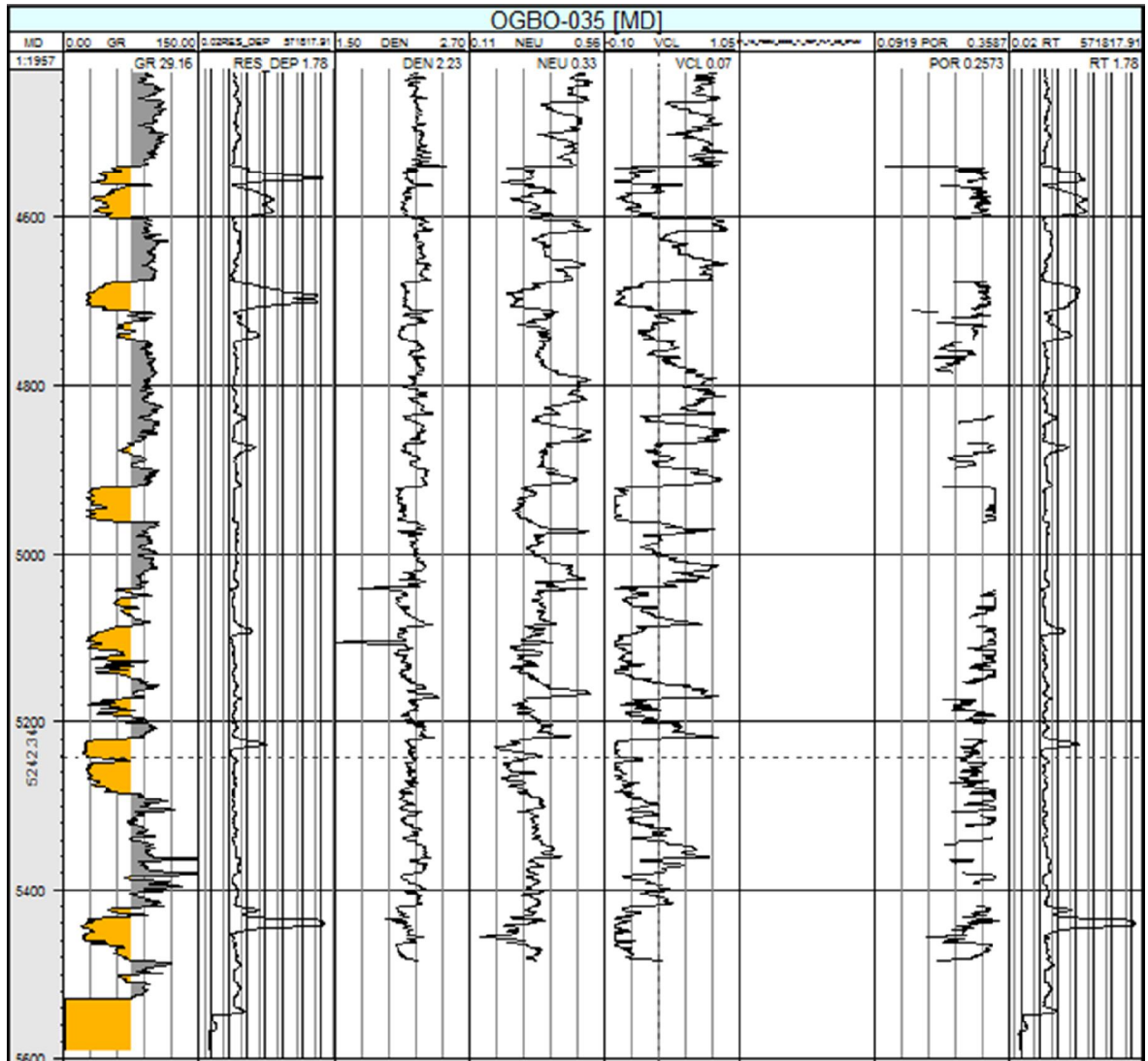


Figure 3. 2: The well log section for OGBO field

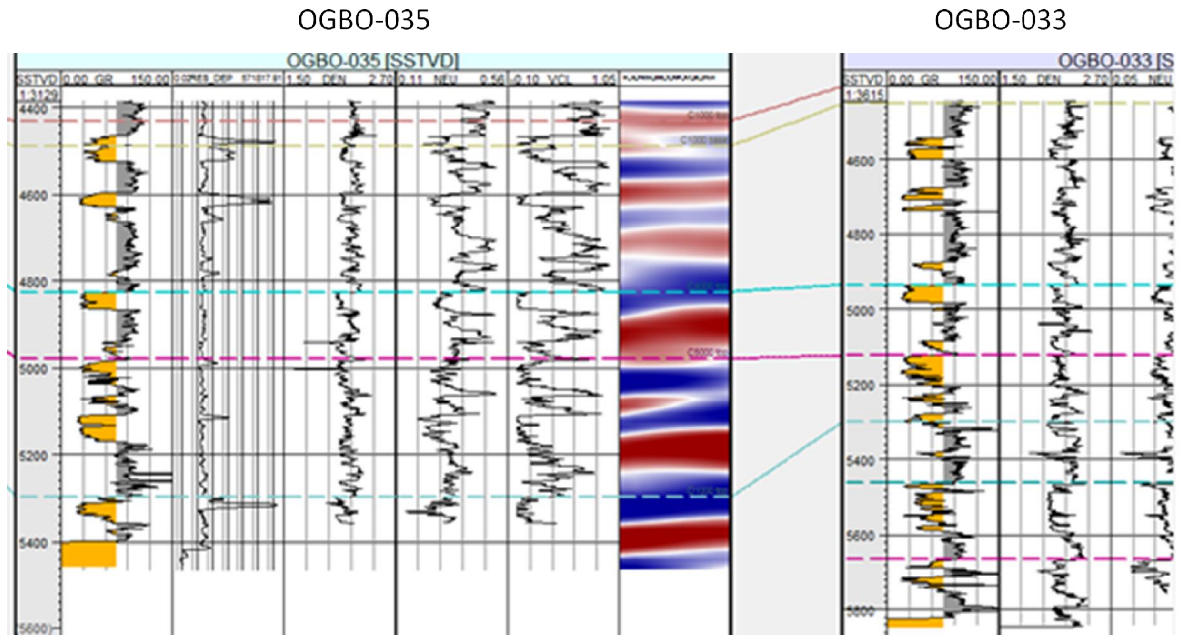


Figure 3. 22: The well log section for OGBO field

These horizons were later correlated in the 3D seismic volume in order to produce time depth structure map horizons. Well to seismic tie was carried out and major and minor faults were identified, traced and assigned in seismic section. The faults were picked at the interval of 10 on the inlines section were subsequently reflected on the cross-lines sections. After the correlation, time and depth structure maps and amplitude extraction maps were produced. The time depth relationship was determined by plotting the checkshot data available using Microsoft Excel. Probabilistic assessment (risk/economic analysis) and estimation of hydrocarbon in place was also carried out to determine the choice of prospect and ranking in the producing field. Seismic data were tied together by the use of 2-way time check shot data.

3.2 DATA SET

The wells used for the study are; OGBO 033, OGBO 035, OGBO 019STI, OGBO 038, OGBO 046, OGBO 005, OGBO 036 and OGBO 056. Biofacies data; The biozone records obtained from the well OGBO 046 (only provided) were the palynological and foraminifera-zones popularly referred to as the P-and F-Zones. Three different pollen zones (P-Zones) and three fauna zones (F-Zones) recognized were P770, P750, P720 and F9507, F9505, F9503, F9501 respectively. The population and diversity of the benthic and planktonic foraminifera were used for environmental and

paleobathymetric interpretation (Figure 3.3 and 3.33). Well log data suites were provided, among which gamma ray logs, neutron Logs, density (FDC.g/cm³) logs, and resistivity (RES_D.OHM.M, RES_S.OHM.M) logs and bottom hole Compensated (BHC.µs/ft) were used. A 3D seismic PSDM volume of OGBO field were acquired, processed and reprocessed in the early 1990s and early 2000s respectively also provided. The quality of the data varies from very good at shallow levels, dropping rapidly to poor quality images at below 2.5 seconds. Check shot data was used for 2-way time interpretation that tied both well logs and seismic data together.

3.2.1 DATA QUALITY AND SOFTWARE APPLICATION

The seismic volume is characterized by a series of nearly parallel reflections that are quite chaotic close to and behind faults and continuous at zones away from faults. Reflections within the upper one second two-way-travel time are slightly discontinuous and of relatively low amplitude. At intervals between one and four second two-way-travel time, the reflections are generally continuous and of relatively high amplitude. Data quality generally deteriorates at depth below four second two-way-travel time characterized by zones of discontinues and chaotic low amplitude reflection; and zones of continuous and high amplitude reflections.

Well log data suites were provided, among which gamma ray logs, neutron logs, density (FDC.g/cm³) logs, and resistivity (RES_D.OHM.M, RES_S.OHM.M) logs and bottom hole Compensated (BHC.µs/ft) were used. In some wells the whole length of the bore were logged while in some others only a small portion, mainly in the productive zone, were logged. The quality of the logs is good mostly where the full length of the well bore is logged. Biostratigraphic data comprises biofacies data, palynological zone (P-Zone) and foraminifera zone (F-Zone). These were calibrated using an established Niger Delta Basin zonation schemes (Figure 3.3 and 3.33, 3.4 and 3.5). The biofacies data contain information on total foraminifera abundance and diversity, total planktonic facies abundance and diversity, total benthic calcareous facies abundance and diversity, total benthic arenaceous facies abundance and diversity, paleobathymetry and environment of deposition for various depth intervals of the well bore. In some wells these are available for the whole length while in others it covers only some intervals of interest. The main computer software used for this research includes Petrel software run on workstations and Microsoft excel.

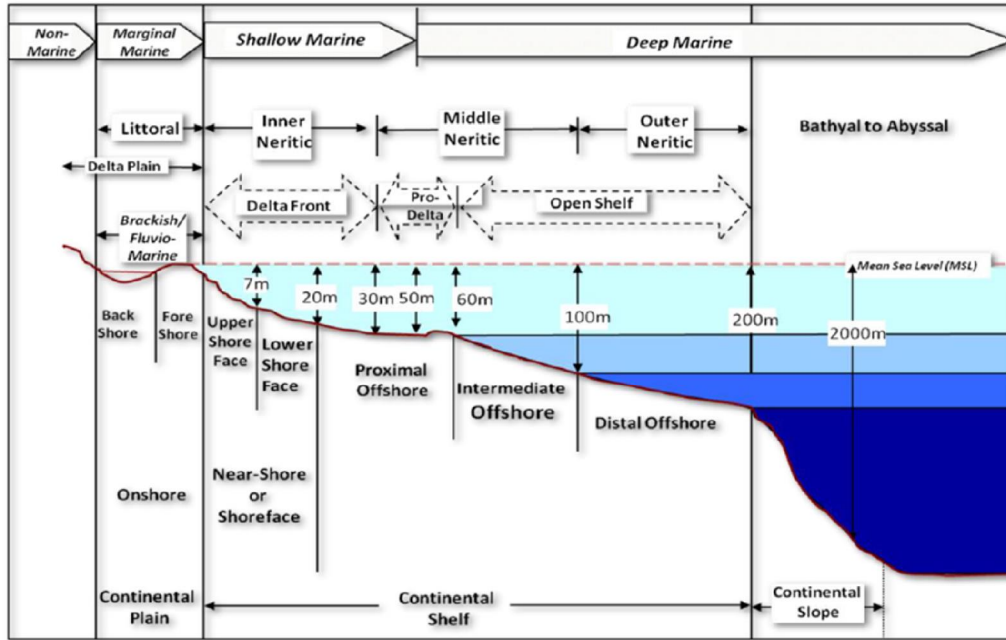


Figure 3.3: Paleobathymetry and Depositional Environment Chart (Modified After Allen, 1965)

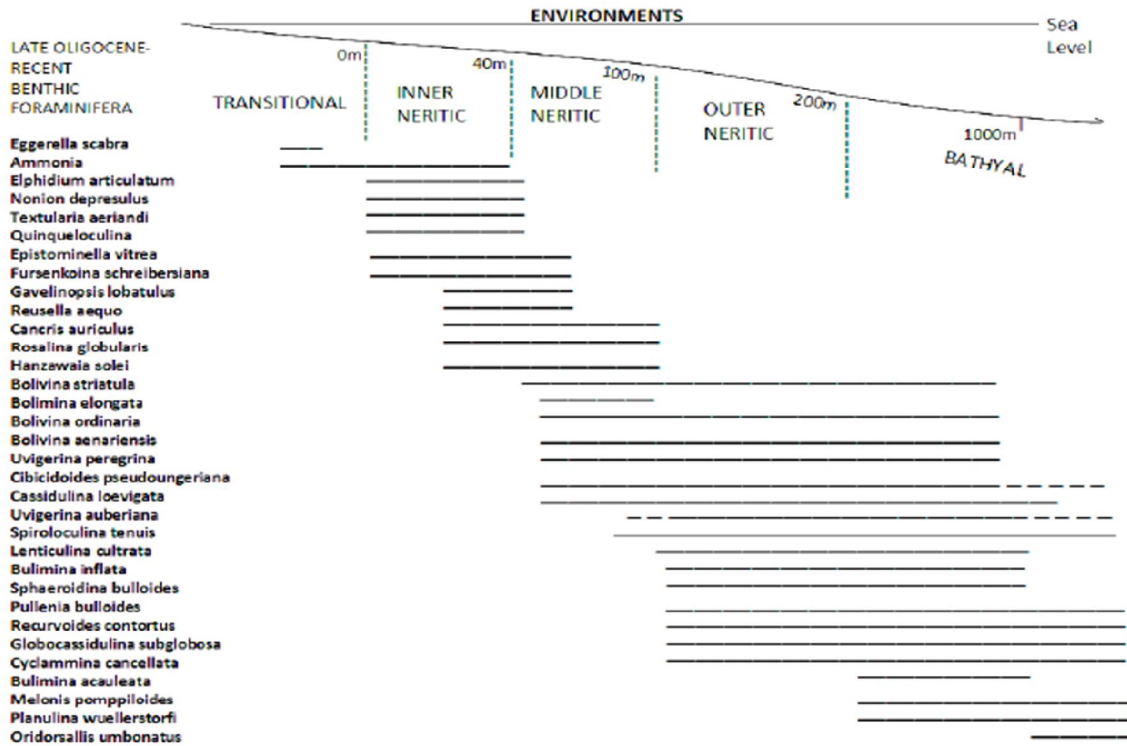


Figure 3.33: Foraminifera biofacies model for the Niger Delta adapted from SPDC in-house Report

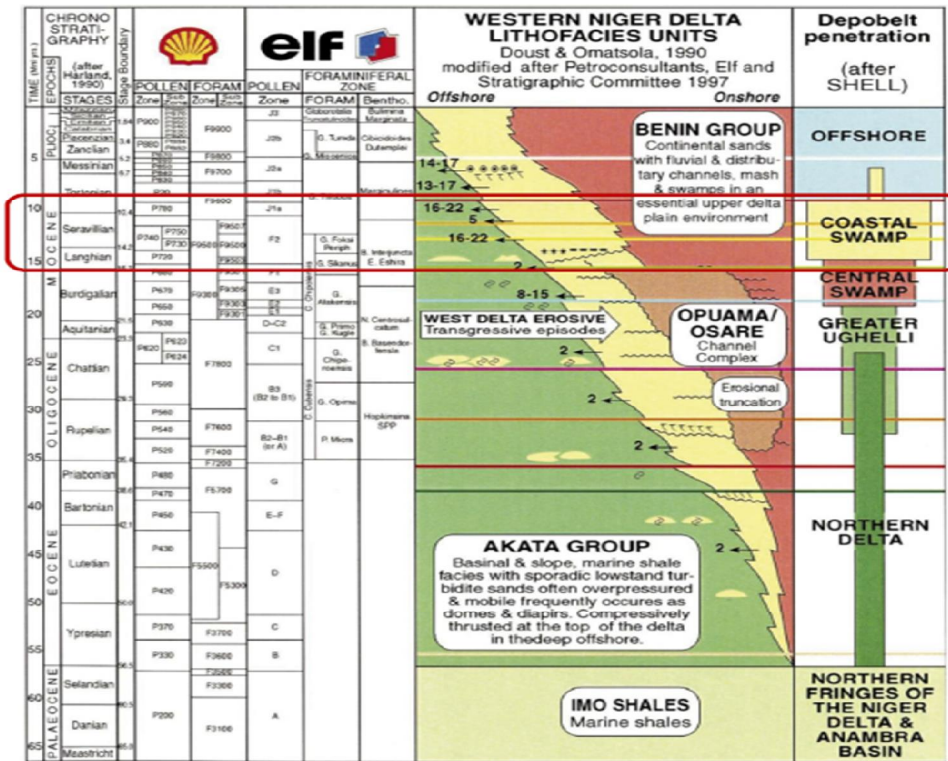


Figure 3.4: Stratigraphic data sheet (west and east halves combined) of the Niger Delta (Reijers, 2011)

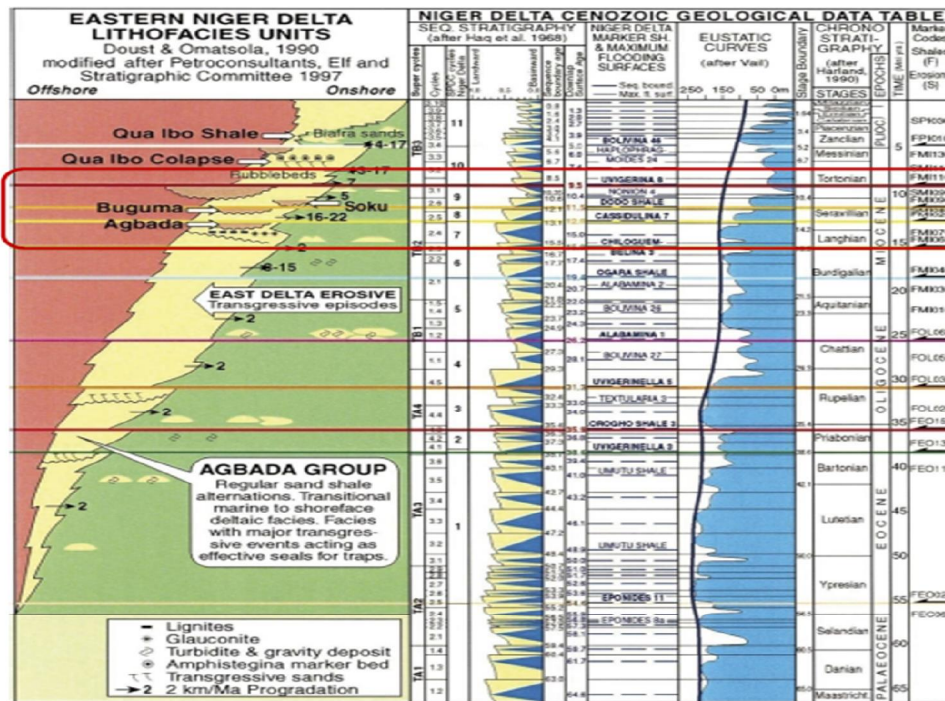


Figure 3.4: Stratigraphic data sheet (west and east halves combined) of the Niger Delta cont'd (Reijers, 2011)

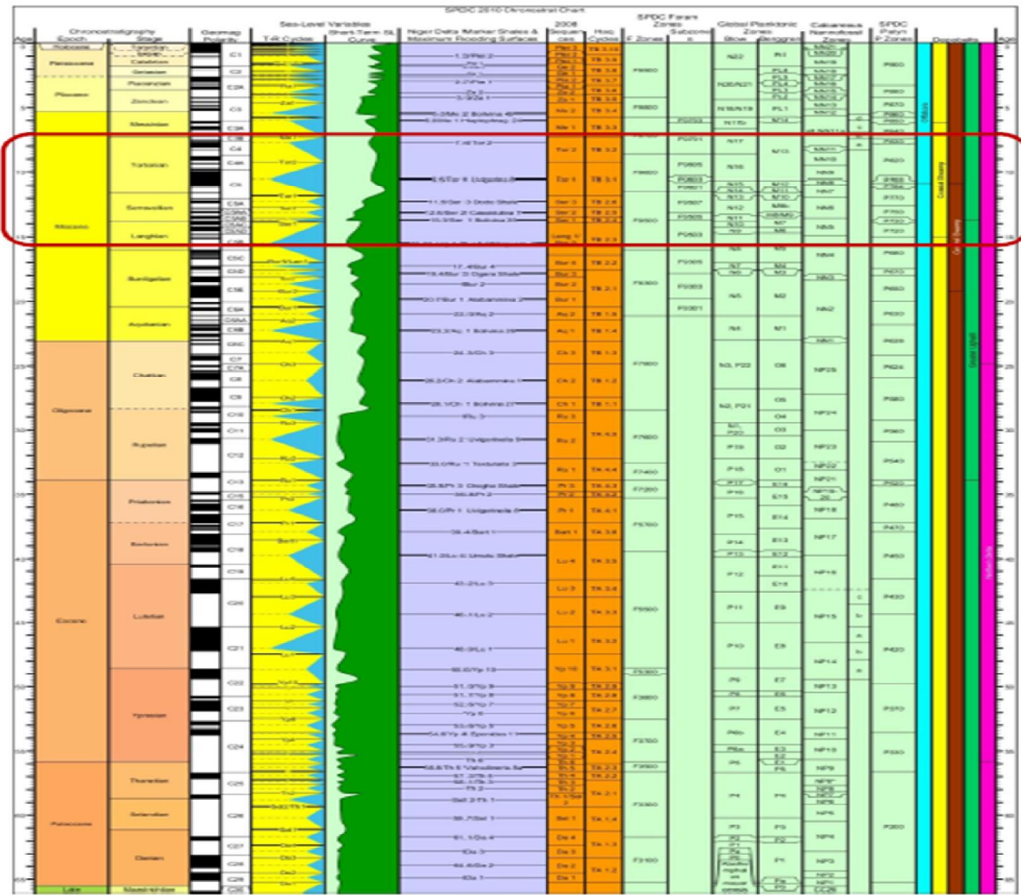


Figure 3.5: Niger Delta Chronostratigraphic Chart (SPDC, 2010)

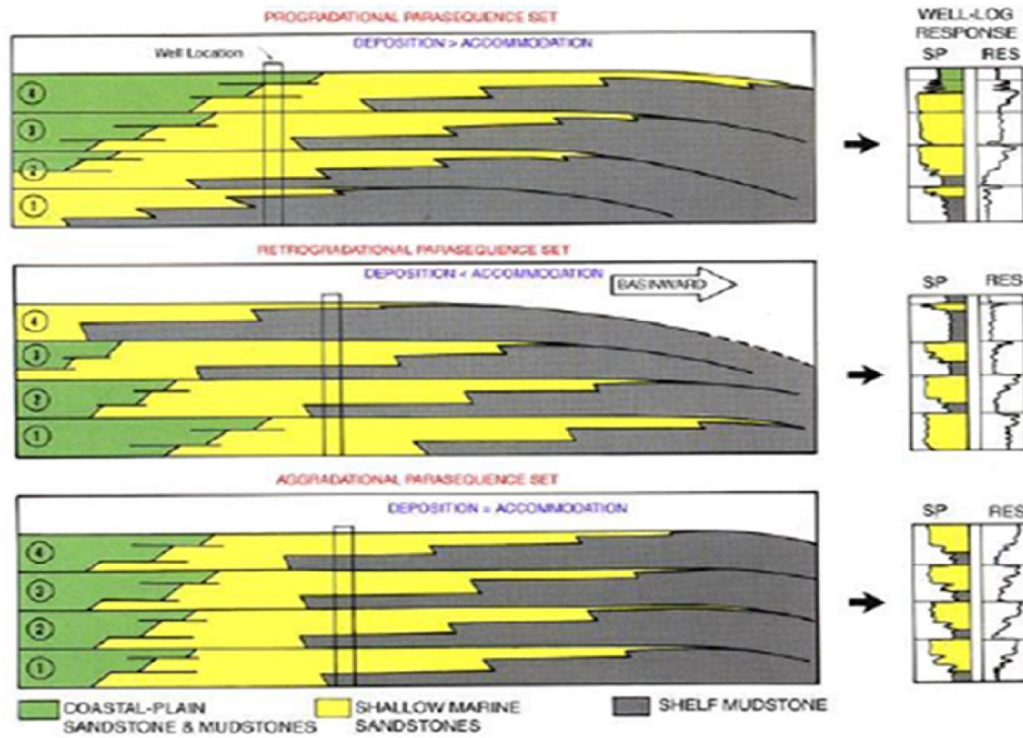


Figure 3.55: Parasequence stacking pattern model (After Van Wagoner et al., 1990)

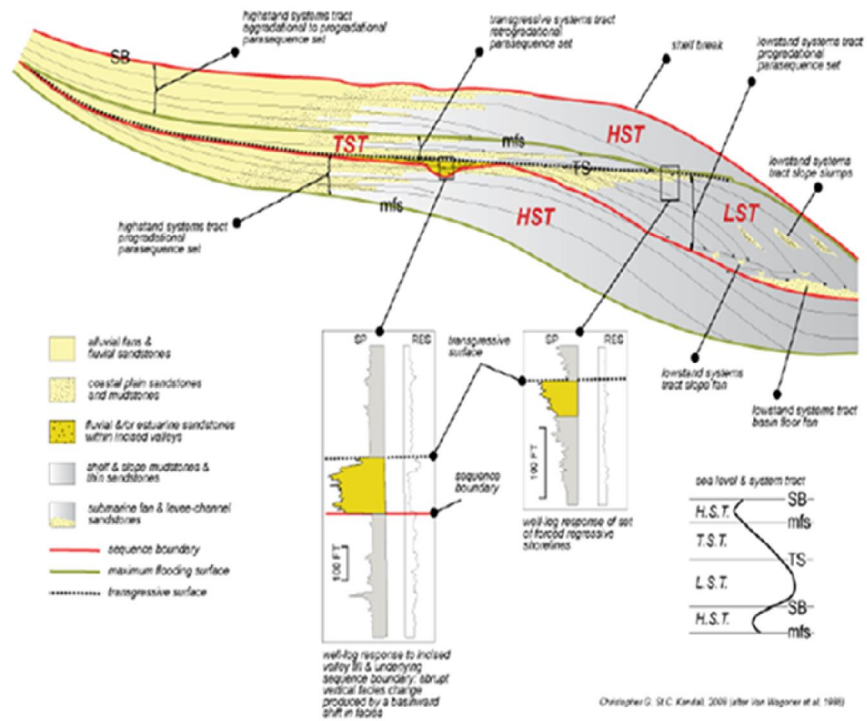


Figure 3.55: Sequence stratigraphic model showing key stratigraphic surfaces and various systems tracts (Kendall, 2008, After Van Wagoner et al., 1988)

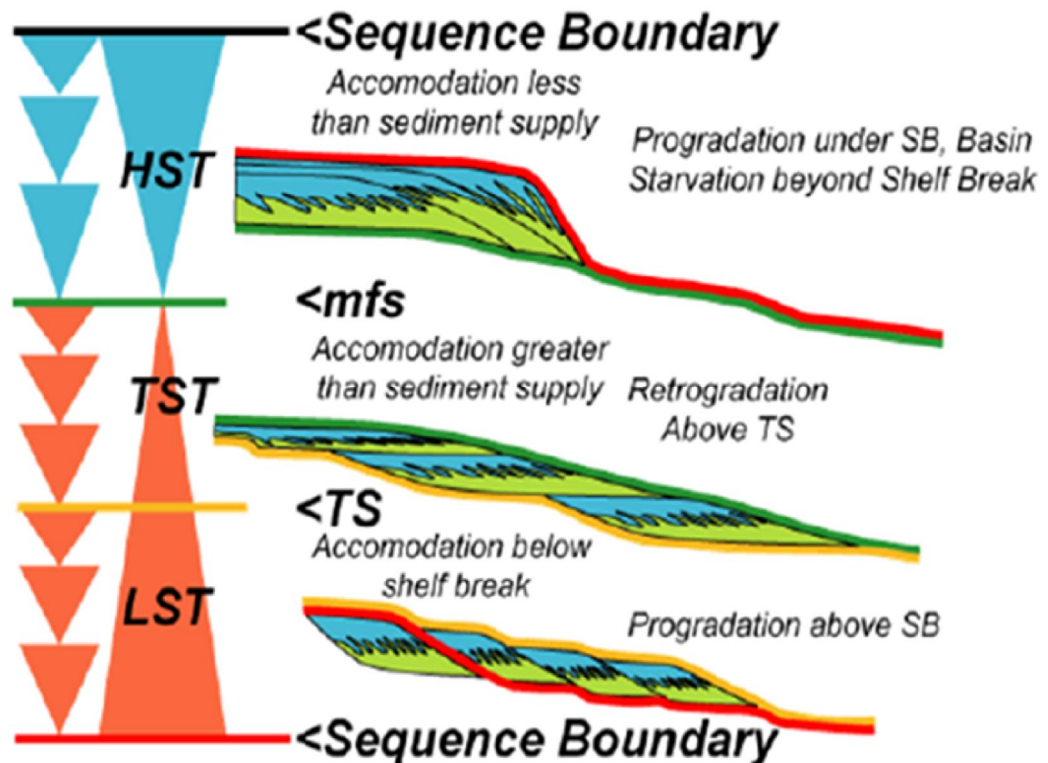


Figure 3.5555: Ideal clastic sequence stacking pattern (Kendall, 2004)

3.3 WELL CORRELATION

The well correlation was carried out in a Petrel software window with surfaces (MFSs and SBs) of same geologic age delimited in the OGBO field. Marine Flooding surfaces were the best markers or datum on which the correlation cross sections were exhibited Beka and Oti (1995). Correlation was arrived at to determine lateral continuity or discontinuity of facies, thereby aiding reservoir studies in the field. The determined MFSs and SBs were dated with marker shales (P and F zones) and by correlation with the Niger Delta Chronostratigraphic Chart (Figure 3.3 and 3.33, 3.4 and 3.5). Relative ages of the surfaces mapped across the fields were determined using the provided biostratigraphic report and correlated with the established works on the study area. The biozone records obtained from the wells were the palynological and foraminiferal zones popularly designated to as the P-Zones and F-Zones. Variety of pollen zones (P-Zones) and fauna zones (F-Zones) were recognized.

3.4 RESERVOIR PETROPHYSICAL ANALYSIS

3.4.1 PETROPHYSICAL ANALYSIS

This involves the use of empirical formulae to estimate the petrophysical properties of the D4100, C4000 and B5000 reservoirs. The reservoirs which were identified through the use of the electrofacies signatures were further characterized quantitatively to arrive at these petrophysical parameters, which include: volume of shale, formation factor, porosity, water saturation, permeability. Etc. Some of these Parameters of the reservoirs were derived from the log (Figures 3.2 and 3.22) which includes:

3.4.1.1 VOLUME OF SHALE: This was derived from the gamma ray log first by determining the gamma ray index IGR, Schlumberger (1985)

$$I_{GR} = (GR_{log} - GR_{min}) / (GR_{max} - GR_{min}) \quad (1)$$

Where IGR = gamma ray index; GRlog = gamma ray reading of the formation; GRmin =

minimum gamma ray reading (sand baseline); GRmax = maximum gamma ray reading (shale baseline).

For the purpose of this project work, Larionov (1969) volume of shale formula for tertiary rocks was used.

$$V_{sh} = 0.083(2^{3.7 \cdot IGR} - 1) \quad (2)$$

3.4.1.2 NET-TO-GROSS RATIO (NTG): This refers to the proportion of clean sand to shale within a reservoir unit. The gross sand is the whole thickness of the reservoir; the non-net sand is the shaly sequences within the whole reservoir thickness; the net sand is thus obtained by subtracting the non-net sand from the gross sand. The Net-to-gross ratio reflects the quality of the sands as potential reservoirs. The higher the NTG value, the better the quality of the sand.

$$NTG = \text{Net sand} / \text{Gross sand} \quad (3)$$

$$\text{Net sand} = \text{gross sand} - \text{shaly intervals} \quad (4)$$

3.4.1.3 TOTAL POROSITY (Φ_T): This was calculated from the density porosity log using the equation below:

$$\Phi_T = (m_a - b) / (m_a - f) \quad (5)$$

Where m_a = matrix density which is taken to be 2.65g/cc for sandstone, b = the bulk density read directly from the log, f = the fluid density which is taken to be 1 for gas and 0.87 for oil.

3.4.1.4 EFFECTIVE POROSITY: This is usually based on an adjustment of total porosity by means of an estimated shale volume.

$$\Phi_{eff} = \Phi_{total} - (V_{sh} * V_{sh}) \quad (6)$$

Where Φ_{eff} = effective porosity, Φ_{total} = total porosity, V_{sh} = log reading in a shale zone, V_{sh} = volume of shale

3.4.1.5 WATER AND HYDROCARBON SATURATION: The water and hydrocarbon saturation are much related. In this research work, water saturation was derived using Archie's (1942) equation for water saturation in uninvaded zone, Archie (1942):

$$S_w = [(a * R_w) / (R_t * m)]^{1/n} \quad (7)$$

$$S_h = 1 - S_w \quad (8)$$

Where S_w = water saturation; R_w = resistivity in the water leg (that is resistivity of formation water); R_t = true formation resistivity derived from the deep induction resistivity log; Φ = porosity; n = saturation exponent usually taken as 2.0; m = cementation factor; a = tortuosity.

3.4.1.6 IRREDUCIBLE WATER SATURATION: sometimes called critical water saturation. It defines the maximum water saturation that a formation with a given permeability and porosity can retain without producing water.

$$S_{wirr} = (F/2000)^{1/2} \quad (9)$$

$$F = 0.81 / \Phi^2 \text{ (in most sandstone reservoirs)} \quad (10)$$

Where F = Formation factor

3.4.1.7 BULK VOLUME OF WATER (BVW): This is the product of water saturation and porosity corrected for shale, Adepelumi et al (2011).

$$BVW = S_w * \phi_{eff} \quad (11)$$

Asquith and Krygowski (2004)

Where BVW = bulk volume of water; S_w = water saturation; ϕ_{eff} = effective porosity

If values for BVW calculated at several depths within a formation are coherent, then the zone is considered to be homogeneous and at irreducible water saturation. Therefore, hydrocarbon production from such zone should be water free, Morris and Biggs (1967).

3.4.1.8 PERMEABILITY: measure of the ease with which a fluid (gas, oil or water) flows through connecting pore spaces of reservoir rock. It is very important in predicting the rate of production from a reservoir.

$$K = 0.136 (4.4/S_{wirr}^2) \phi \quad \text{Timur, 1968} \quad (12)$$

Where K = permeability (millidarcy); ϕ = porosity; S_{wirr} = irreducible water saturation)

3.4.1.9 FLUID TYPE: Delineation of fluid type contained within the pore spaces of formation is achieved by the observed relationship between the Neutron and Density logs. Presence of hydrocarbon is indicated by increased Density log reading which allows for a cross-over. Gas is present if the magnitude of cross-over, that is, the separation between the two curves is pronounced while oil is inferred where the magnitude of cross-over is low, Asquith and Krygowski (2004).

After the petrophysical attributes were estimated, the reserves for the three horizons mapped were estimated. The parameters used were derived from both the logs and the seismic sections as follows:

3.4.1.10 VOLUMETRIC EQUATION

$$= \text{Area} * \text{thickness} * (1 - S_w) * \phi * NTG \quad (13)$$

3.4.1.11 OOIP

$$= (7758 * \text{thickness of oil column} * SH * \text{NTG}) \quad (14)$$

Where OOIP = original oil in place, SH = hydrocarbon saturation

3.4.1.12 STOOIP

$$= (OOIP * FVF \text{ oil}) \quad (15)$$

Where STOOIP = stock tank original oil in place, FVFOil = formation volume factor (oil)

3.4.1.13 RESERVE (oil)

$$= (STOOIP / RF) \quad (16)$$

Where RF = recovery factor

3.4.1.14 OGIP

$$= (43,560 * \text{area} * \text{thickness of oil column} * SH * \text{NTG}) \quad (17)$$

Where OGIP = original gas in place

3.4.1.15 STOGIP

$$= (OGIP * FVF \text{ gas}) \quad (18)$$

Where STOGIP = stock tank original gas in place, FVFgas = formation volume factor (gas)

3.4.1.16 RESERVE (gas)

$$= (STOGIP / RF) \quad (19)$$

3.5 SEISMIC SECTION

A 3Dimensional pre-stack seismic volume in SEG-Y format covered by a grid of 3D seismic data acquired, processed and reprocessed in early 1999 and 2009 respectively approximately 300 Km² were used for this study. The data set has a bin size of 25m by 25m in both inline

and crossline directions. The quality of the data varies from very good at shallow levels, dropping rapidly to poor quality images at depth below approximately 2.5 seconds and beneath major faults. Faults were recognized from the seismic section by distinct discontinuity or abrupt jump of seismic reflection events. By using the synthetic seismogram created, the tops of the sands identified on the logs were tied to the seismic reflection events on the seismic sections. Horizons were interpreted based on the tops and were traced through the whole seismic volume. The horizons were interpreted on every 10 inlines and 10 cross-lines. Attribute maps were generated. The RMS amplitude attribute was extracted for each horizon. Time structure maps were produced for each horizon. The time maps were then converted to depth maps using a simple velocity model. Check shot data was used for 2-way time interpretation that tied both well logs and seismic data together. Petrel software was used for the interpretation.

CHAPTER FOUR

RESULTS, DATA ANALYSIS AND INTERPRETATIONS

4.1 LITHOFACIES AND DEPOSITIONAL ENVIRONMENTS

The lithology interpretation of the well logs across the six wells studied indicates predominantly sand and shale. The vertical and lateral facies changes of the area are largely the function of the variability in the sand and shale thicknesses known as sand percentage. Sand percentage was adopted as one of the dependable ways of expressing lithofacies and this was calculated from gamma ray log per hundred feet (100ft) interval. However, Wornardt (1994) proposed the various sand percentages that can indicate the different lithofacies. Lithofacies interpreted from sand percentages and well logs can be used for reservoir characterization, burial history and lithofacies zonation. The stratigraphic column of the wells in the area is divided into four lithofacies, namely: (1) Coarse Grained Basal Sandstone Facies; (2) Mudrock Facies; (3) Heterolithic Facies; (4) Sandstone/ Shaly Facies.

4.1.1 COARSE GRAINED BASAL SANDSTONE FACIES (FACIES 1)

This facies consists of combined and separated sharp-based fining upward sand bodies characterized by blocky to bell-shaped gamma ray log motif without much separation on the neutron-density logs (Figure 4 and 5). The sand units are locally separated by thin bands of mudstone/shale and are without marine fauna. The facies found to exist in wells OGBO 019STI, 038, 046, 036 and 056, and absent in 005 well. Based on the Log motif character alone, this facies may be interpreted as fluvial channel deposits based on these forms. These channel deposits is deposited in a coastal plain setting landward of the tidal zone (MaCabe et al., 1992). The blocky log pattern is characteristic of incised valley fills (Allen and Posamentier., (1993). The lack of serration in the gamma ray log signature and absence of marine fauna indicate minimal or complete absence of tidal influence.

OGBO WELL 019 STI

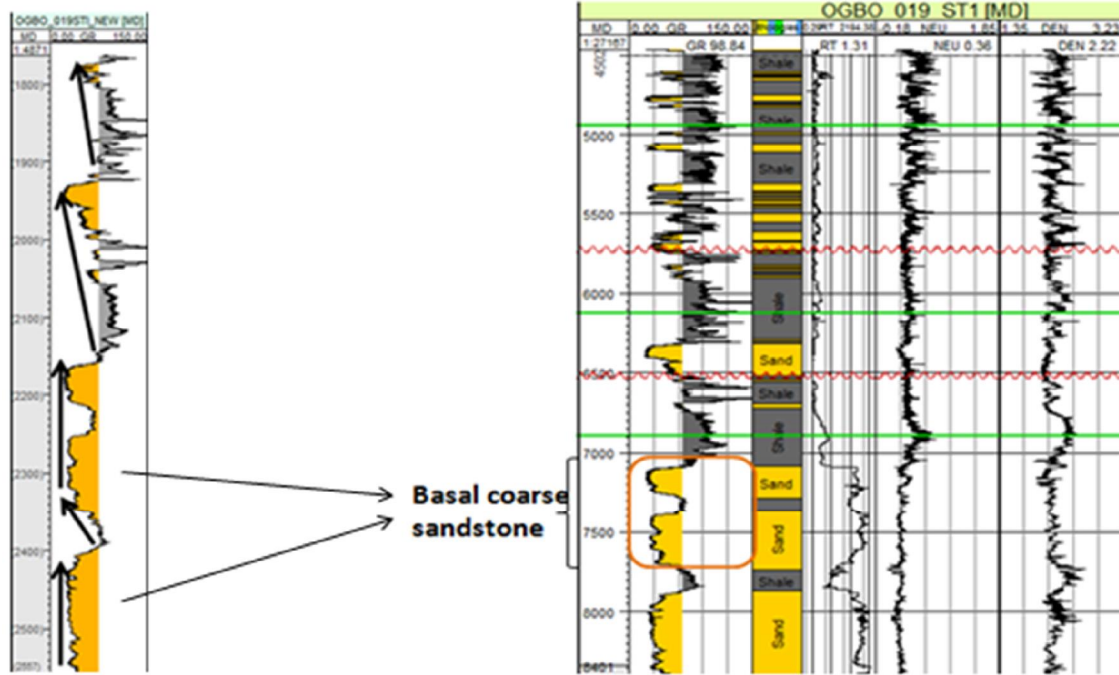


Figure 4.: Coarse grained basal sandstone facies represented by blocky gamma ray log in well OGBO 019ST1

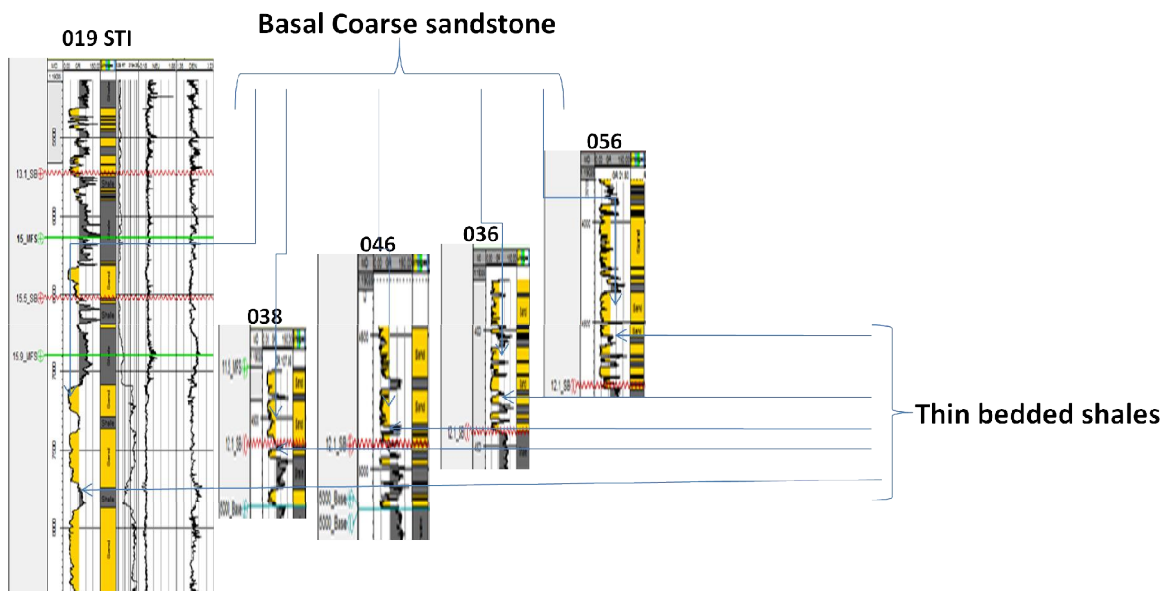


Figure 5: Course grained basal sandstone facies represented by blocky gamma ray logs enlarged

4.1.2 MUDROCK FACIES (FACIES 2)

This facies has great number of shale units with thin siltstone intercalations showing a retrogradational parasequence pattern (Figures 6 and 7). However, the facies also showed a property of high frequency and diversity of foraminifera particularly those of outer neritic (ON) to bathyal (BA) depositional environments. The predominant shale units with occasional thin siltstones and foraminifera abundance indicates deposition in the offshore setting.

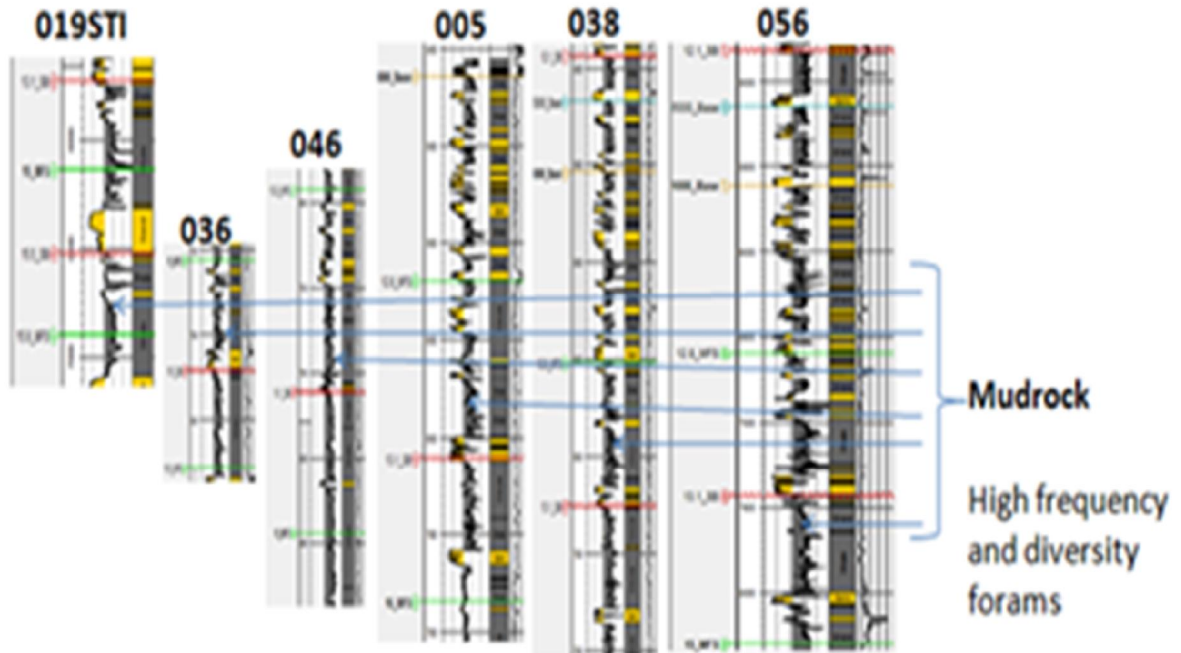


Figure 6: Mudrock facies represented by high gamma ray log signature enlarged (high frequency and forams diversity)

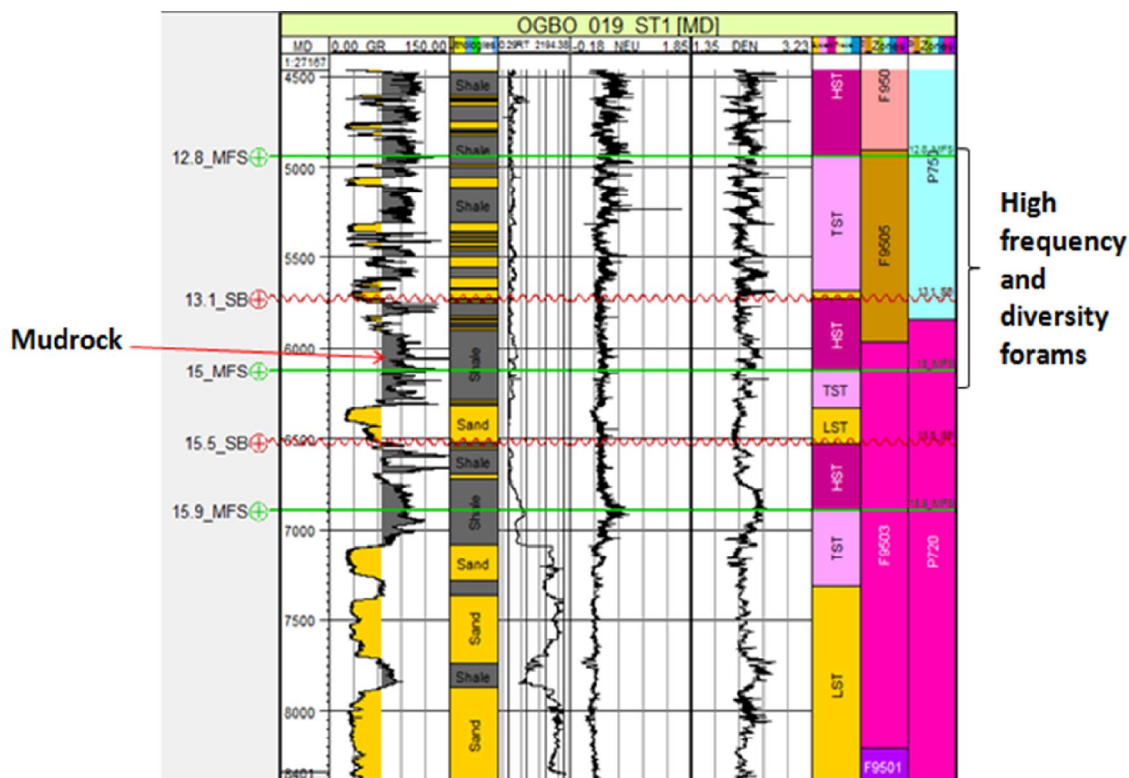


Figure 7: Mudrock facies represented by high gamma ray log signature in well OGBO 019ST1 (high frequency and forams diversity)

4.1.3: HETEROLITHICS FACIES (FACIES 3)

This facies is interpreted as mudstone and sandstone heteroliths. The sandstone unit is delineated as upward cleaning units on the gamma ray log trend. The crescent trend in the gamma ray log (Figures 8, 9, 10 and 11) show a cleaning up trend overlain by a dirtying up trend without any sharp break. This facies features indicate inner- middle neritic (IN-MN) depositional environments and it may be inferred upper shoreface deposits. Crescent log pattern (Figure 12) is without regard to specific details the result of waning and waxing clastic sedimentation rate Emery and Myers., (1996). The serrated nature of the gamma ray log signature is revealing clearly of wave and tide activity Emery and Myers., (1996) and the heteroliths likely reflect deposition from waning storm generated flows, Boggs (1995). The muddy portion which is characterised by high gamma ray values with biofacies bathymetry in the Neritic environment expressed storm emplacement or inter-storm pelagic sedimentation Walker and Plint.,(1992).

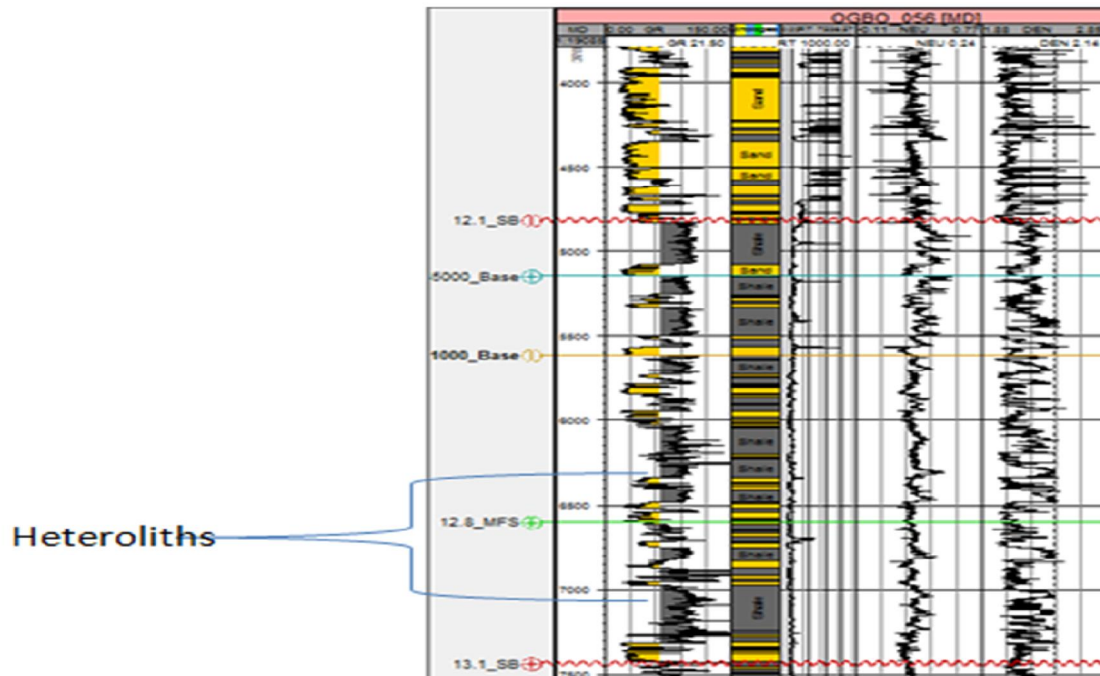


Figure 8: Heterolithic facies encountered in OGBO 056 well

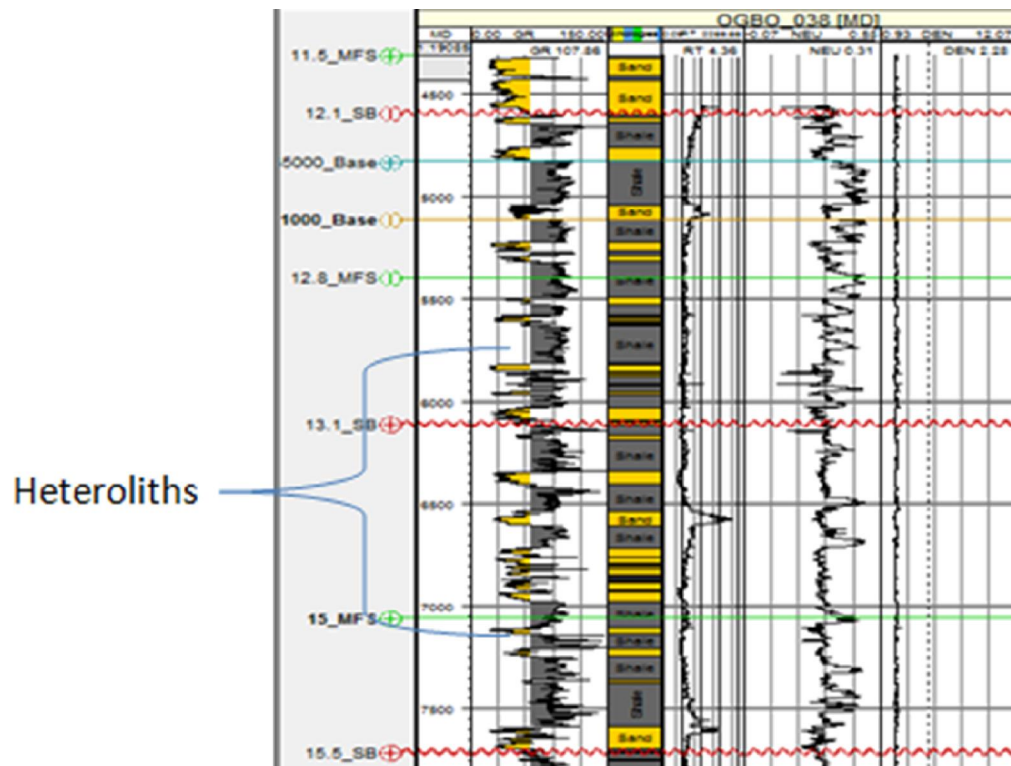


Figure 9: Heterolithic facies encountered in well in OGBO 038 well

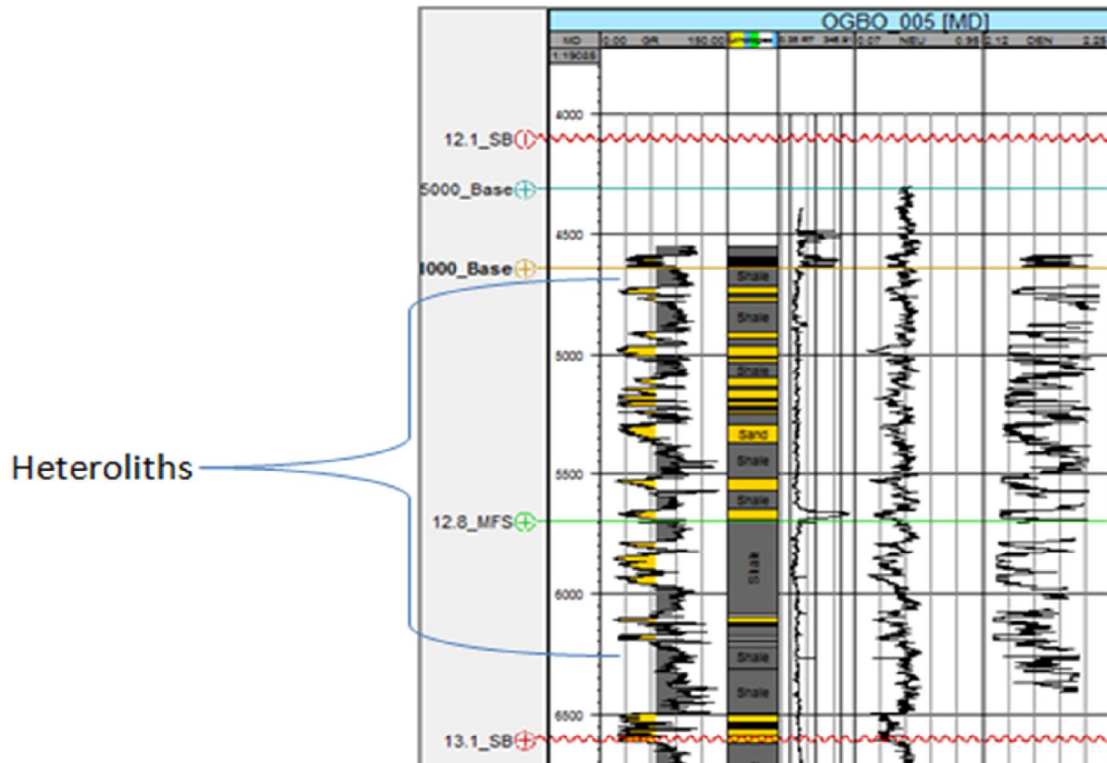


Figure 10: Heterolithic facies encountered in OGBO 005 well

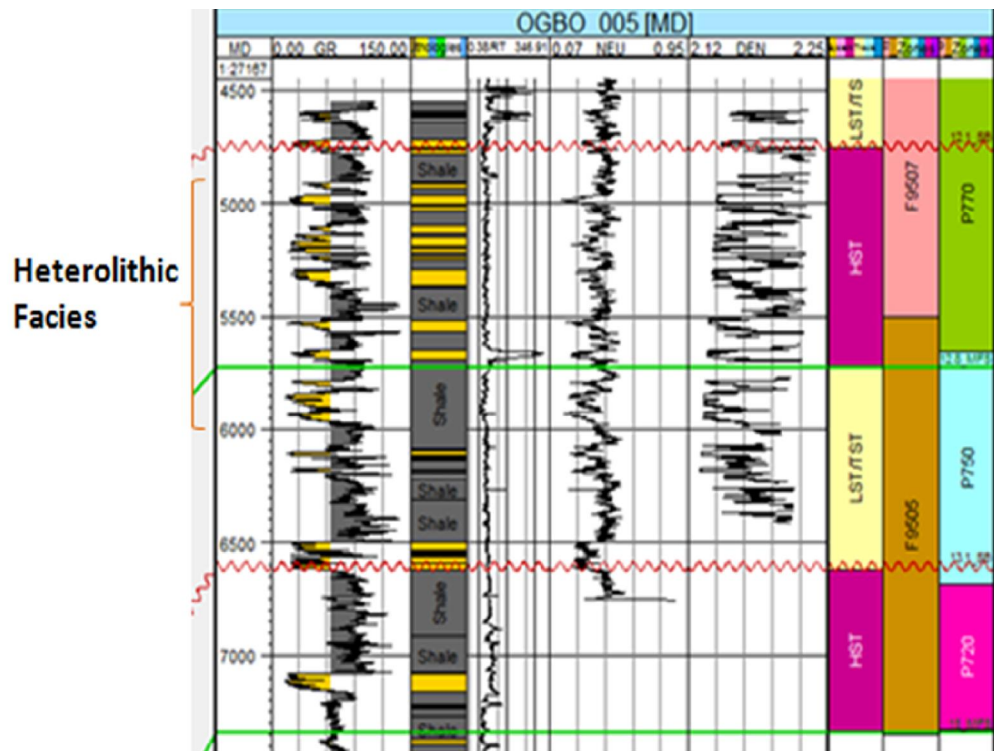


Figure 11: Heterolithic Facies encountered in OGBO 005 well with Biofacies data

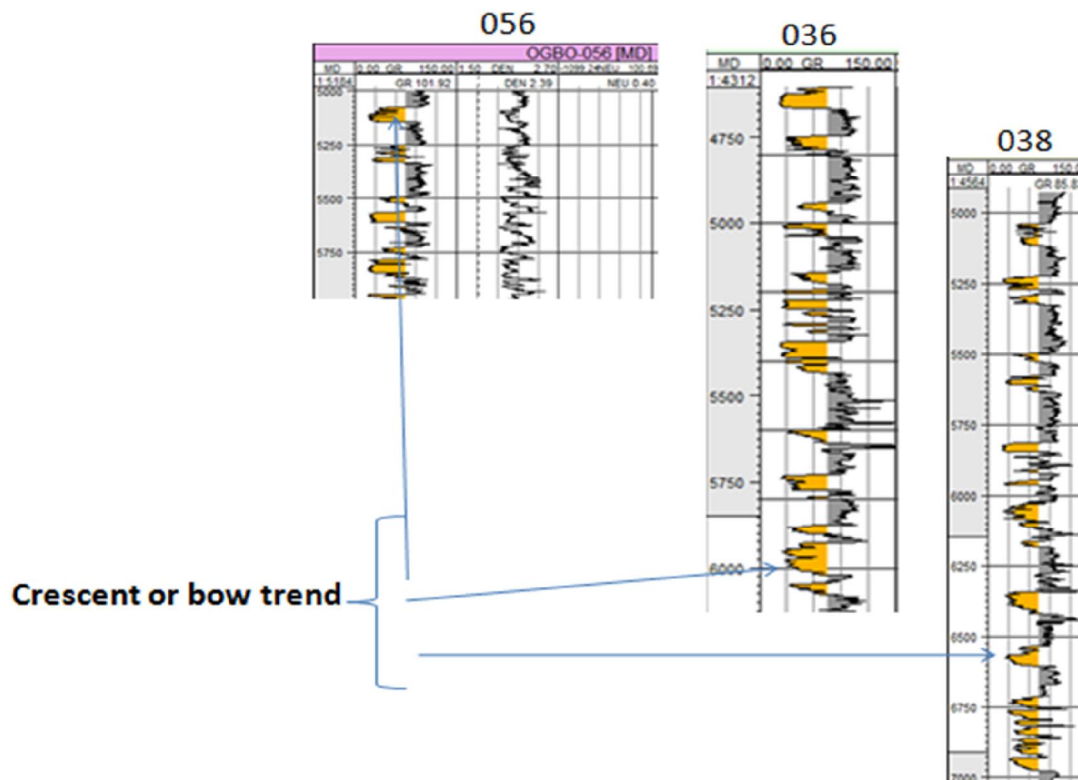


Figure 12 Crescent or bow trend expressed in OGBO 056, 036 and 038 wells

4.1.4 SANDSTONE/SHALY FACIES (FACIES 4)

The sandstone/shaly facies (Figures 13 and 14) is identified by its fine-medium grained sandstones and shale/mudstone interbeds. It consists of saw-toothed funnel shaped gamma ray log pattern and sometimes saw-toothed bell to blocky shaped patterns at some intervals. These intervals are also characterised by high value in neutron and density porosity log with not much separation. The biofacies information suggests that the intervals exhibit low frequency and low diversity of foraminifera belonging to the Inner-Outer Neritic (IN-ON) depositional environment. This facies may be interpreted as tide dominated estuarine deposits based on the cyclic alternation of mudstone and sandstones presence. From the log motif, each funnel shape is characterized as a succession of coarsening upward from mud to shallow/ marginal marine sandstones. Rhythmic alternation of high gamma ray log response and serrated funnel, bell and blocky gamma ray log motif resulted from frequent fluctuations in current strength which is characteristic of tidal processes. The successions are inferred to have been deposited in a prograding, estuarine environment, believed to be deposits of beach sands, barrier bars or alluvial fans. The alluvial fans show thick bedded sandstone indicating

aggrading pattern at some interval. The biofacies data showed low diversity forms at shallow water depths within the sandstone units and increase in foraminiferal assemblages pointing towards progressive deeper water bathymetry within the mudstone units. Sandstone/shaly facies occurred in all the wells OGBO 019STI, 038, 046, and wells OGBO 005, 036, and 056 in dip section of the field.

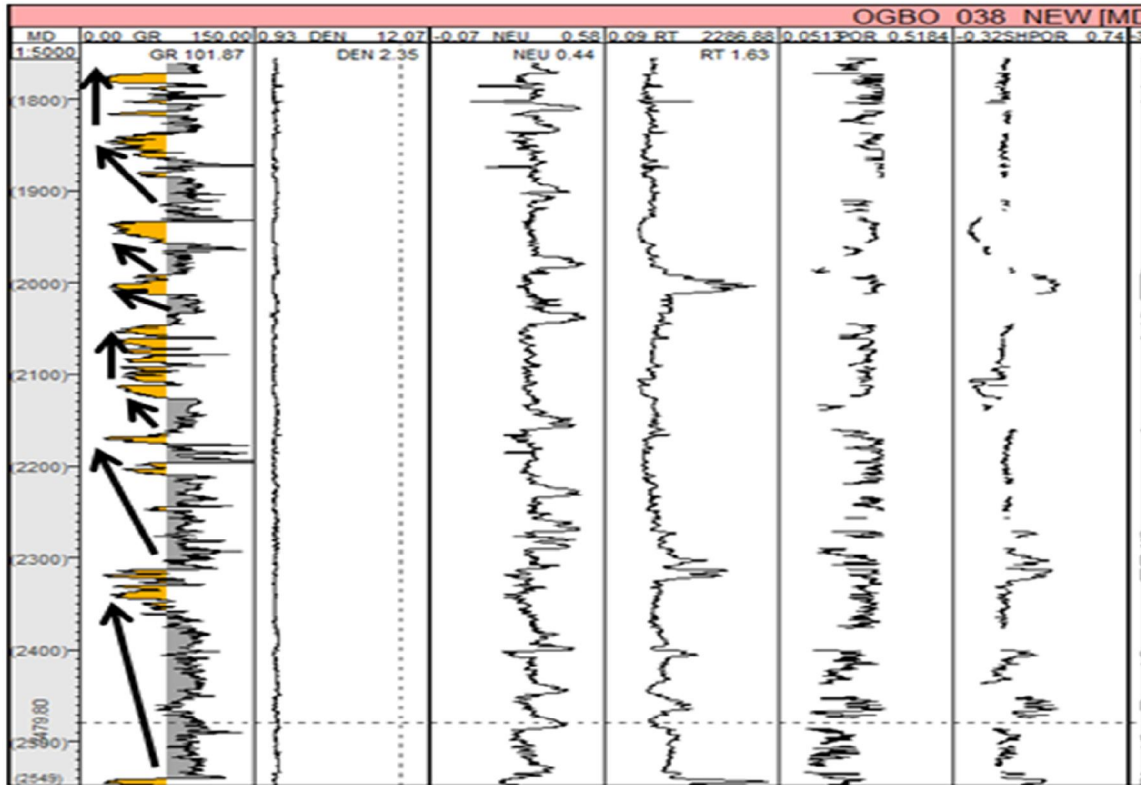


Figure 13: Sandstone/ shaly facies defined by funnel-shaped gamma ray logs

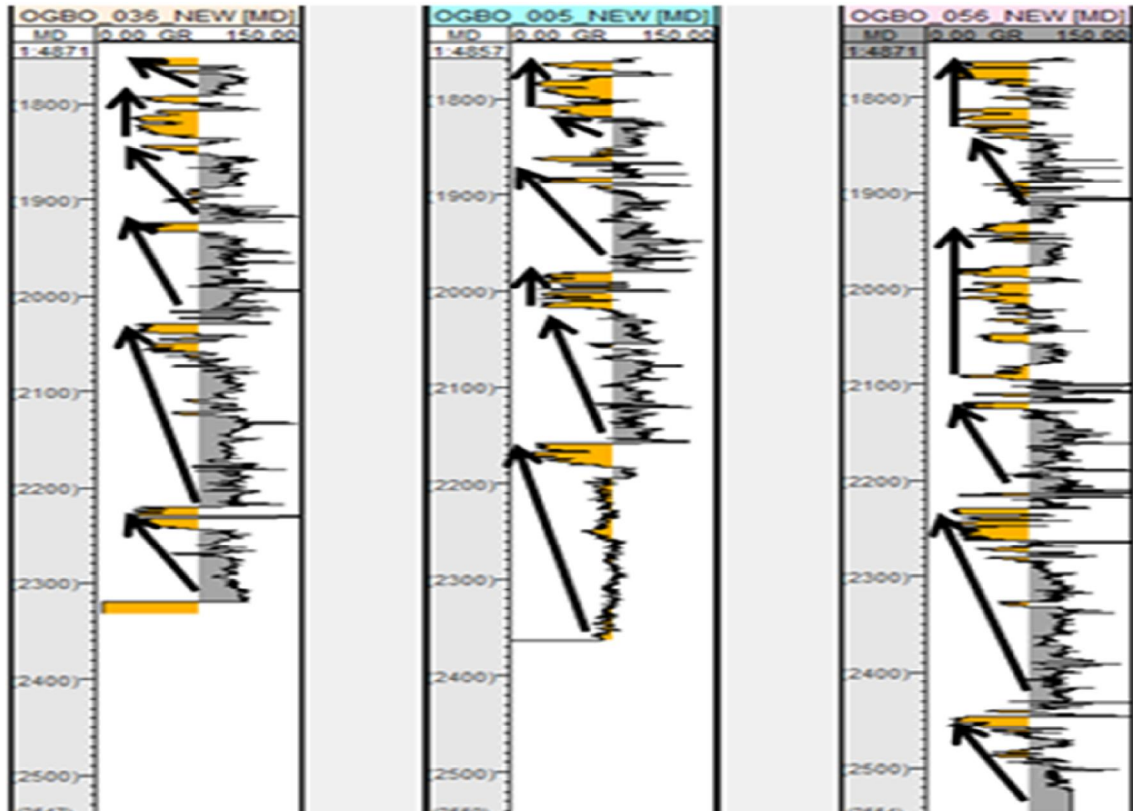


Figure 14 : Sandstone/shaly facies defined by funnel-shaped gamma ray logs

4.2 ENVIRONMENT OF DEPOSITION (EOD) DELINEATION AND INTERPRETATION

4.2.1 ENVIRONMENT OF DEPOSITION DELINEATION BY INTEGRATION APPROACH

Making meaningful interpretation for EOD makes it necessary to adopt variety approach and minimize speculation (Figure 15).

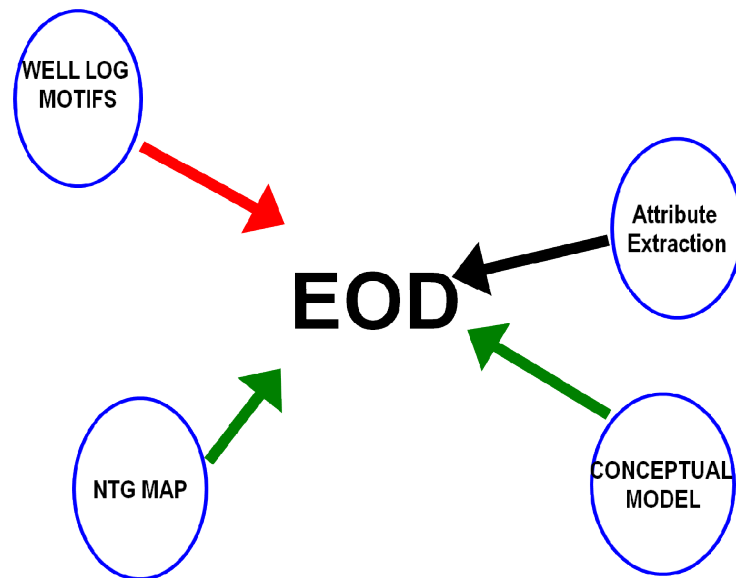


Figure 15: Integrated workflow for environment of deposition delineation

Conceptual Model approach to environment of deposition delineation

(Figures 15 and 16) Conceptual sedimentary depositional model, Bevis (2014) with this schematic guide revealed the transport system of the sediments and their associated sedimentary structures. The sediments moved from mainland, floodplain, distributary channels, fluvial delta plain, delta front, pro delta to the shelf. The associated structures are concretions and bands for prodelta zone, tabular crossbedding for channel, trough crossbedding and ripple marks for distributary mouth bar and flaser bedding for distal bar

environment. Their sand capacity size decreases as the transporting energy decreases, the geometry of the sediment and the surrounding environment. From the shoreface depositional model (Figure 16) comprising Beach backshore zone, Back beach zone with eroded storm berm with eroded clasts structures to Foreshore (swash) zone with beachrock cement with planar wedge sets structures down to Shoreface zone (lower shoreface having bioturbation presence and upper shoreface with trough crossbedding structure and wave breaker bars and finally to Offshore zones with mainly turbidite sedimentary structures.

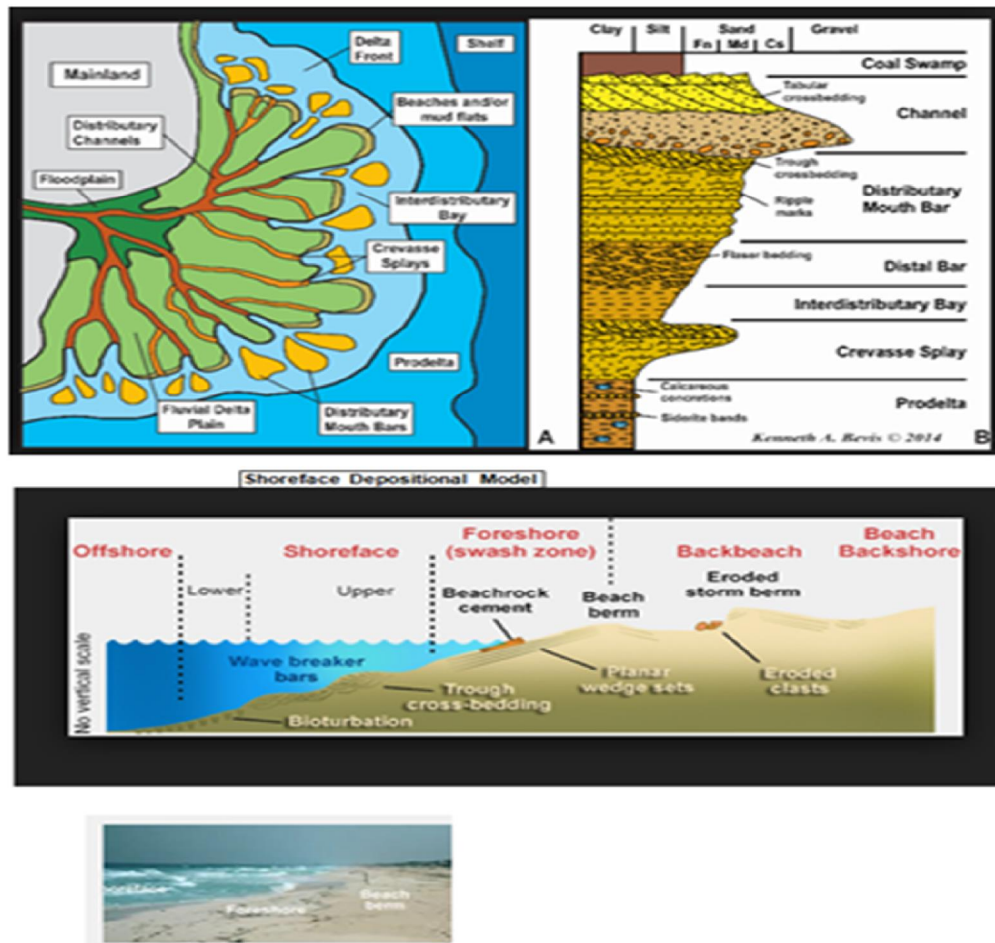


Figure 16: Conceptual sedimentary depositional model, Bevis (2014)

Table 2 below represents the summary of the depositional environments from well log motifs of various electrofacies analysis from Cant (1992) as shown in Gonzales (2003) and Kendall (2008), inferred reservoir different sand shapes and their depth intervals adopted for OGBO wells from 019STI to 046 in the strike direction to 005 to 056 in the dip direction.

Table 2 represents the summary of the depositional environments from well log motifs of various electrofacies analysis from Cant (1992) as shown in Gonzales (2003) and Kendall (2008)

Well	Cant (1992) as shown in Gonzales (2003)	Kendall (2008)	Inferred Reservoir	Depth (Ft)	Sands	Shape
OGBO 019STI	Cylindrical Shaped: (Aggrading; even block with sharp top and base) Clean, No Eolian, braided, fluvial, carbonate shelf, reef. Irregular Shaped: (Aggrading; Saw teeth) (Mixed Clean and Fluvial flood plain, carbonate slope, clastic slope, canyon fill.	Cylindrical Shaped: (Aggrading; even block with sharp top and base) Eolian, braided, fluvial distributary channel-fill, submarine, canyon-fill, carbonate shelf margin, reef, evaporate fill of basin. Serrated Shaped: (Aggrading; Saw teeth) Fluvial floodplain, storm-dominated shelf, and distal deep marine slope.		7100-7180.	A1 -A4,	Cylindrical
				7190-7800.	A5-A8	Irregular/Serrated
				7850-8400.		
OGBO 038	Funnel Shaped: (Prograding; Coarse up and sharp top) Abrupt Top Coarsening. Crevasse splay, distributary mouthbar, clastic strand plain, Barrier Island, shallow marine sheet, sand-stone, carbonate shoaling upward sequence, submarine fan lobe.	Funnel Shaped: (Prograding; Coarse up and sharp top). Crevasse splay, river mouth bar, delta front, shoreface, submarine fan lobe, change from clastic to carbonates. Bell Shaped: (Retrograding; fine up and sharp base). Fluvial point bar, tidal point bar, deep tidal channel fill, tidal flat, transgressive shelf sands.		5000-5100.	B1-B3	Irregular/Serrated
				6500-6700.	B4Base	Funnel
					B4	Irregular/Serrated
				7500-7700.	Middle	
					B4 Top	Symmetrical
					B5	
					B6	Symmetrical
				B7-B12	Cylindrical	
B13	Irregular/Serrated					
B14						

Table 2 Continues

Well	Cant (1992) as shown in Gonzales (2003)	Kendall (2008)	Inferred Reservoir	Depth (Ft)	Sands	Shape
	<p>Bell Shaped: (Retrograding; fine up and sharp base) Abrupt Base Fining. Fluvial point bar, tidal point bar, deep sea channel, some transgressive shelf sands.</p> <p>Symmetrical Shaped: (Prograding and retrograding; Hour glass) Irregular. Sandy offshore bar, some transgressive shelf sands, amalgamated coarsening-upward and fining-upward units.</p>	Symmetrical: (Prograding and retrograding; Hour glass).rework offshore bar, regressive to transgressive shore face delta.				
OGBO 046					C1-C6 C7 C8-C13	Irregular/Serrated Bell Irregular/Serrated
OGBO 005				5700-5800. 7100-7250.	D1 D2 D3 D4 D5-D11 D12 D13-D17	Irregular/Serrated Funnel Irregular/Serrated Funnel Irregular/Serrated Funnel Irregular/Serrated

Table 2 Continues

Well	Cant (1992) as shown in Gonzales (2003)	Kendall (2008)	Inferred Reservoir	Depth (Ft)	Sands	Shape
OGBO 036				5560-5570.	E1-E11	Irregular/Serrated
OGBO 056				5500-5570. 6600-6620. 8200-8300.	F1-F10	Irregular/Serrated

LOG SHAPE AND INFERRED ENVIRONMENT

Table 3: Different log motifs for the six correlated wells in OGBO Field

OGBO 019STI	OGBO 038	OGBO 046	OGBO 005	OGBO 036	OGBO 056
Cylindrical. Irregular/Serrated	Irregular/Serrated, cylindrical, bell, symmetrical	Irregular/Serrated, bell	Irregular/Serrated, funnel	Irregular/Serrated	Irregular/Serrated

Table 3 showcased six OGBO wells and their well log motif shapes representative. Deductions from the log motif in interpretation that the inferred environment ranges from retrograding tidal point bar to shoreface tidal inlet and regressive to transgressive shoreface delta sands, Cant (1992) and Kendall (2008).

NTG MAP AT DIFFERENT INTERVALS AND INFERRED ENVIRONMENT

(Figures 17, 18, 19 20 and Table 3) show the analysis of the depositional environments delineation from intervals 4000ft, 5000ft and 6000ft which characterize the inferred reservoir net to gross (NTG) contour mapping at 4000ft, 5000ft and 6000ft depth intervals adopted for OGBO wells from 019STI to 046 in the strike to 005 to 056 in the dip section in the study.

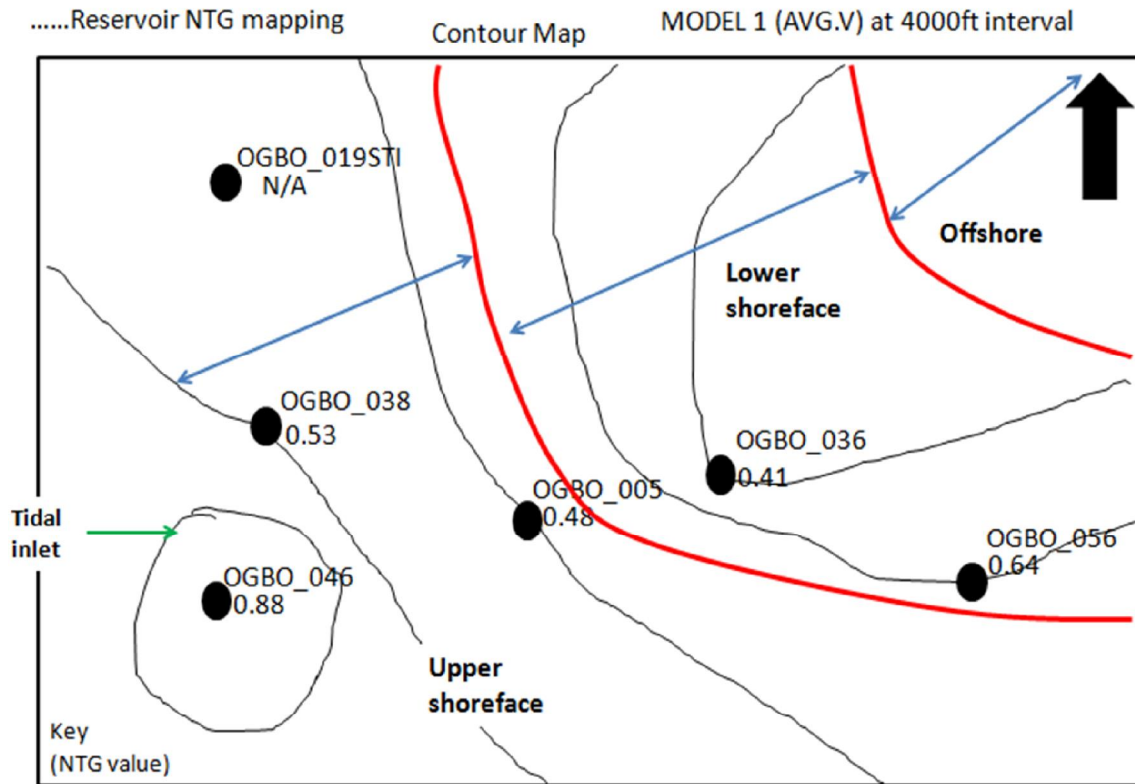


Figure 17: Net to Gross plot at 4000ft interval from six well location and inferred Environment of Deposition Trend

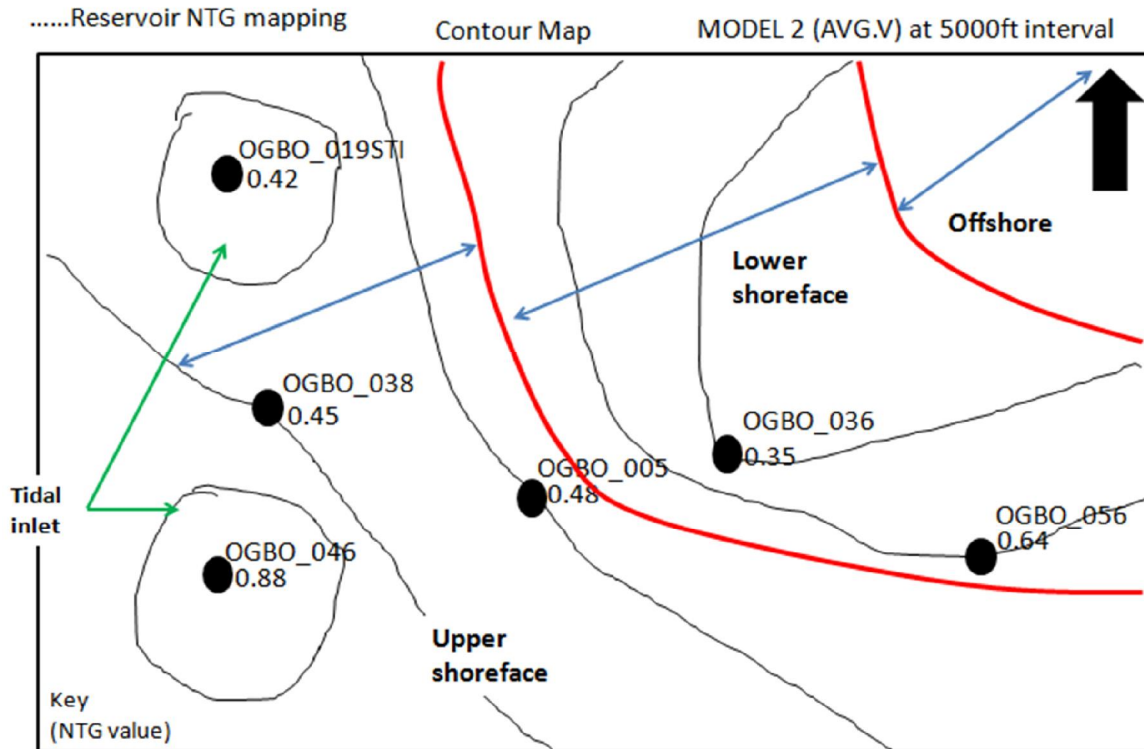


Figure 18: Net to Gross plot at 5000ft interval from six well location and inferred Environment of Deposition Trend

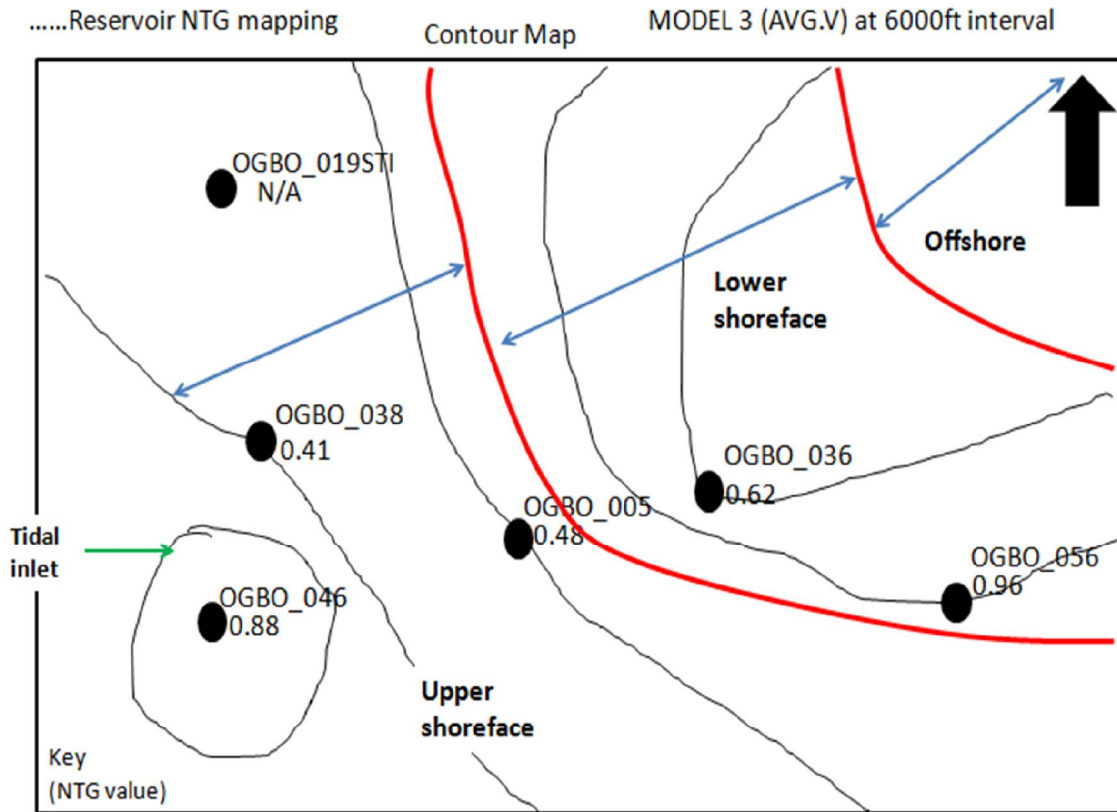


Figure 19 Net to Gross plot at 6000ft interval from six well location and inferred Environment of Deposition Trend

No clear observation was made using the net-to-gross values shown. Reason being that the wells are quite few and not enough statistics to make that interpretation. However, deductions from the three NTG values (map pattern) at intervals 4000ft, 5000ft and 6000ft shows increasing values from SW to NE portion of the area study, based on the contour trend inferred that the environment (typical of a shoreface EOD) ranges as a shallow marine shoreface environment of deposition, starting with progression from upper shoreface (proximal) to offshore (distal) whereas areas with circle are sub-environment within a shallow marine shoreface environment of deposition- Tidal inlet. To ensure that changes in the NTG across wells are related primarily to the depositional process. Higher NTG values are expected for proximal wells along the depositional profile.

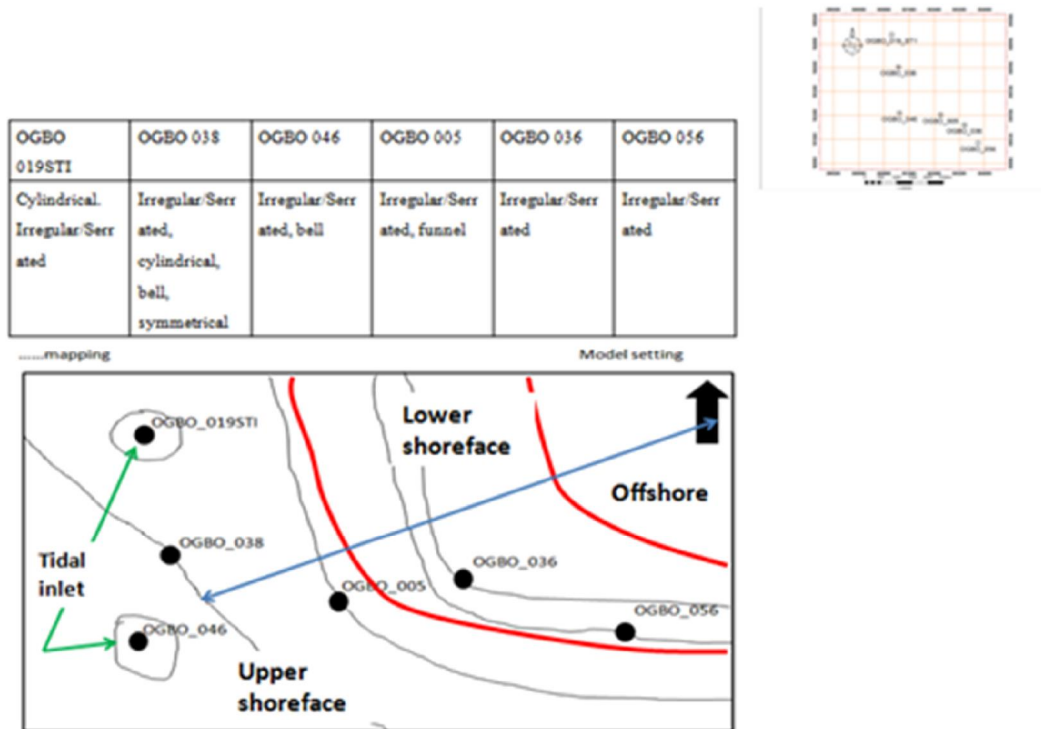


Figure 20: Well location representation of the well log motif interpretation and NTG map Environment of Deposition Trend and the inferred field environment

AMPLITUDE EXTRACTION (AMPLITUDE TREND) AND INFERRED ENVIRONMENT

By placing the log motifs for each well on the RMS map and wells with high NTG (good sand) plot in the high/bright/positive amplitude area correspond to sand presence (Figure 21), while wells with low NTG (poor sand) infer high negative amplitude correspond to presence of shale. Portions with absence or no relationship between high/low amplitude trend and sand presence, inferred the amplitude does not indicate sand presence. This may be due to noise in the seismic data or acquisition artifacts error. Availability of seismic data (attribute extractions) is used to aerially constrain EOD boundaries determined from well data. Hydrocarbon effect was observed to have the most dominant influence on seismic attributes. There was also no systematic change in the map pattern of the attribute that could be related to lithologic variation from one environment to another.

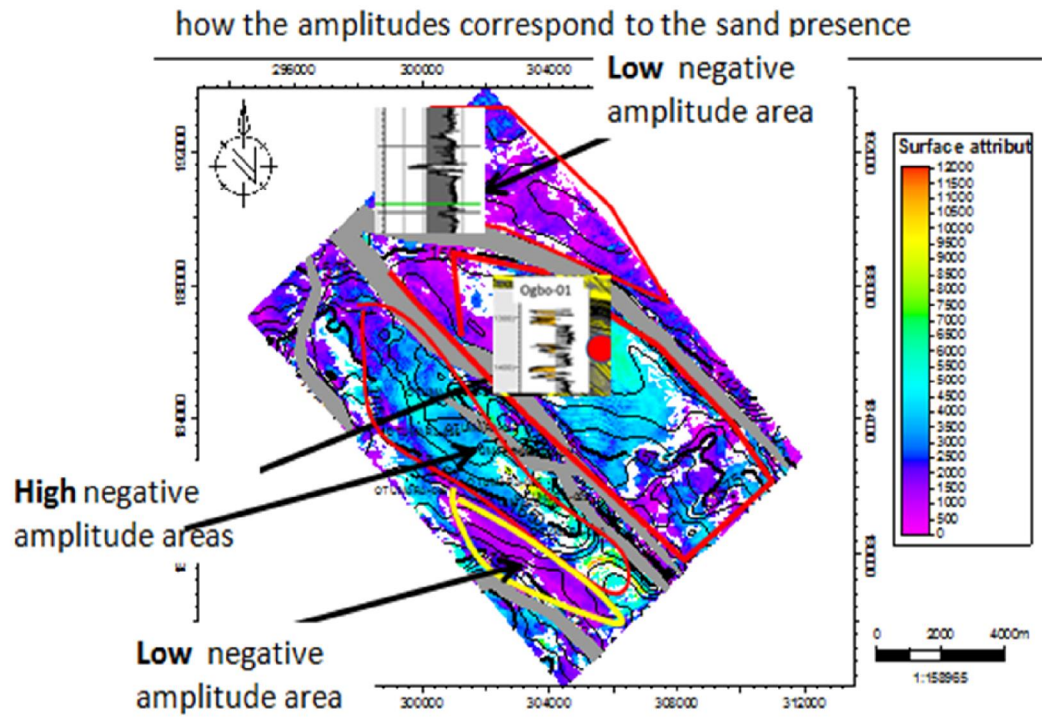


Figure 21: RMS Amplitude map for horizon B5000 surface interval with well log motif and amplitude analysis

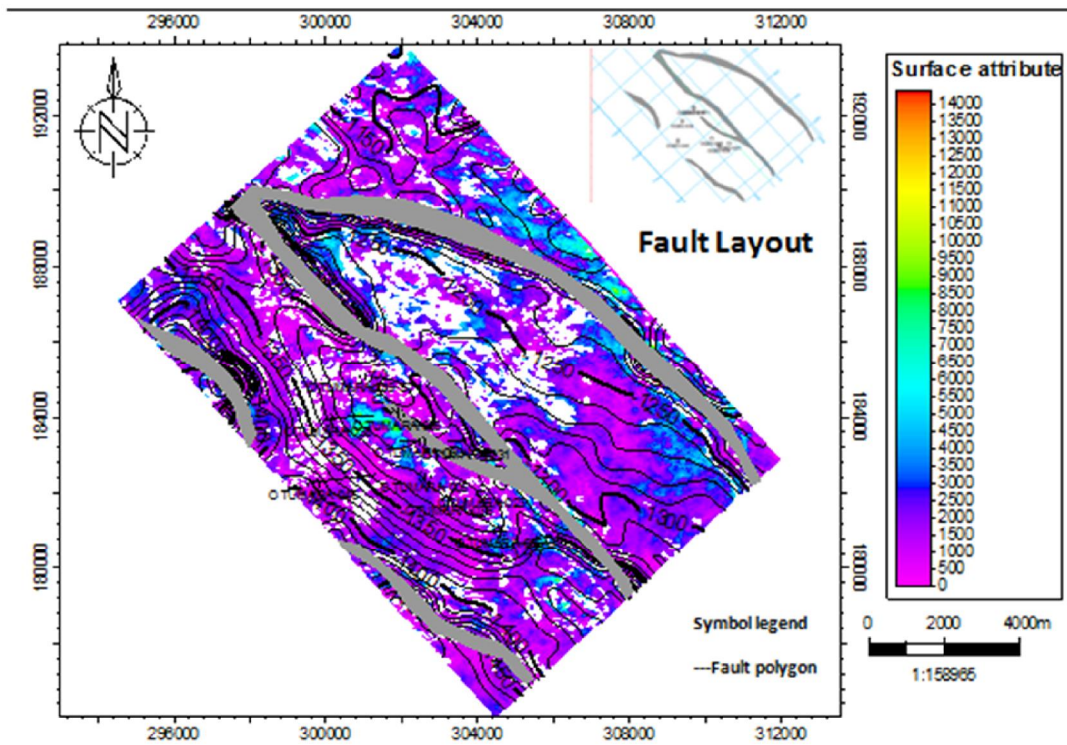


Figure 22: RMS Amplitude map for horizon B5000 surface interval

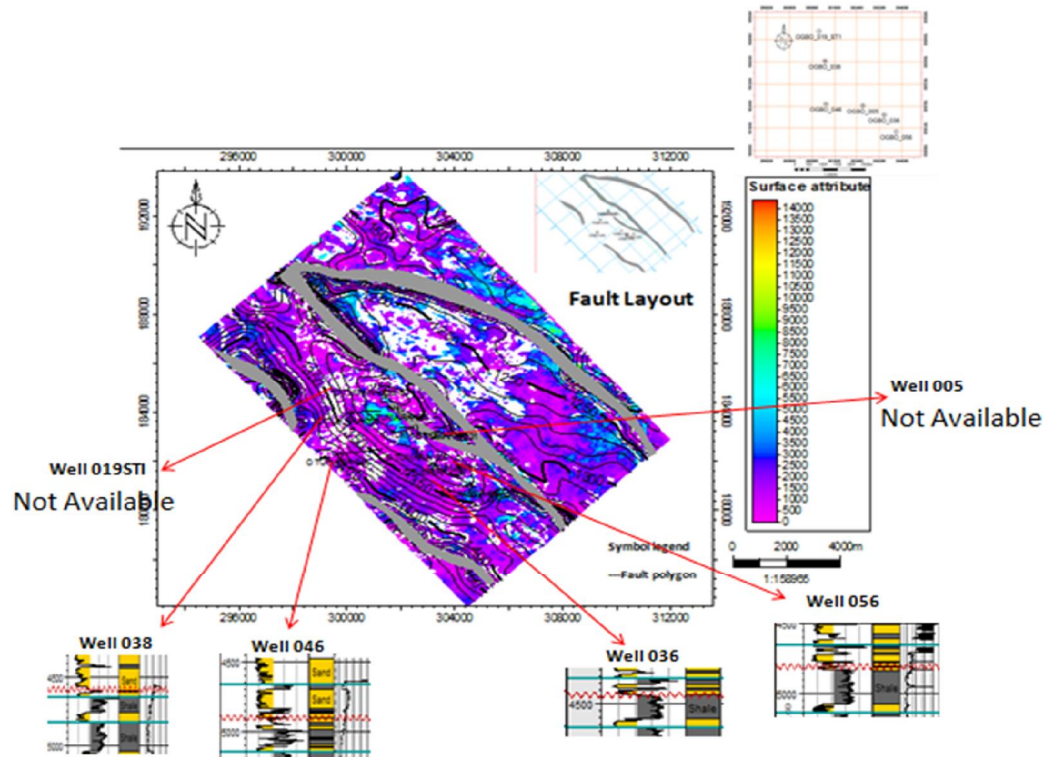


Figure 23: RMS amplitude map for horizon B5000 surface interval- (for amplitude extraction at 4500ft depth gamma ray log motif)

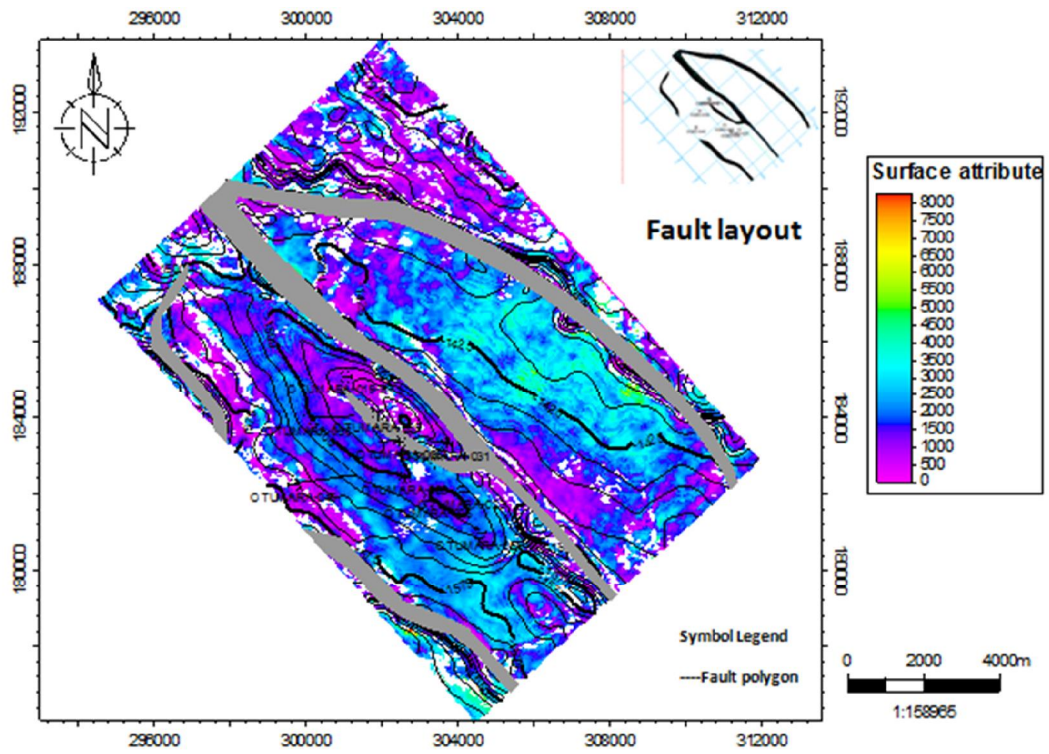


Figure 24 RMS Amplitude map for horizon C4000 surface interval

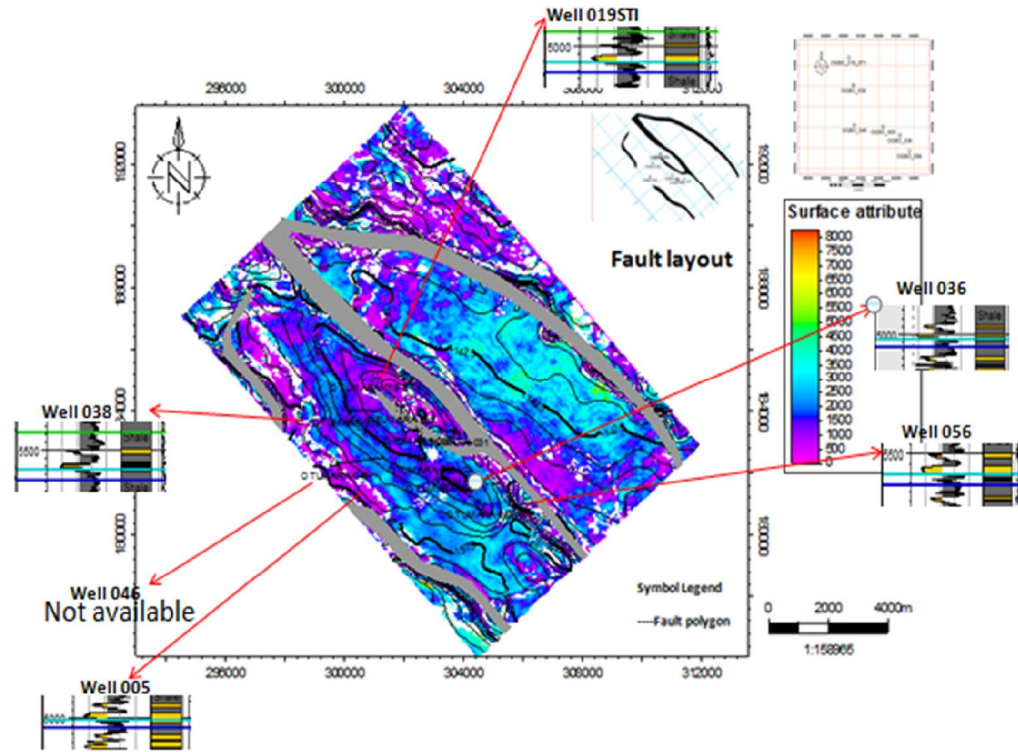


Figure 25: RMS amplitude map for horizon C4000 surface interval- (for amplitude extraction at 5500ft depth gamma ray log motif)

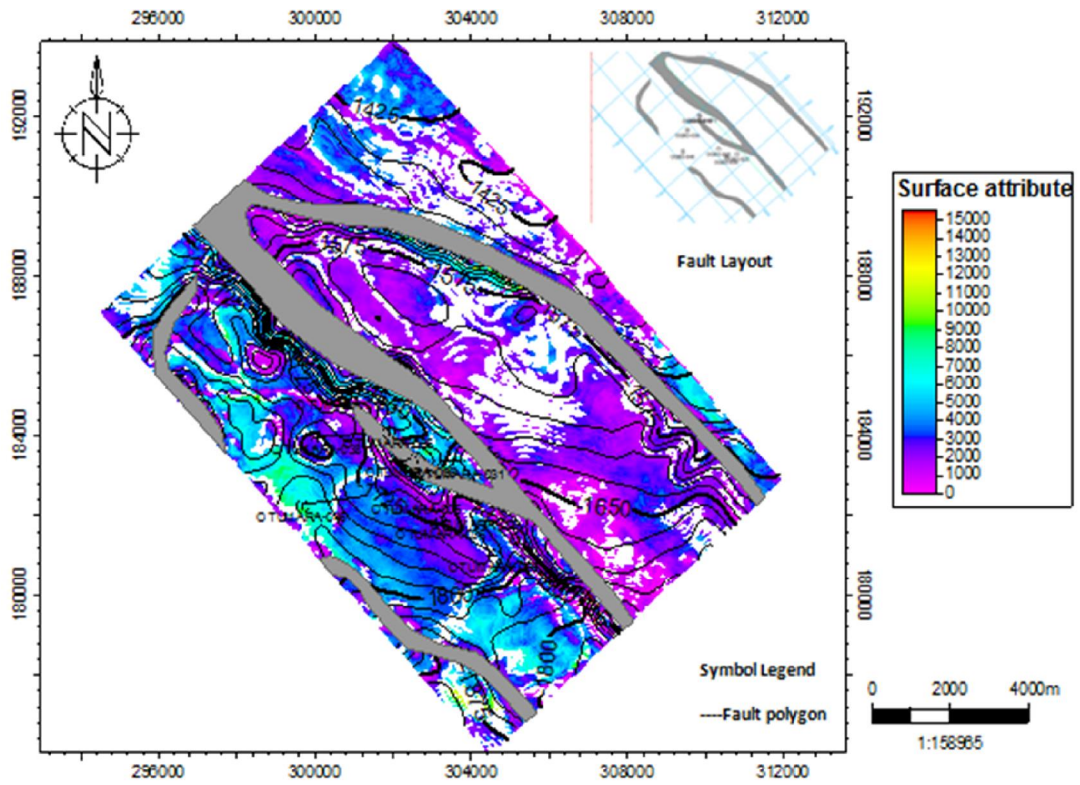


Figure 26: RMS Amplitude map for horizon D4100 surface interval

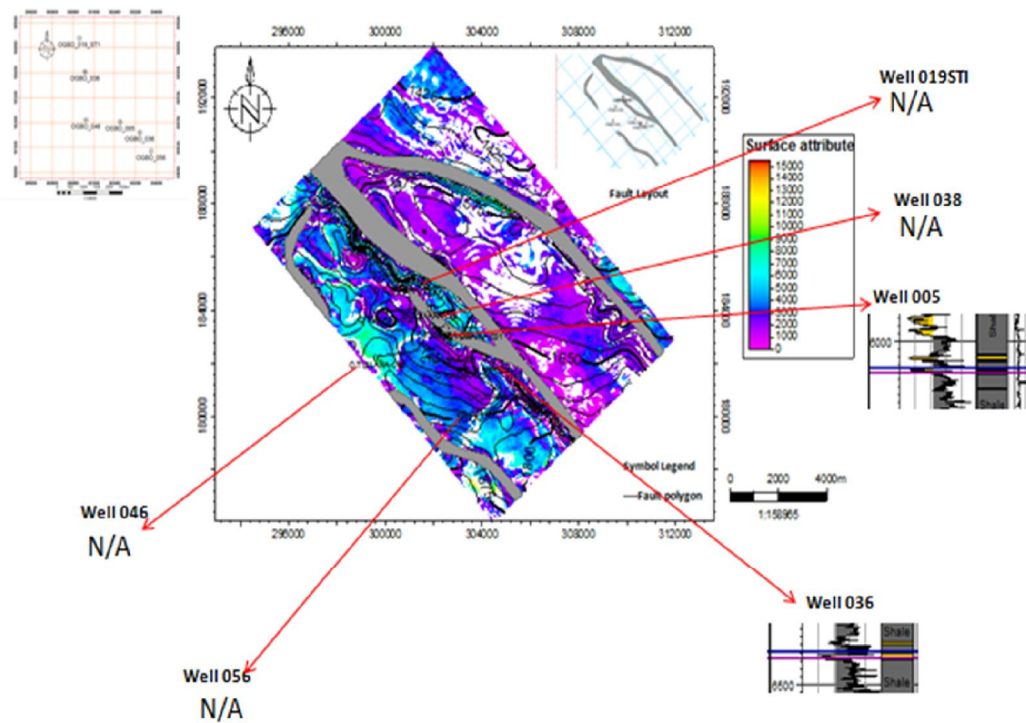


Figure 27: RMS amplitude map for horizon D4100 surface interval- (for amplitude extraction at 5500ft depth gamma ray log motif)

Observations made:

No much observation was made using the extraction map. This is because, (i) it is not clear what top and base was used to generate each estimation due to short fall of the check shot data at that interval of interest and (ii) whether the sands shown actually ties to the interval in question on the seismic section (regarding the need for proper seismic-well for this intervals).

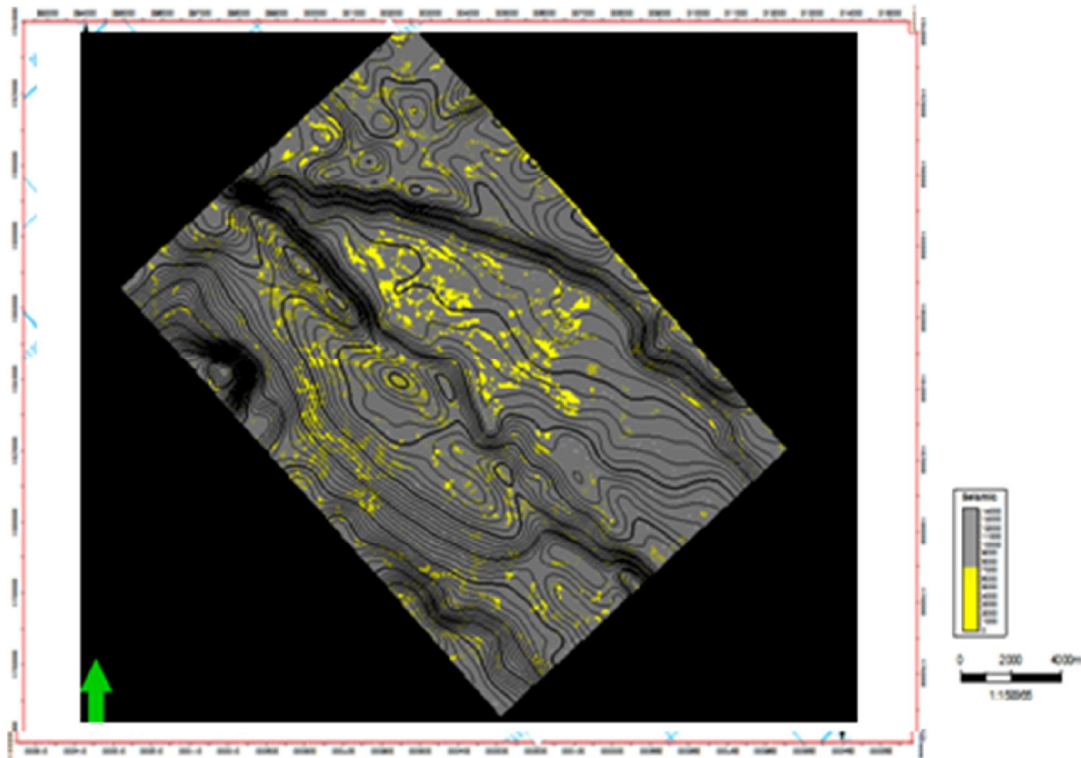


Figure 28: Map pattern of B5000 surface interval amplitude extraction in yellow and black colour background

Based on (i) the location of OGBO field in the sub-regional sense, i.e. Coastal-shelf position, (ii) the map pattern of one of the extraction (Figure 28), (iii) and considering that some of the log motif for this interval showed generally coarsening-upward grain trends (i.e. funnel-shaped GR log motif), there is a chance of inferring shallow marine environment probably upper-middle shoreface region. However, there is also the occurrence of some serrated cylindrical GR motifs. Although this is not very clear since the log appear compressed, if this observation is true, then we might infer that there is fluvio-tidal influence in this area. Hence a combination of shoreface and tidally-influenced fluvio-deltaic systems. However, it is key to suggest that the sand trends (inferred from the attribute maps) might have been strongly influenced by the basin ward dipping faults. This further makes the interpretation a bit

ambiguous. Otherwise, one can say that the sand fairway is the result of the interplay between structural and depositional influences.

Discussion on Environment of Deposition (E O D)

Well data may therefore, augmented by the use of depositional model. A tide dominated shoreline depositional models was adopted for the western portion of the field while a fluvial and wave dominated type was adopted for the Eastern portion of the field. The use of analogous depositional model proved very valuable as it was used to constrain the NTG maps and subsequent EOD interpretation of individual portions of the study area. Utilizing all the data sets namely; reservoir facies (amplitude extraction), well log motif, petrophysical parameter (NTG) and depositional model was analyzed and integrated to generate EOD framework for each (portion) reservoir inferred. Deduction of EOD In the upper OGBO field inferred a southward prograding wave dominated shoreline. The shoreline was fairly linear with good quality upper to proximal lower shoreface sands. Sand quality decreases as you move from distal lower shoreface to offshore deposits of the field.

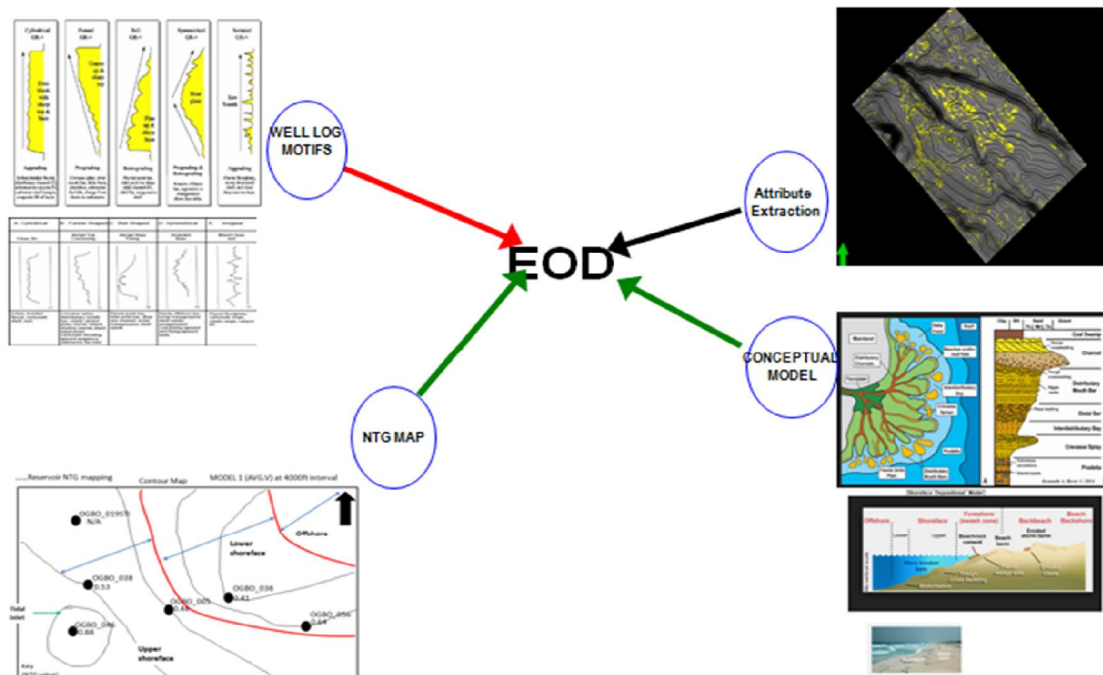


Figure 29: Environment of deposition delineation: by integrated model approach

EOD framework provided a comprehensive description of the spatial and vertical distribution of depositional facies along with their inherent reservoir properties for the individual flow units. It is hoped that the EOD framework would serve as the tool in conveying geologic data observations and interpretations to both the geologic property models for exploration, production project plan and entire life line of the reservoir management of the field. In addition, consistent, detailed integrated approach adopted for the EOD gave insight to reservoir description and geared effort towards improved stratigraphic framework definition for the OGBO field. This was achieved at a flow unit scale with the aid of available data at hand. (Figure 29) showed the integrated approaches adopted in delineation of environment of deposition in this study. EOD interpretation involve the integration of different elements to arrive at a model. The different elements include well log motifs, NTG map pattern, amplitude trend and conceptual depositional model. For the purpose of minimizing speculation, integration of these elements to arrive at a model was the destination. The stratigraphic framework is helpful in achieving more reliable reservoir connectivity analysis. It is anticipated that the stratigraphic framework will prove its worth in helping to achieve a satisfactory history match and reliable production forecasting. This leads to a better grade depletion plan for the maturing OGBO field.

4.3 SEQUENCE STRATIGRAPHIC ANALYSIS

(Tables 4, 5, 6 and Figures 30, 31, 32 and 33) analyzed sequence stratigraphy application in OGBO field.

4.3.1 MAXIMUM FLOODING SURFACES (MFS)

Maximum Flooding Surface (MFS_{15.9}) was correlated across OGBO 019STI and OGBO 038 wells and was dated 15.9 Ma using a regional marker, Chiloguembelina 3. The surface occurrence of the event is within P720 and F9501/F9503 biozones.

Maximum Flooding Surface (MFS_{15.0}) was correlated across OGBO 019STI, 038, 046, 005,036 and 056 wells and was dated 15.0 Ma using a regional marker, Bolivina 25. The surface occurrence of the event is within P720 and F9501/F9503 biozones.

Maximum Flooding Surface (MFS_{12.8}) was correlated across OGBO 038, 046, 005,036 and 056 wells was dated 12.8 Ma using a regional marker, Cassididulina 7. The surface occurrence of the event is within P720/P750 and F9503/F9505 biozones.

Maximum Flooding Surface (MFS_11.5) was correlated across OGBO 038 well was dated 11.5Ma using a regional marker, Dodo Shale. The surface occurrence of the event is within P770 and F9505 biozones. The summary of the recognized and identified MFSs and the depth at which they occur in the wells are shown in (Figures 30, 31, 32, 33 and Table 4)

The well correlation across various and delineated bounding surfaces (Surface of Erosion - Sequence Boundaries and flooding surfaces - Maximum Flooding Surfaces) and the depth at which they occur in the wells are shown in (Figures 30, 31, 32, 33 and Table 4) .

Table 4: Table showing the delineated MFS, marker fauna and biozone studied summary for six wells studied

CHRONO SURFACE	AGE(Ma)	MARKER FAUNA	BIOZONES		DEPTH (Ft)
			P-ZONE	F-ZONE	OGBO 019STI well
MFS1	15.9	Chiloguembelina 3	P720	F9503	6889
MFS2	15.0	Bolivina 25	P720	F9503	6145
MFS3	12.8	Cassididulina 7	P750	F9505	4907
MFS4	11.5	Dodo Shale	N/A	N/A	N/A
			P-ZONE	F-ZONE	OGBO 038 well
MFS1	15.9	Chiloguembelina 3	P720	F9503	8277
MFS2	15.0	Bolivina 25	P720	F9503	7084
MFS3	12.8	Cassididulina 7	P750	F9505	5400
MFS4	11.5	Dodo Shale	P770	F9507	4307
			P-ZONE	F-ZONE	OGBO 046 well
MFS1	15.9	Chiloguembelina 3	N/A	N/A	N/A
MFS2	15.0	Bolivina 25	P720	F9505	8449
MFS3	12.8	Cassididulina 7	P750	F9505	6500
MFS4	11.5	Dodo Shale	N/A	N/A	N/A

Table 4: Table showing the delineated MFS, marker fauna and biozone studied summary for six wells studied continued

CHRONO SURFACE	AGE(Ma)	MARKER FAUNA	BIOZONES		DEPTH (Ft)
			P-ZONE	F-ZONE	OGBO 005 well
MFS1	15.9	Chiloguembelina 3	N/A	N/A	N/A
MFS2	15.0	Bolivina 25	P720	F9505	7340
MFS3	12.8	Cassididulina 7	P750	F9505	5695
MFS4	11.5	Dodo Shale	N/A	N/A	N/A
			P-ZONE	F-ZONE	OGBO 036 well
MFS1	15.9	Chiloguembelina 3	N/A	N/A	N/A
MFS2	15.0	Bolivina 25	P720	F9505	7602
MFS3	12.8	Cassididulina 7	P750	F9505	6021
MFS4	11.5	Dodo Shale	N/A	N/A	N/A
			P-ZONE	F-ZONE	OGBO 056 well
MFS1	15.9	Chiloguembelina 3	N/A	N/A	N/A
MFS2	15.0	Bolivina 25	P750	F9505	8308
MFS3	12.8	Cassididulina 7	P750	F9505	6600
MFS4	11.5	Dodo Shale	N/A	N/A	N/A

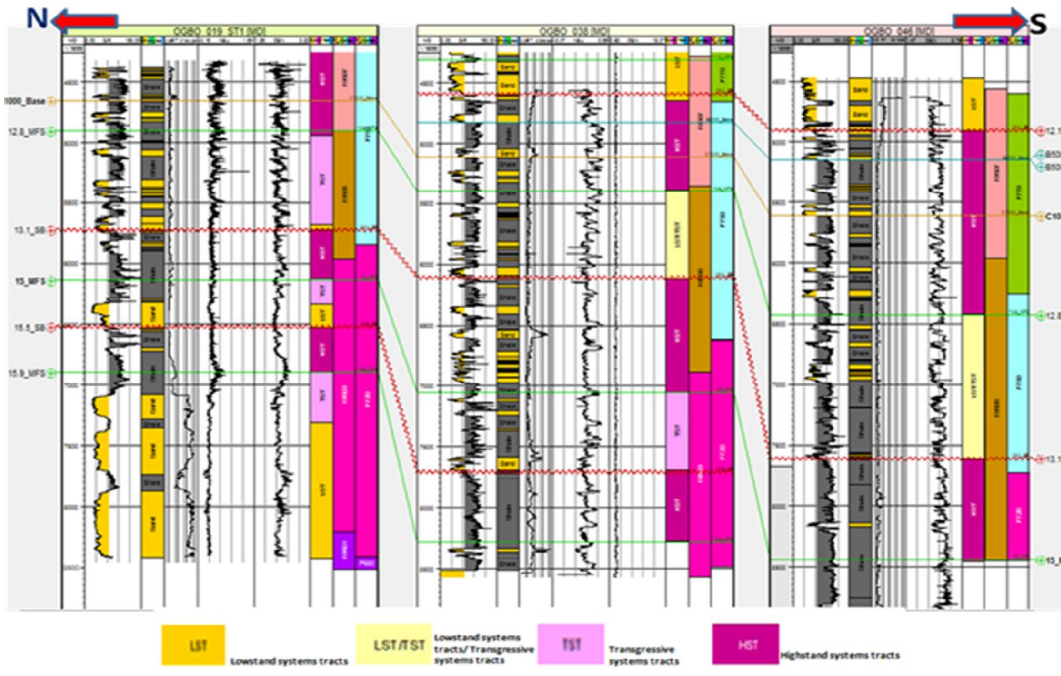


Figure 30: Well Log Sequence Stratigraphic Interpretation and Correlation across Strike within the Field and wells

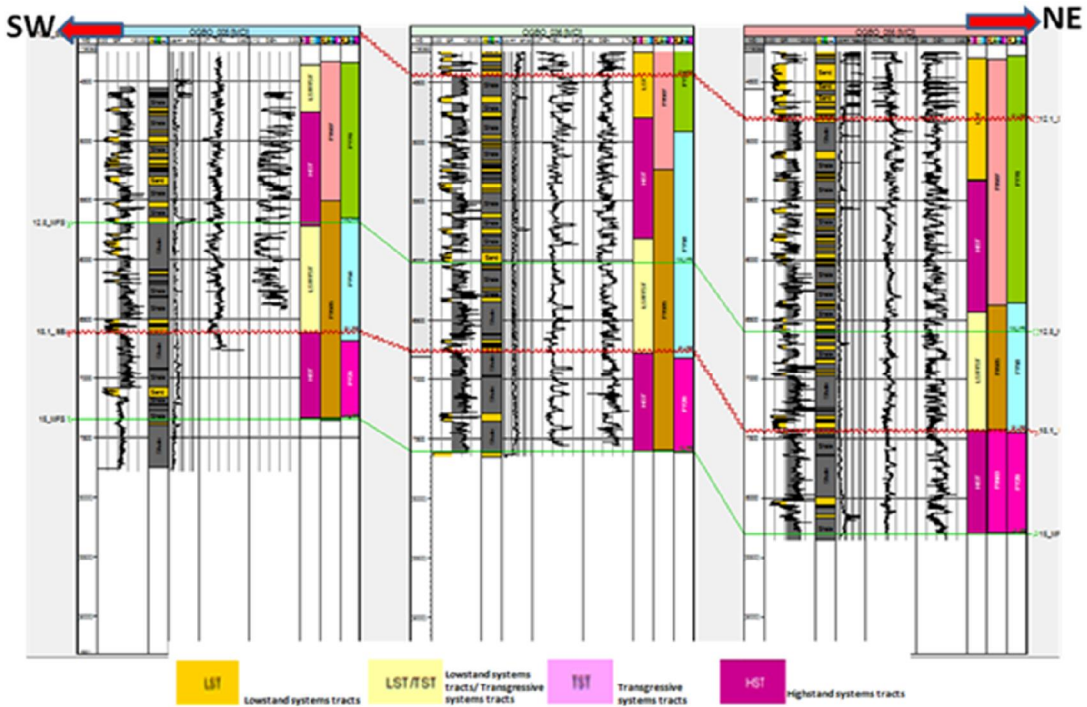


Figure 31: Well Log Sequence Stratigraphic Interpretation and Correlation across Dip within the Field and wells

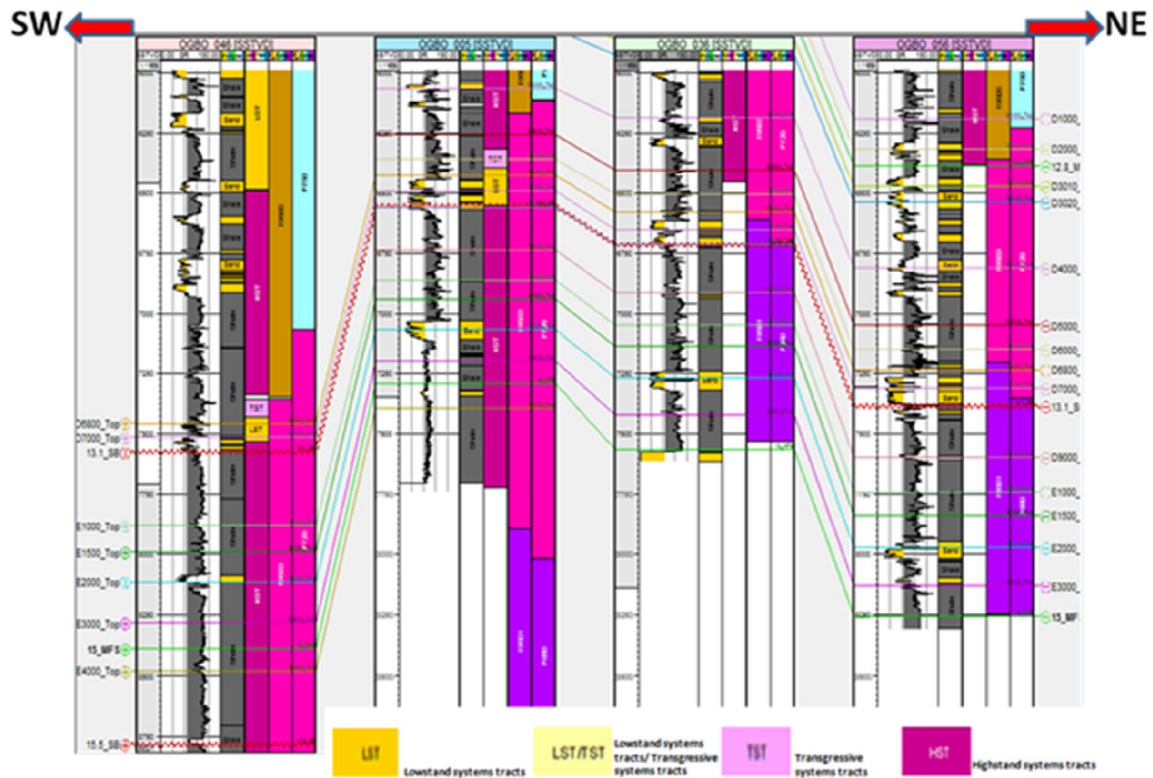


Figure 32: Well log sequence stratigraphic interpretation and correlation across Dip with surfaces interval within the field and wells

4.3.2 SEQUENCE BOUNDARY (SB) AND TRANSGRESSIVE SURFACE OF EROSION (TSE)

The oldest Sequence Boundary (SB1) recognized in the well field was dated 15.5 Ma. The surface represents an erosional surface defined before the MFS of 15.9 Ma (Figures 30, 31, 32, 33, Tables 4 and 5). SB1 (SB_15.5Ma) is lie upon in the down dip section by a thick and sharp-based sand unit identified as incised valley fills and in the up dip areas by sharp-top facies of the uppermost prograding Highstand parasequence. The thickness of the sand units overlying SB1 in the down dip section of the well field, thus, widely different from well to well due to local erosion of the sands (ravinement) at the onset of rising sea level and beginning of a retrogradational facies that starts with initial substrate erosion: the Transgressive Systems Tract (TST). Other Sequence Boundaries (SB2 and SB3) are dated 13.1 Ma and 12.1 Ma respectively, based on their relative positions in the stratigraphic sections, also with reference to the Niger Delta Chrono- stratigraphic Chart (Haq et al., 1988)

Recognized Transgressive Surfaces of Erosion, lie close to the SBs marking sharp changes from progradational facies to retrogradational facies and substantially caused diminution of sand thickness deposited during sea level fall.

4.3.3 DEPOSITIONAL SEQUENCES AND SYSTEMS TRACTS

(Figures 30, 31, 32, 33, Tables 4 and 5) depositional systems in the OGBO field comprise Lowstand Systems Tracts (LSTs), Transgressive Systems Tracts (TSTs) and Highstand Systems Tracts (HSTs). In this study, LST/TST infers Lowstand Systems Tracts (LSTs)/Transgressive Systems Tracts (TSTs) as model to bridge the relationship between them and validate the operation and check error due to inference.

Table 5: Table showing summary of the delineated system tracts and inferred depth studied for six wells

Event/Age (Ma)	019STI(Ft)	038 (Ft)	046 (Ft)	005 (Ft)	036 (Ft)	056(Ft)
SB3 (12.1)	N/A	LST @ 4600	LST@ 4908	N/A	LST/TST @ 4400	LST/TST @ 4600
SB2 (13.1)	HST/TST @ 5725	LST/TST @ 6100	LST/TST @ 7652	LST/TST @ 6619	LST/TST @ 6725	LST/TST @ 7500
SB1 (15.5)	LST/TST @ 6500	TST @ 7700	N/A	N/A	N/A	N/A
MFS3 (12.8)	HST @ 4900	HST @ 5400	HST @ 6425	HST @ 5588	LST/TST @ 6000	LST/TST @ 6500
MFS2 (15.0)	TST/HST @ 6000	TST/HST @ 7200	HST @ 8446	HST @ 7400	HST @ 7510	HST @ 8300
MFS1 (15.9)	HST/TST @ 8000	HST @ 8250	N/A	N/A	N/A	N/A

Events and Inferred lithologies:

TST = Sand, LST = sand (erosional/ truncated surface TSE), LST/TST =Shale/sand, HST = shale, MFS = shale, SB = sand

4.3.3.1 STRATIGRAPHIC SEQUENCES AND SYSTEMS TRACTS

Two (2) complete depositional sequences (First/DSQ1 and Second/DSQ2), and the others are categorize as INC.DSQ (incomplete depositional sequence), also the accompanying systems

tracts were assigned and mapped in the OGBO well field (Figures 30, 31, 32, 33, Tables 5 and 6), based on logomotifs of the various reference wells (OGBO-019STI, OGBO-038, OGBO-046, OGBO-005, OGBO-036 and OGBO-056) and the spatial distribution of the recognized constrained surfaces (MFSs and SBs). In this study, DSQ1 and DSQ2 formed the deepest (oldest) and top- most (youngest) complete depositional sequences respectively. First sequence is an incomplete sequence and approximately about 2000 ft and is bounded top and bottom by 15.5 Ma Sequence Boundary. INC. DSQ refers to an incomplete sequence. DSQ1 is enveloped on top by the 15.5 Ma SB, which was revealed exclusively in wells OGBO-019STI and OGBO-038 that examined deeper stratigraphic sections of the well field. Accompanying Lowstand Systems Tract/ Transgressive Systems Tract (LST/TST) contained marine shales rich in fauna with minor sand unit enveloped on the top by the 13.1 Ma SB. The transgresssive sand units have been recognized as shoreface sands deposited in the shelfal region during rising sea levels. Highstand Systems Tract (HST) of the sequence was deposited in the Middle Neritic (MN) setting inferring mainly progradational-aggradational stacking patterns. DSQ2 is bounded top and bottom by 13.1 Ma and 12.1 Ma Sequence Boundaries, respectively. The Lowstand Systems Tract/ Transgressive Systems Tract (LST/TST) of this sequence formed thick sand deposits recognized as basin floor fans (BFF), deposited in the Outer Neritic (ON) to Bathyal (BA) depositional settings. The LST was observed to be unconformably overlying the 12.1 Ma SB and underlies a TST. Another INC.DSQ overlies the 13.1 Ma SB and it lies at the top by the 12.1 Ma SB. The sequence was identified in the wells OGBO-038, OGBO-046, OGBO-036 and OGBO-056. The sequence displayed predominantly fluvial and tidal processes (progradational stacking pattern) as shown in the parasequence stacking pattern of the western wells OGBO-038 and OGBO-046. LST of this sequence contains reworked channel sand deposits which were more pronounced in the down dip wells. Incomplete DSQ is the topmost (youngest) for incomplete sequence in the study area (present in OGBO-019STI well). It rests unconformably on the 12.1 Ma SB. The sequence consists of thick sand units at its base, deposited during relative sea level lows. The sequence was deposited within the Neritic paleodepositional environment. The 11.5 Ma MFS was recognized in this Sequence.

Table 6: Table showing the delineated Sequence Boundary with depth penetrated

KEY SURFACE	AGE(Ma)	DEPOSITIONAL SEQUENCE	DEPTH (Ft)					
			019STI	038	046	005	036	056
SB1	15.5	1	6518	7705	N/A	N/A	N/A	N/A
SB2	13.1	2	5725	6108	7611	6605	6754	7437
SB3	12.1	2	N/A	4590	4902	(4273	4437	4814

4.3.4 WELL CORRELATION

Correlation across the OGBO field was done using the recognized and identified constrained chronostratigraphic surfaces expressed indirectly by Maximum Flooding Surfaces (MFSs) and Sequence Boundaries (SBs) (Figure 34). Correlation contributed to the categorizing of the stratigraphic section and makes clear validity of how the surfaces correlated along dip and strike at certain depths within the depositional basin, thus gives the description of the basin geometry and depositional sequences in the whole extent of the well field (Figures 30, 31, 32, 33 and Tables 4, 5 and 6). The above correlation sheet model gives evidence that the stratigraphic column appears to be dipping in E-W direction and striking in the NW-SE direction (Figure 34). Deposition have a tendency to be thicker in wells OGBO-019STI, OGBO-038, OGBO-046, OGBO-036 and OGBO-056, which were located down dip. The occurrence of the identified chronostratigraphic surfaces at different depths along dip and strike lines in the OGBO field studied wells showed indication of faulting in the well field. The structural setting of the studied area as portrayed by the correlation figures indicates fault line depositional representative and displacement of sediments across the fault lines by rollover fault structure, prominent in the depobelt and entire Niger Delta basin.

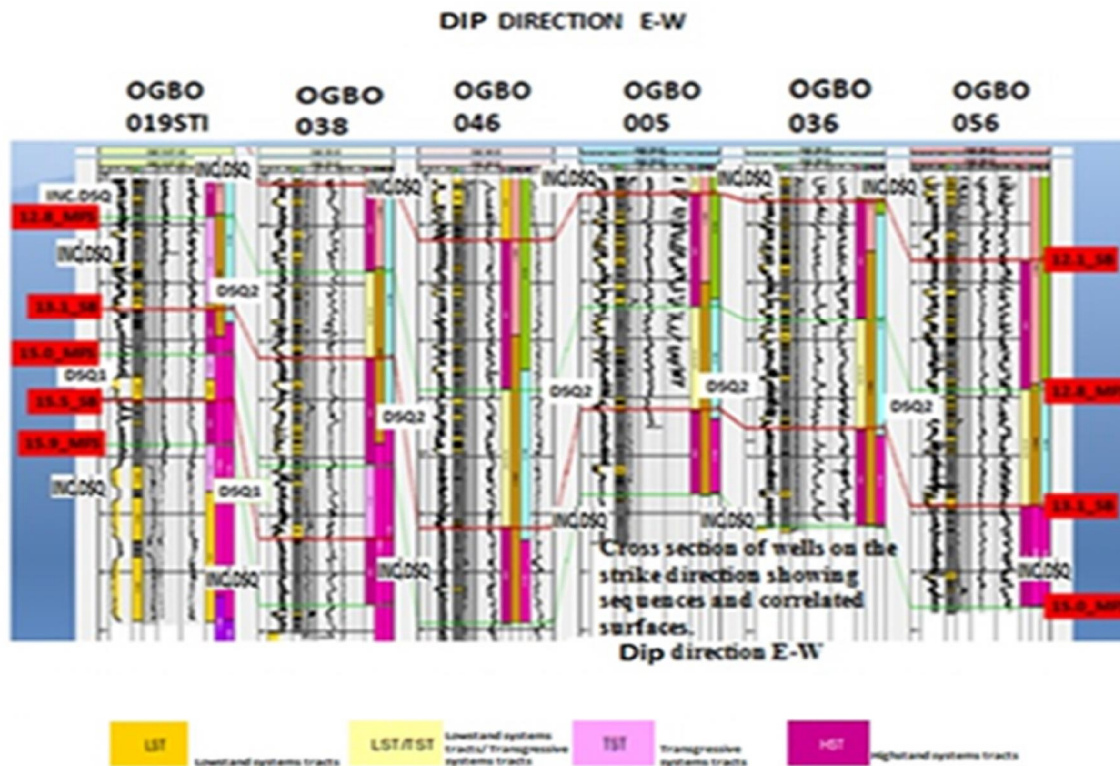


Figure 33: Cross section of the studied wells showing sequences and correlated surfaces

4.4 SEISMIC DATA INTERPRETATION

Seismic data interpretation in this study entailed the generation of synthetic seismograms, the interpretation of seismic data, and the extraction of seismic attributes from the seismic data. The seismic volume used for this study extends to 2.5 seconds two way travel time (TWT), below which reflection continuity is generally poor (Figures 34, 35, 36 and 37). The seismic volume is characterized by series of parallel/divergent reflection offset and formed by major listric growth faults, the character of the seismic volume changes with depth. The basal part of record (below 3.0s TWT) is disrupted by several zones with low to highly discontinuous reflection patterns, while the reflections between 3.0 to 0.75 TWT have moderate to good continuity and high amplitude variations. The second fault to the Northeast dipping basinward formed the major fault. The structural configuration changes with depth as the number and throw of faults increases. Contour closures against the major structure building faults represent a faulted anticlinal structure juxtaposed against the fault. In addition to the stratigraphic traps, these structures form the majority of structural traps in the Niger Delta.

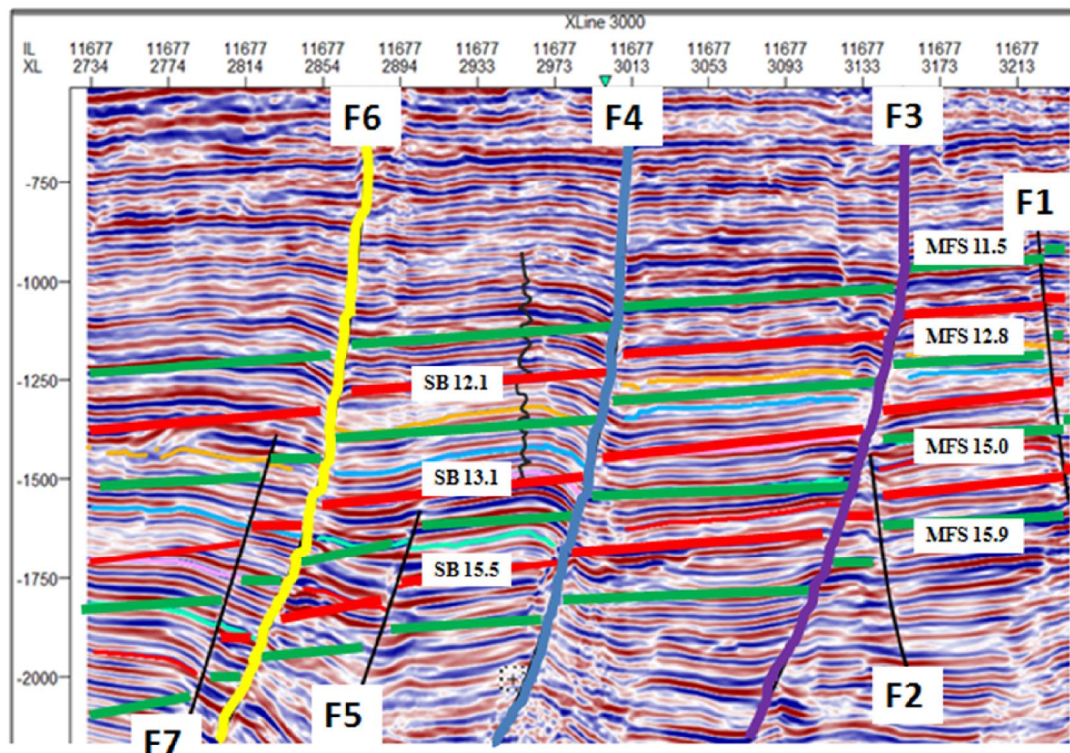


Figure 34: Seismic interpretation well OGBO 046 (vertical) inline 11677 showing the SB's, MFS's and the faults

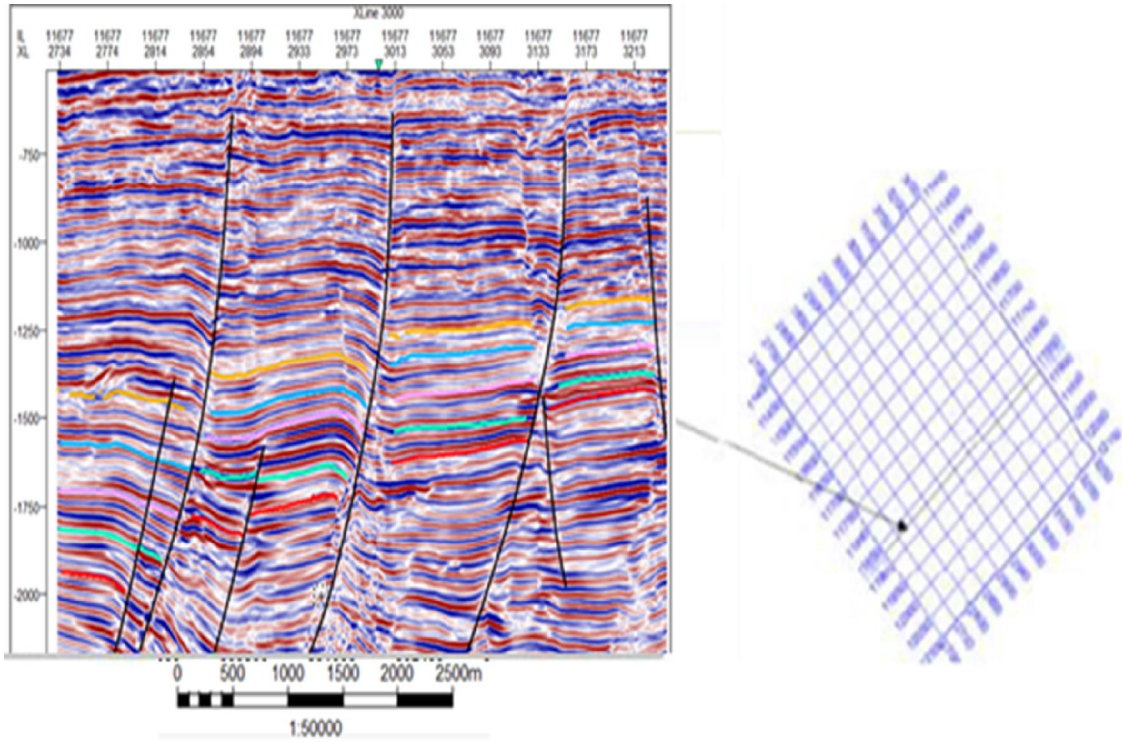


Figure 35: OGBO field seismic section showing fault sticks

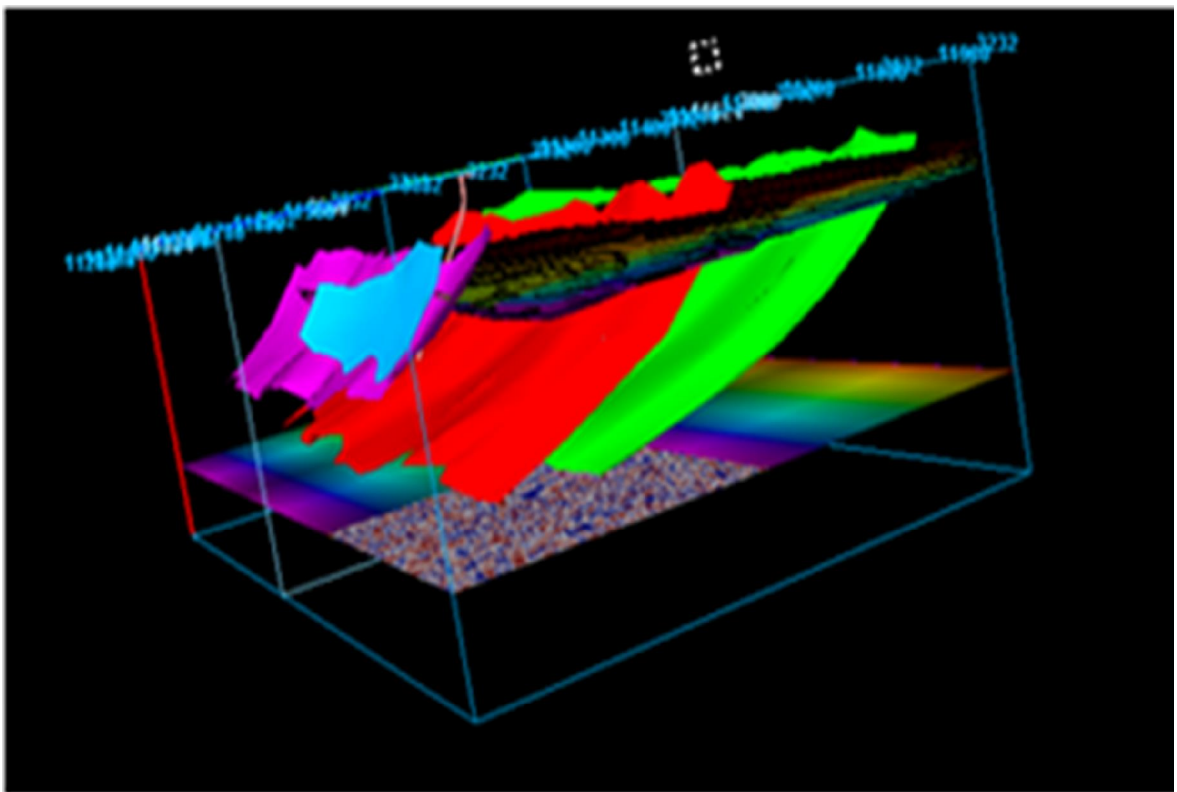


Figure 36: 3D seismic map showing the faults with hydrocarbon trap configuration and some wells in the OGBO Field

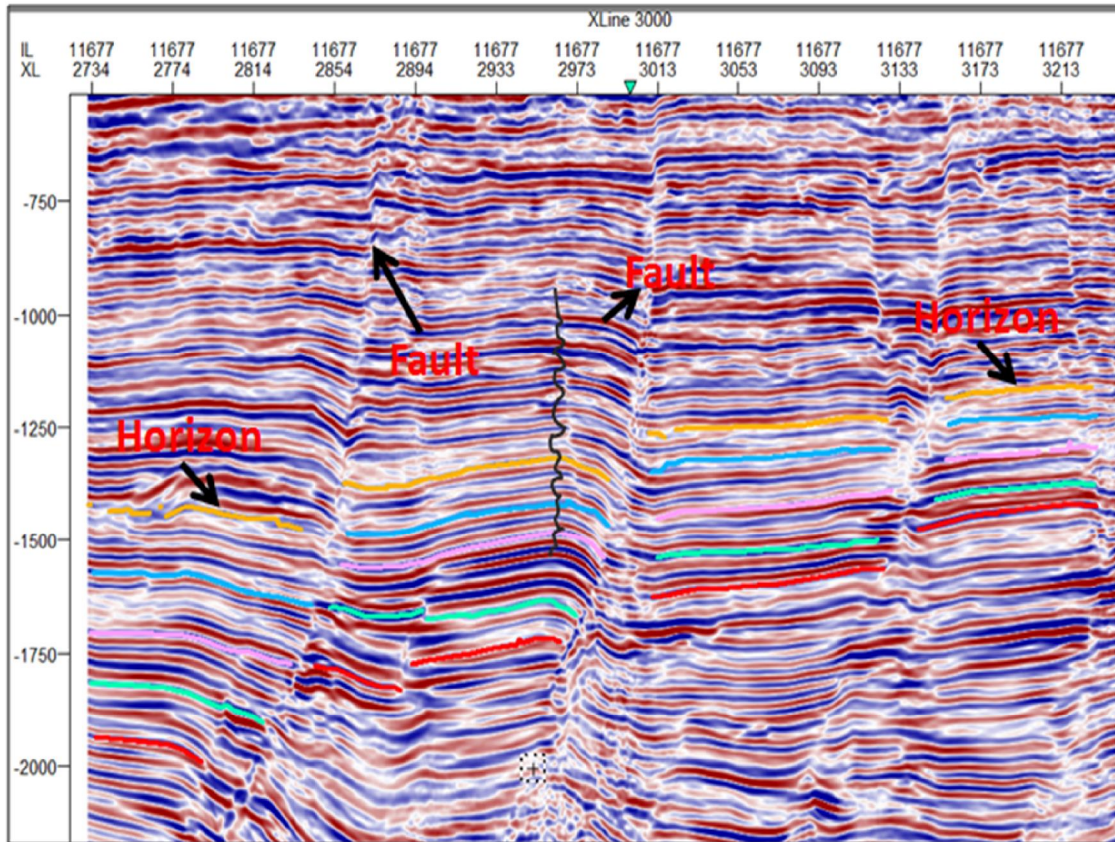


Figure 37: Seismic section showing the horizons, faults and well position between faults

4.4.1 SYNTHETIC SEISMOGRAM AND WELL-TO -SEISMIC TIE

Synthetic seismogram

Synthetic seismogram is a direct forward model of acoustic energy traveling through the layers of the earth. It is used to show the expected seismic response for comparison with the real seismic data and also to know if the target horizon is peak or trough in seismic sections. It is believed that the quality of the match between a synthetic seismogram depends on well log quality, seismic data processing quality, and the ability to extract a representative wavelet from seismic data. The synthetic seismogram was constructed by convolving the reflectivity derived from digitized acoustic/sonic and density logs with the wavelet that was extracted from the OGBO field 3D seismic data. In this study, Petrel software was used to derive a best fit wavelet that will be used to find best fit impedance from the traces around the neighborhood of the well. Sonic and density from OGBO 046 well logs were used to generate a synthetic seismic trace. The synthetic trace is compared to the real seismic data collected near the well location. The extracted wavelets were modeled with Ricker wavelets (Figure

38). Sonic and density logs were edited manually for spikes and inconsistent data points. Appropriate median filters were applied to eliminate undesirable noise. Sonic log data were linearly extrapolated from the approximate velocity of 200 s/ ft (e.g., Mitchell et al., 2004) at the datum (mean sea level) to the velocity at the top of the formation (or where data recording started). Density logs were projected to the surface (mean sea level) from the start of recording at a constant value that ranged between 1.8 and 2.2 g/ cm³, depending on the trend of the formation density (Figure 3.2 and 3.22). Curves of acoustic impedance were generated as a product of the edited sonic and density logs. Reflection coefficients derived from the impedance curves (Figure 38) were convolved with extracted wavelets from seismic data within the proximity of OGBO well 046. The extracted wavelets were filtered, thus the synthetic seismograms were successively tied to the seismic data by iteratively matching the waveforms of the synthetic seismograms with the wave forms of the 3-D seismic data that were extracted in the vicinity of the synthetic source well. (Figures 38 and 39) showed the synthetic seismogram generated from the study. The closed region in the figure shows a good match of the stratigraphy and seismic.

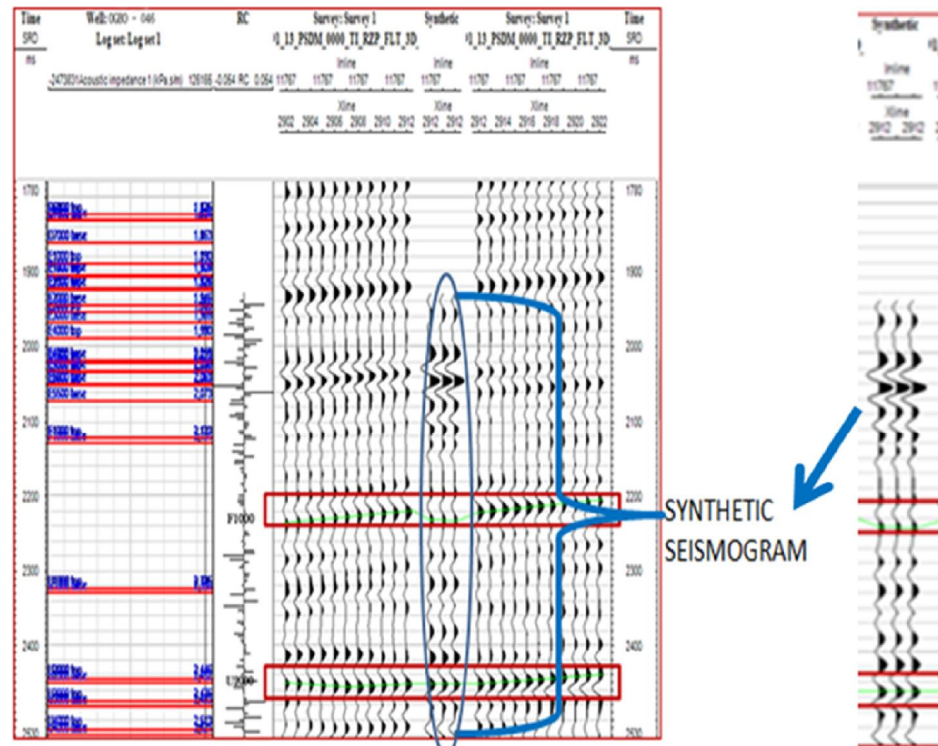


Figure 38: Synthetic seismogram showing high correlation between seismic and stratigraphy

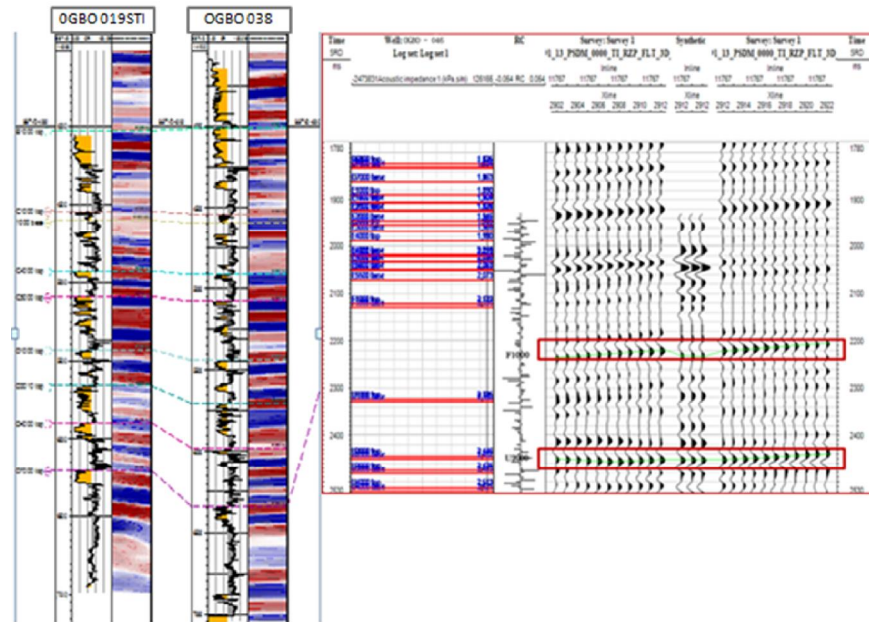


Figure 39: Synthetic seismogram showing well OGBO 019STI and OGBO 038 correlation between seismic and stratigraphy

Well to Seismic tie

Seismic to well tie requires a wavelet estimated from the seismic data. A wavelet is a wave-like oscillation with amplitude that starts out at zero, increases, and then decreases back to zero. Typically, a reflection coefficient series from a well within the boundaries of the seismic survey is used to estimate the wavelet phase and frequency, this is because accurate wavelet estimation is critical to the success of any seismic to well tie. In the same way, the inferred shape of the seismic wavelet may strongly influence the seismic to well tie results and thus, subsequent assessments of the reservoir quality. Good estimation of seismic wavelet is used to estimate seismic reflection coefficients in acoustic impedance calculation. If we think of the subsurface as a number of layers, each with its own acoustic impedance A , then the reflection coefficient at the n th interface for P-waves at zero-offset is given by the formula

$$\text{REFLECTION COEFFICIENT} = (AI_2 - AI_1) / (AI_2 + AI_1)$$

Where AI_1 and AI_2 are the acoustic impedance above and below the interface; acoustic impedance is the product of density and seismic P-wave (sonic) velocity. For a simple particular case, valid for normal incidence, of the Zoeppritz relations, which described how

the reflection coefficient varies as a function of incidence angle. Ziolkowski et al., (1998) stated that accurate wavelet estimation requires the accurate tie of the impedance log to the seismic. To ensure quality, the Reflection Coefficient (RC) result was convolved with the wavelet to produce synthetic seismic traces which are compared to the original seismic. Looking at the method of Ziolkowski et al., (1998), Ricker wavelet was extracted using well OGBO 046 together with PSDM data using offset range of 17m to 22m at 1m radius in the neighborhood of the well. The extraction window starts from 0 ms to 4250 ms with wavelength of 200ms, 25 ms Taper length at sample rate of 4 ms.(Figures 40 ó 43) showed the wavelet extraction window panel and Wavelet history.

WAVELET EXTRACTION

The wavelet extraction workflow adopted in this Seismic to well tie process involved performing deterministic wavelet extraction by selecting the seismic volume and input logs of interest (OGBO 046 well logs provided). The position of the extraction location changed interactively based on predictability to optimize on the wavelet to use. Changing the extraction location automatically updates the extracted wavelet with its corresponding power and phase spectra, as well as the resulting synthetic trace.

ZERO-PHASING

Zero phase wavelet has maximum energy at time zero. Most of the seismic sources do not generate a zero phase pulse, because that implies an output before time zero. Seismic processing is carried out according to the source signatures. In seismic acquisition, we go for minimum phase wavelet and during processing it can be converted into zero phase. The wavelet zero phase helps to line up known acoustic interfaces with picks or troughs in the seismic data. The zero-phase wavelet is of shorter duration than the minimum phase equivalent. This wavelet is symmetrical with a maximum at time zero. The fact that energy arrives before time zero is not physically realizable but the wavelet is useful for increased resolving power and ease of picking reflection events (peak or trough) for modeling purpose. This wavelet used is a special type of wavelet called the Ricker wavelet which is defined by its dominant frequency.

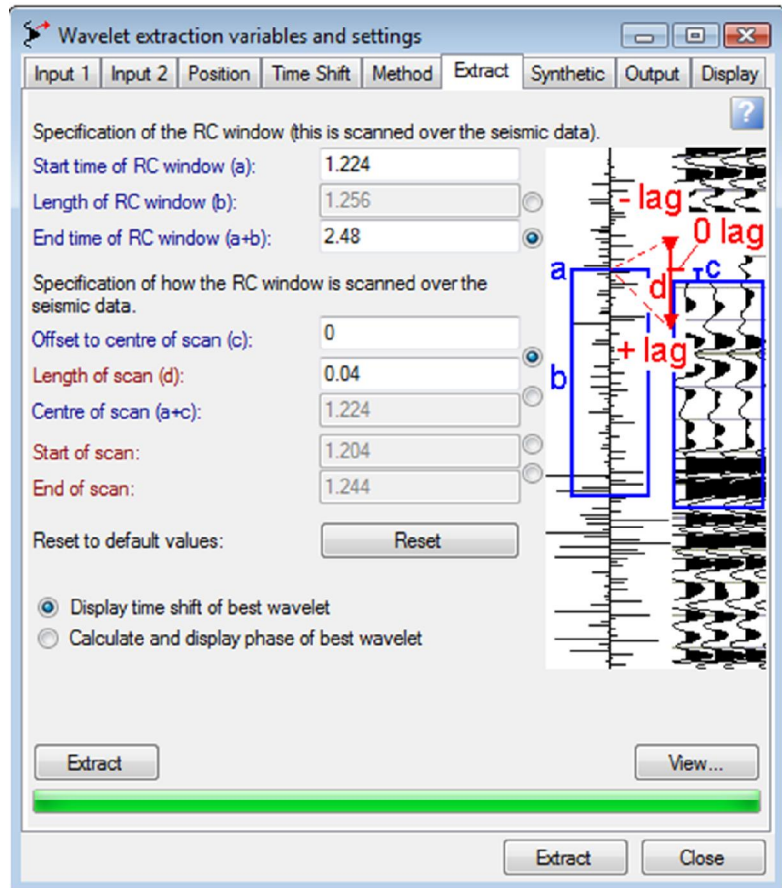


Figure 40: Wavelet Extraction window showing variables and settings

The Ricker wavelet is by definition zero-phase, but a minimum phase equivalent can be constructed. This wavelet is used because it is simple to understand and often seems to represent a typical earth response. (Figures 44a, b and c) showed the wavelet time, amplitude and phase response of the earth in the study area.

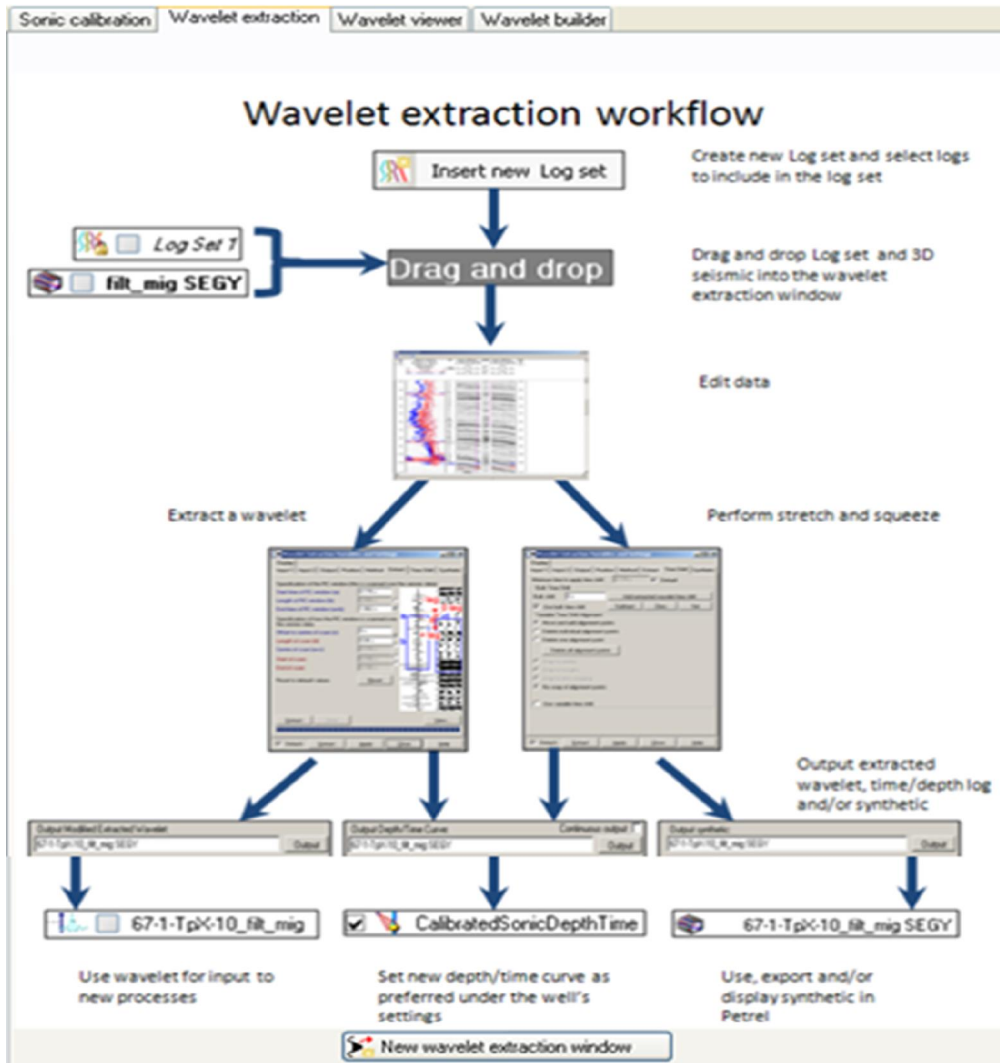


Figure 41: Wavelet Extraction workflow

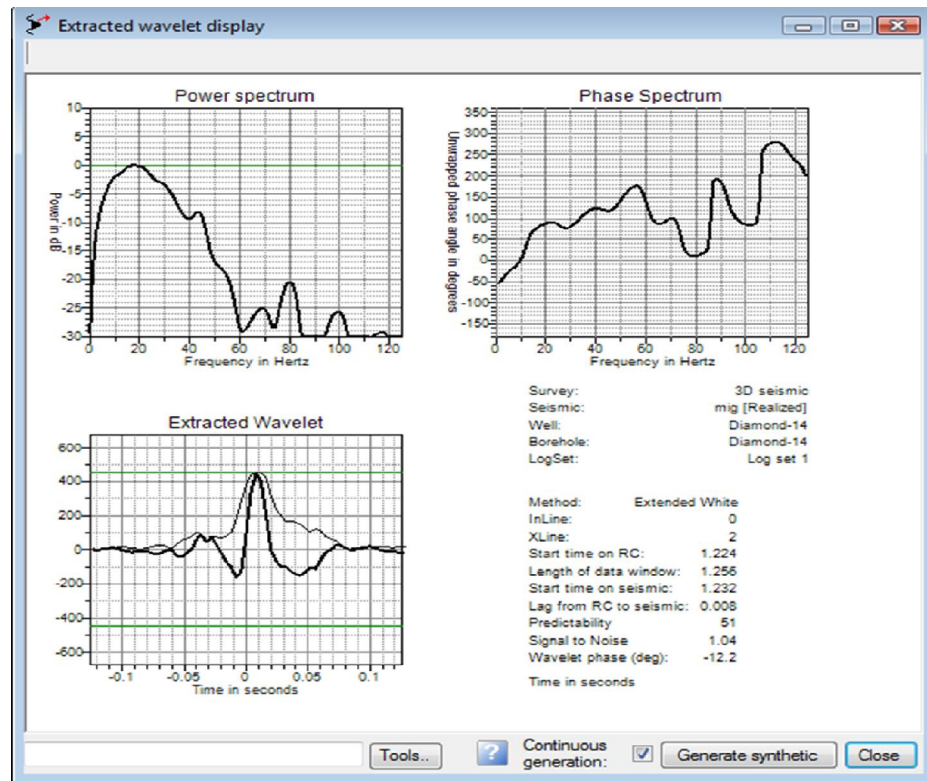


Figure 42: The Petrel wavelet extraction summary

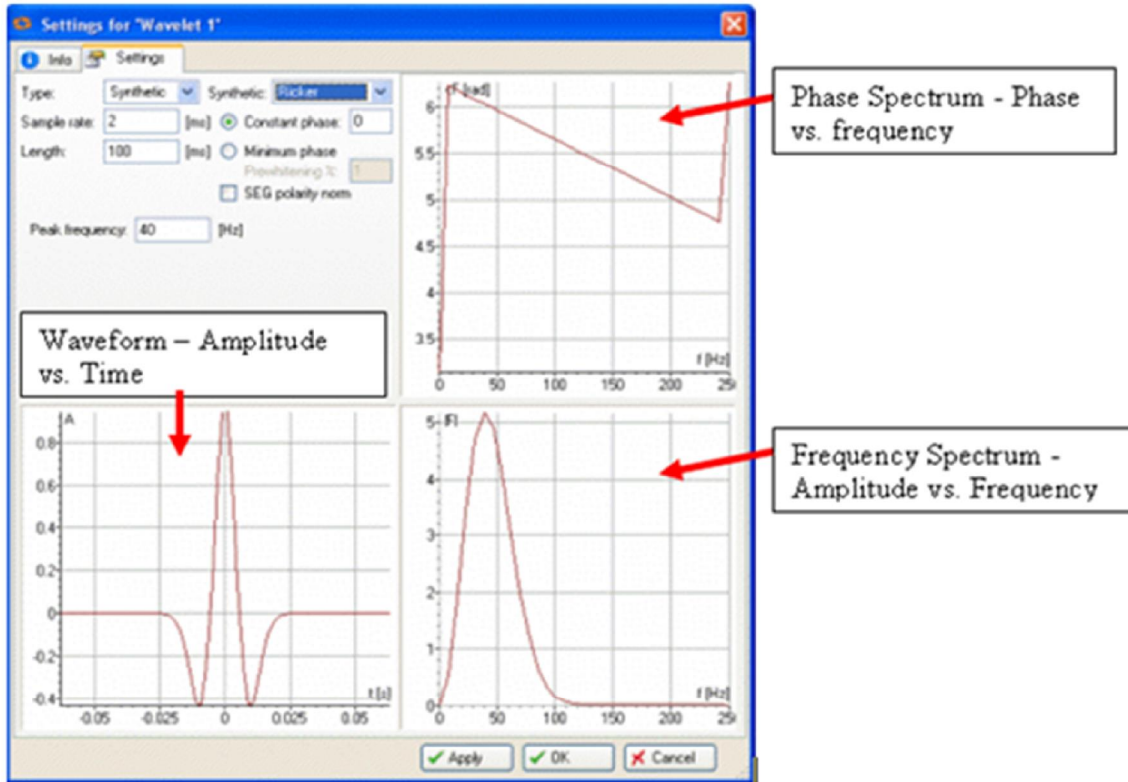


Figure 43: The spectrum for a Ricker wavelet

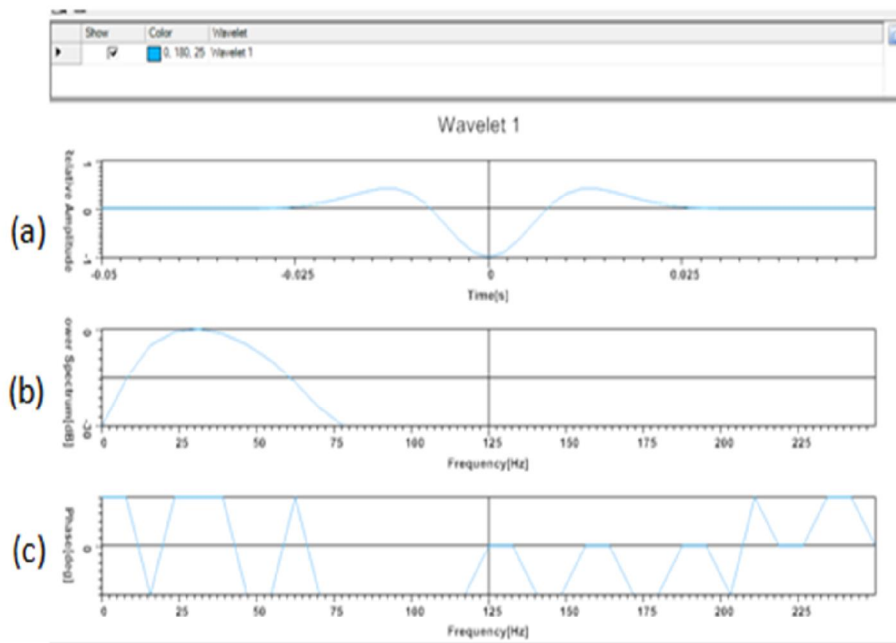


Figure 44: (a) Zero phase wavelet time response at an interval of -0.025 to 0.025 ms, (b) (Wavelet frequency window) Wavelet frequency and amplitude band response at 5Hz to 75Hz. (c) Wavelet amplitude spectrum

Wavelet amplitude spectrum almost completely overlies the seismic amplitude spectrum suggesting a good match.

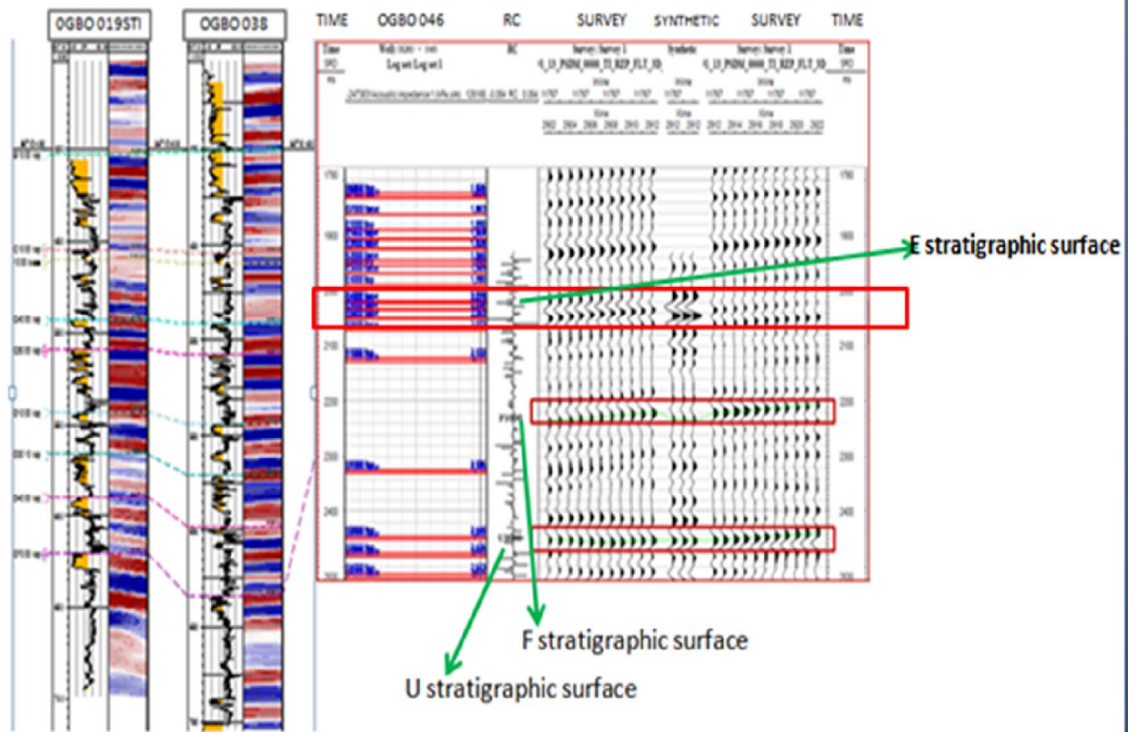


Figure 45: Well to Seismic tie showing the good character match

Wells are registered in units of depth ó feet or meters while Seismic data is recorded and usually worked with a vertical scale of 2-way travel time. To relate well data to seismic data, and vice versa, result to great need to handle this change in vertical scale units. Accurately tying of wells and seismic information is a necessary step in reservoir characterization. The objective is to identify an accurate time-depth relationship between the geology and seismic interface, so that horizons on the zero phase of the processed seismic data can be picked in time or depth units. To cross this bridge, one needs to go from seismic ÷wigglesö to the rocks that produced the ÷wigglesö and the interpretation of the subsurface geology. Well-seismic ties allow well data, measured in units of depth, to be compared to seismic data, measured in units of time. This allows us to relate horizon tops identified in a well with specific reflections on the seismic section such as doing mapping, e.g., mapping a significant erosional unconformity or a flooding surface, then our tie within 1 or 2 seismic cycles (peaks

or troughs) of the seismic data. To tie well data, e.g., the top of a stratigraphic horizon/ marker within $\frac{1}{2}$ a cycle, know the seismic event within $\frac{1}{2}$ a cycle, the shape of the real and modeled seismic trace is similar. Obtaining a good character (shape) tie between the real and synthetic traces, enables extraction of various seismic attributes. The synthetic seismogram generated revealed that OGBO 046 well has a good time depth tie with a trough to trough and peak to peak match. Well to-seismic tie revealed that the mapped hydrocarbon bearing reservoirs lie on the trough of the rollover anticlines on seismic sections (Figure 45). A chance of 100% confidence for the tie was limited due to shortage of full checkshot data availability. Available data comprised of very short range stratigraphic surfaces interval in deeper horizons (between E, F and G surfaces only where my tie lies), whereas B5000, C4000 and D4100 (shallower horizons) stratigraphic surfaces were mapped and interpreted in this study, thereby confining one taking a shot in the dark.

4.4.2.1 HORIZON AND FAULT INTERPRETATIONS

The 3-D seismic data were interpreted, using Petrel, in a grid of 10 traces by 10 inlines. Horizon/events were mapped, interpreted and correlated all through the study area. Horizon picks were done iteratively in in-line and cross-line directions, and corrected for misties. In areas where reflection quality and characteristics are of good quality, lines are picked at larger intervals while at areas where reflection quality is relatively poor and characterized by discontinuities and chaotic, lines were picked at closer intervals in order to reduce misties to acceptable minimum. (Figure 34) Three major Horizons were mapped namely; MFS_15.9, MFS_15.0, MFS_12.8 and MFS_11.5 respectively. B5000, C4000 and D4100 shallower stratigraphic surfaces horizons were mapped and interpreted in this study.

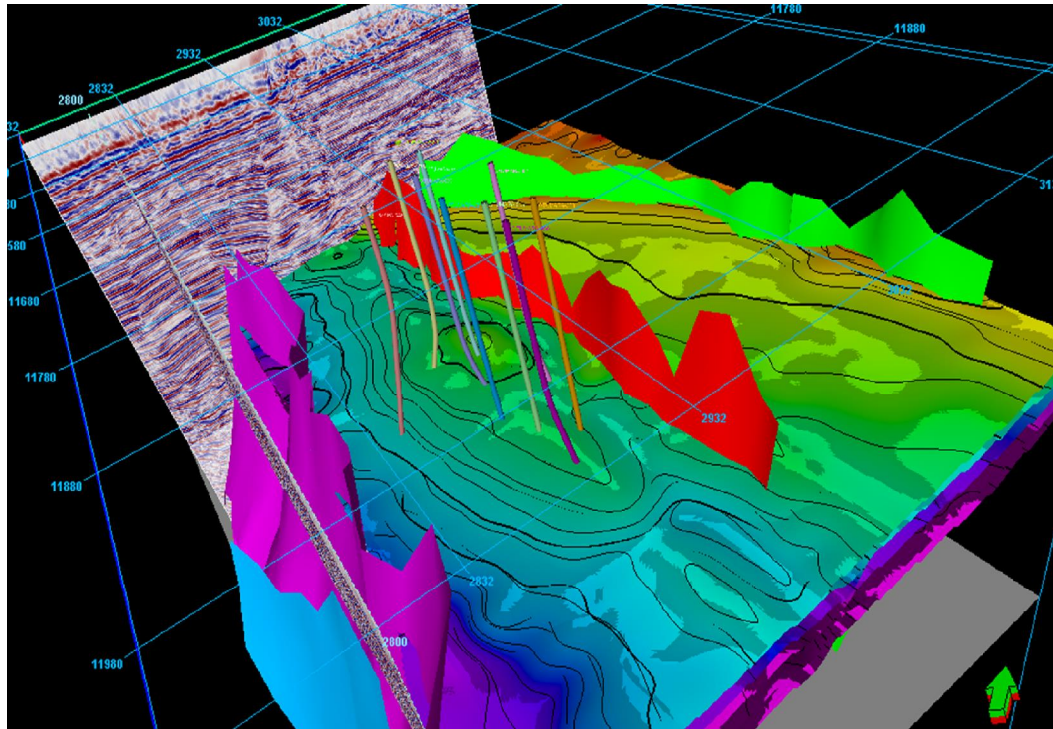


Figure 46: Structural/Trapping styles - Upper extensional zone of listric faults and simple-rollover anticlines

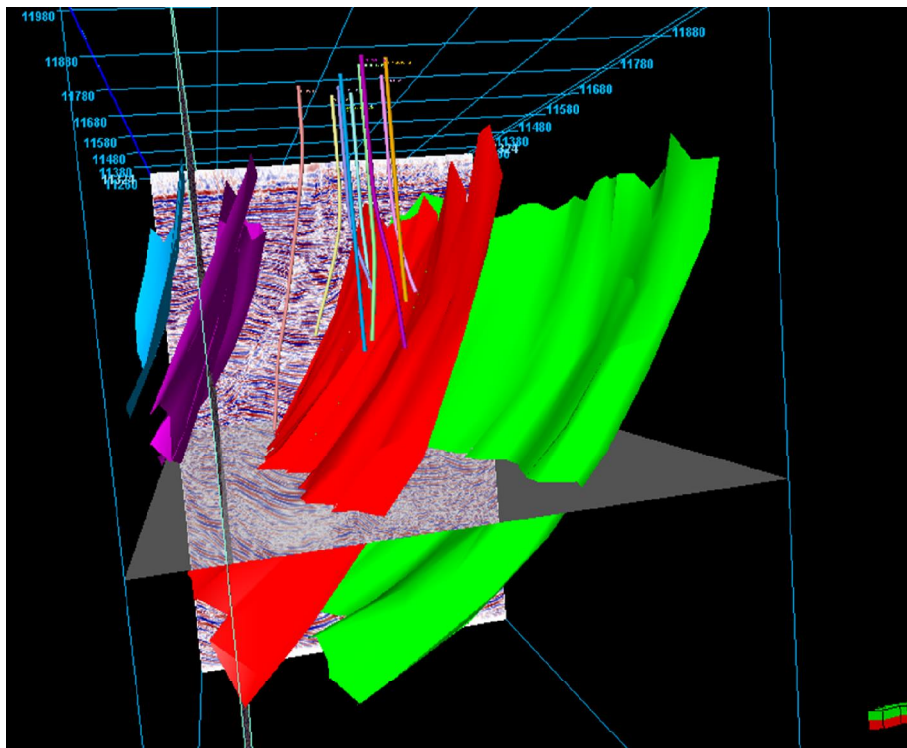


Figure 47: Gridded fault and event on cube Volume view showing Structural and stratigraphic Framework of study area on Plan and Dip section

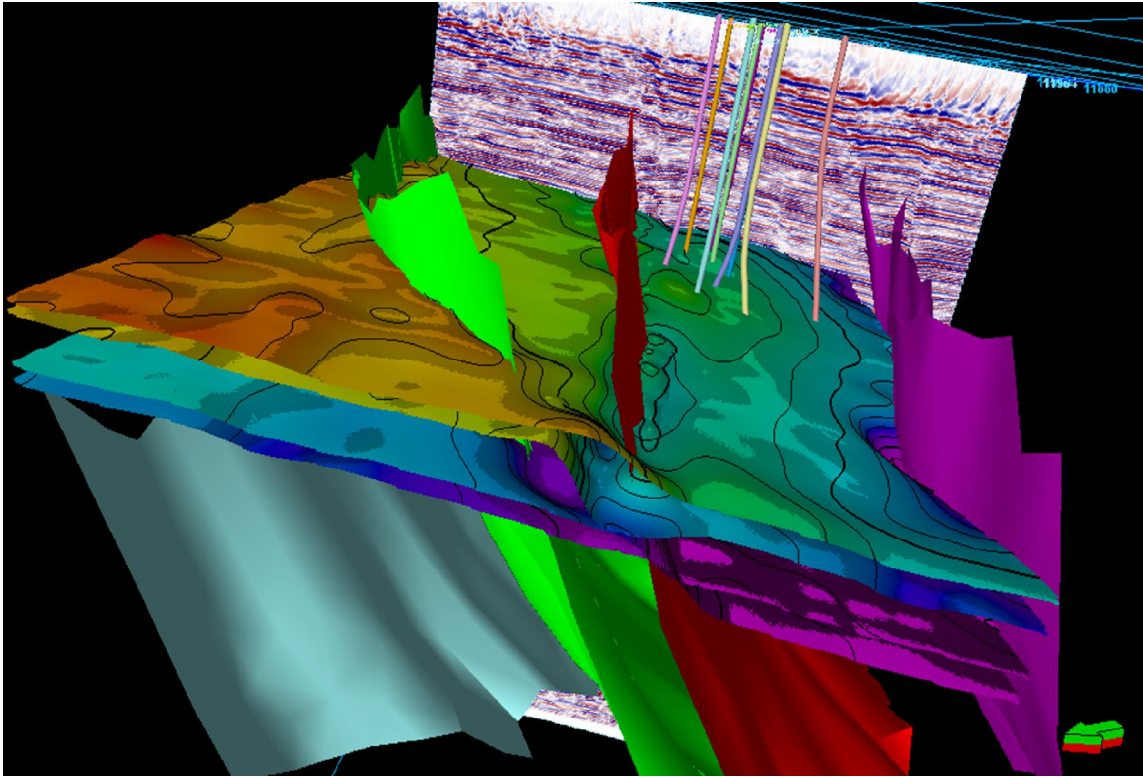


Figure 48: 3D seismic map showing the faults with hydrocarbon trap configuration and some wells in the studied field

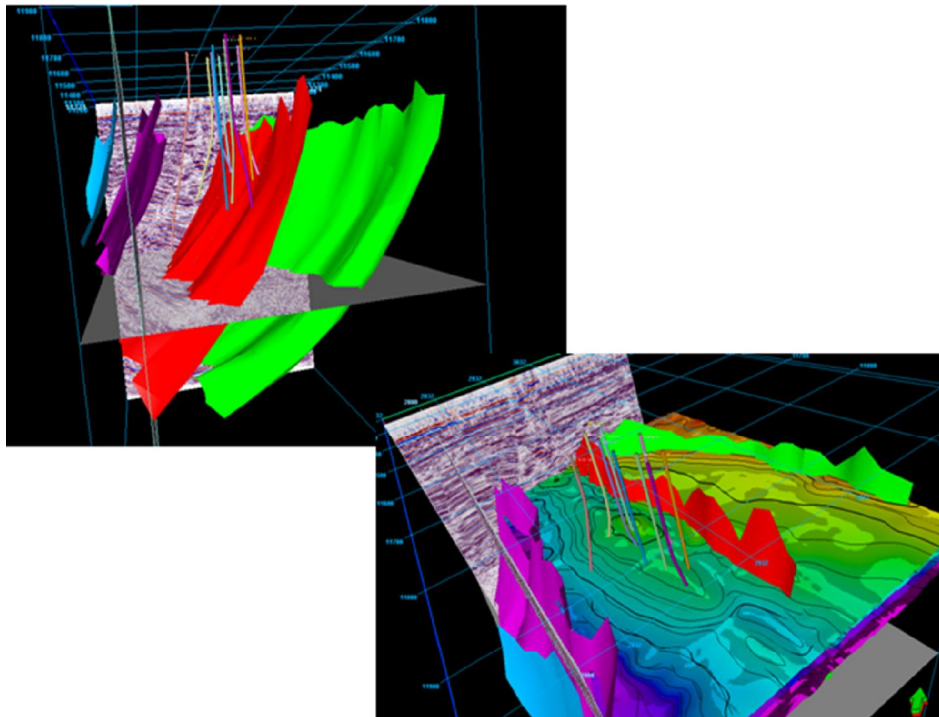


Figure 49: Gridded fault and event on cube Volume view showing Structural and stratigraphic Framework of study area on Plan from Dip section to strike section

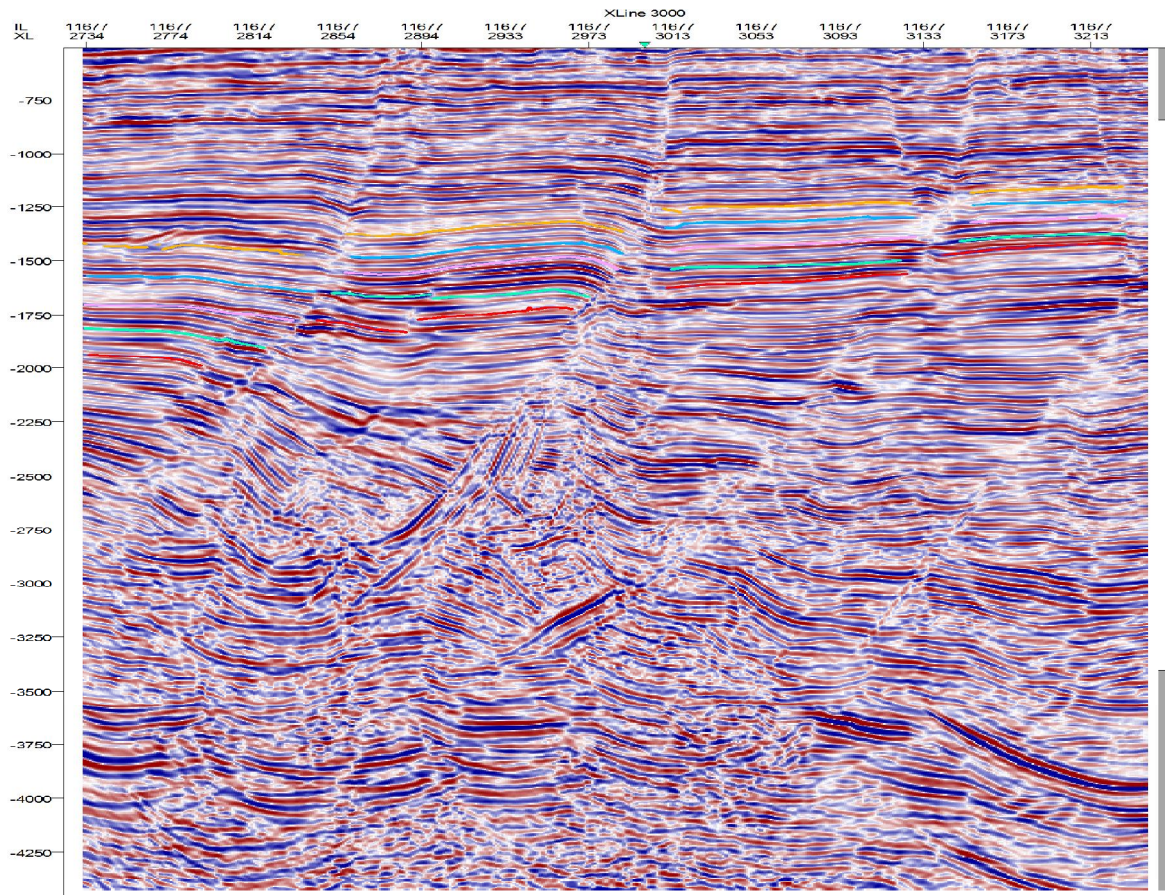


Figure 50: Seismic section of OGBO field

This comprised of depositional environments of sediments determination from seismic reflection characteristics. (Figure 50) These characteristics include reflection continuity, architectural arrangement, amplitude and others in this study. Based on seismic amplitude continuity and reflection frequency Weimer et al., (1988) the seismic volume is divided into two different facies. Facies one comprised of high frequency, continuous, parallel/divergent reflections while facies two comprised of lower amplitude, chaotic, discontinuous/inclined internal reflection. The various reflection patterns, observed on seismic sections are described below which indicated the reflection arrangement and the nature of cycle termination at seismic facies boundary. Reflection characteristics between 0s and about 1.35s two way travel time observed from seismic record show a characteristics low amplitude observed from the seismic record show a characteristics low amplitude, parallel, and discontinuous reflection patterns of the field. Based on regional studies and the uniformity blocky, low-value gamma ray patterns observed within this interval, this portion can be inferred as the Benin Formation. The upper part showed a characteristic where the sandstone intervals are

thicker than the shale, whereas in the lower part, a reversed situation is the case. This zone is equivalent to the zone of 1.35s to 2.80s two ways travel time, observed from the seismic record and can be assigned to the Agbada Formation Doust and Omatsola (1990); Owoyemi (2004)

High amplitude reflection and high continuity: This reflection pattern occurs within the section of about 1.25s to 2.50s in trace 11677 inline, from the East towards the western part of the section within the parallel/divergent reflection pattern. To the south west, it grades into a low continuity, variable amplitude facies. The high continuity of the reflection facies calls to mind a continuous bed deposited in a relatively widespread and uniform environment. The high amplitude reflections are inferred as inter-bedding of shale with relatively thick sands, which indicates inter-bedding high and low energy deposits which points to a shelf environment. This establishes the findings of Posamentier and Kolla (2003) and Sangree and Wimier (1979)

Low amplitude reflection: This is observed between 1.0s to 1.8s on traces 11677 inline. Low amplitude facies is an indication of zone of one common lithologic type speculatively. Following Sangree and Wimier (1979), this massive sand associated with low amplitude reflections tend to be near shore to fluvial sands that are transported and deposited by high energy fluvial and wave processes.

Chaotic arrangement: This is seen on the section as a discontinuous discordant reflections at the base of the section. This chaotic configuration gradually developed as one moved within the section of about 2.25s to 3.50s where it is more unfolded. The chaotic configuration arrangement points to a disordered reflection surfaces which show a relative high energy and variability of deposition or disruption of beds after deposition, Sangree and Wimier (1979). This arrangement has variably sharp transitions to diffuse gradational boundaries which are interpreted to be reflection deposits that have been fractures by overpressures and moved upward under the weight of overlying strata during fault displacement.

4.4.2.3 STRUCTURAL INTERPRETATION

Fault mapping and picking of horizons: Seismic volume revealed the presence of patterned reflection discontinuities which are identified and interpreted as faults (Figures 32, 33, 34, 35,36, 37, 46, 47, 48 and 49). The regional growth faults which are listric in nature and are concave basinwards. They are mainly synthetic, dipping in the same direction as the main fault with a few antithetic faults that dip in opposite direction to the main fault. The main OGBO fault and the minor faults were picked by tracking an alignment of terminating events. The faults were identified, correlated, assigned unique names and marked with different colours. Interpreting fault plane geometry was quite difficult in most areas due to poor reflection characteristics around fault ó a seismic acquisition and processing artifact error. Also mapping faults detachments at depth was difficult and sometimes impossible as data quality deteriorated greatly with depth. However simple extrapolations were made to constrain interpretation picks. Identification of faults on the seismic section was based on the following criteria: (a) Reflection discontinuity at fault plane (b) Vertical displacement of reflection (c) Mis-closures in tying reflections around loops (d) Abrupt termination of events (e) Overlapping of reflections (f) Change in pattern of events across the faults.

A horizon is the interface between two different rock layers and it represents a mappable isochronous geologic time surface. It is associated with continuous and reliable reflection on the sections that appear over a large area. However, criteria (a) to (d) above were used in picking of the horizons. The horizons were tied to the well picks and also interpreted in a grid of 10 traces by 10 inlines. The interpreted horizons were interpolated and edited for consistency. Using the well logs, the reservoir sands B, C and D were focused on, while the sands B5000 surface, C4000 surface and D4100 surface were used to pick the horizons. The horizons were picked using the time equivalent of the sands B500 surface, C4000 surface and D4100 surface located on the well path. The depth of these sand were converted to time using the checkshot data, and the nearest, brightest and most continuous reflection were mapped on the in-lines. OGBO 046 well was generally used as control.

4.4.2.3.1 GENERATION OF MAPS:

Reservoir Attribute Maps

Seismic attributes were extracted from a 30 ms window from the reservoir intervals of the TWT maps of B5000, C4000, and D4100 to provide additional stratigraphic information. The extracted seismic attributes maps were generated to aid in the data interpretation. These Seismic structural maps were generated to evaluate the geometry of the mapped horizons. These maps also give a 3D perspective of the mapped surfaces. The corresponding time values of the three horizons on all the cross-lines were picked with the use of the in-lines to generate the time map. About five different types of maps were generated to aid in the data interpretation. These maps include: Time structure map, Depth structure map, RMS amplitude map and Maximum amplitude maps. The RMS amplitude attribute extracted for each horizon B5000, C4000 and D4100 were characterized by low to high or variable amplitude reflections with moderate to good continuity. There are truncations in some places which are caused by faults. Time structure maps were produced using the interpolated seismic seed grids for each horizon. The time maps were then converted to depth maps using a simple velocity model. The RMS amplitude maps for B5000, C4000 and D4100 horizons outlined a paleo-geomorphology of tidal inlet and shoreface. The RMS amplitude maps also indicated the lateral variations in sand/ shale content similar to De Angelo and Wood (2001). Amplitude anomalies may be attributed to constructive or destructive interference caused by two or more closely spaced reflectors and/or variations in net sand within a thin bed unit .The dull colors (or the lower RMS amplitude values) occurred predominantly in the shaly portion whereas the bright colors (or the higher RMS amplitude values) occur in the predominantly sandy portion. Seismic reflection amplitude information helped to identify unconformities, reefs, channels, and gas/fluid accumulations. The RMS amplitudes are sensitive to sandstone-bearing systems tracts within the reservoir-bearing succession and helped define spatial distribution of genetically related depositional successions De Angelo and Wood (2001). The sandy shoreface reservoirs were clearly highlighted by RMS amplitude in the Eastern portion of the three reservoir intervals, just as the sandy fills were highlighted in the western portion. The high RMS amplitude values tend to occur in the sandier portions of the respective reservoir interval, irrespective of the paleo-environment. Representatives of these maps are shown in (Figures 22, 24, 26, 51, 52, 55, 53, 54, 56 and 57).

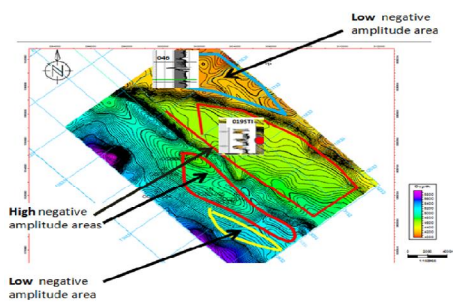


Figure 51: Depth structure map for horizon B5000 surface with well log motif

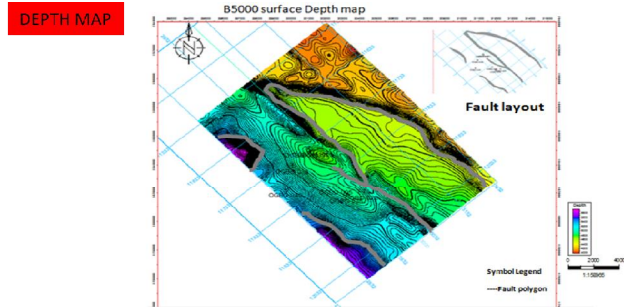


Figure 52: Depth structure map for horizon B5000 surface

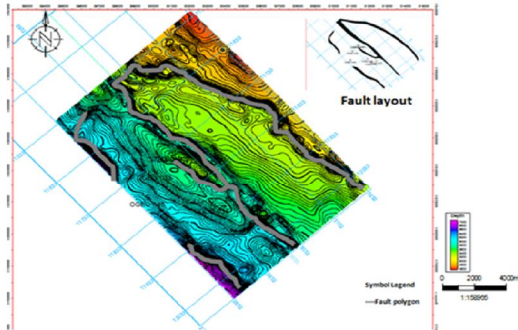


Figure 53: Depth structure map for horizon C4000 surface

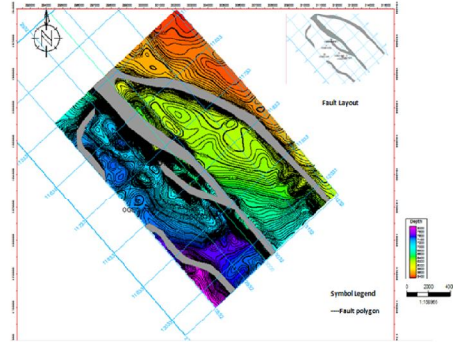


Figure 54: Depth structure map for horizon D4100 surface

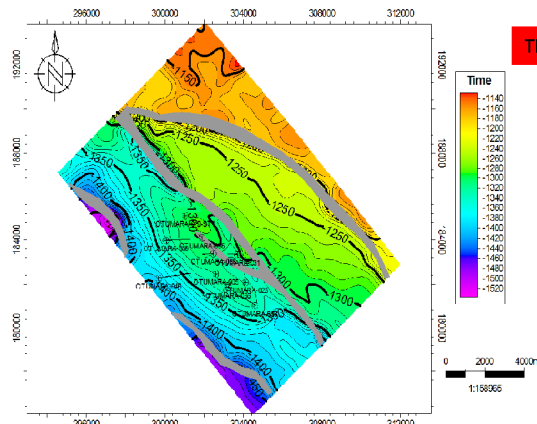


Figure 55: Time Structural map for horizon B5000 surface

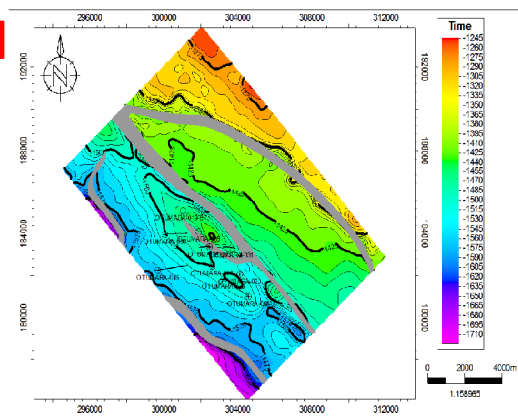


Figure 56: Time Structural map for horizon C4000 surface

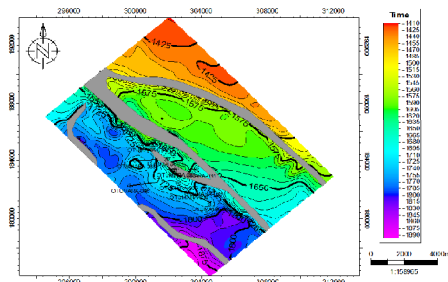


Figure 57: Time Structural map for horizon D4100 surface

4.4.2.3.2 STRUCTURAL DISCUSSION

Prospectivity for hydrocarbon reserves in bye-pass zones is the aim of this study leads to critical look at structures of the interested areas. The prospects were identified (Figures 22, 24, 26, 51, 52, 55, 53, 56, 57, 58 and 59). This was done by identifying structural traps or closures found around fault blocks. The new Prospects (leads) are areas represented on a structural map where hydrocarbons are likely to accumulate. The structural maps shown for B5000 horizon surface (Figure 59), the wells have been drilled into the structural highs (2-way and 3-way fault dependent closures). The areas circled in white (prospect) may not hold with high confidence because it appeared to be on the structural lows (i.e. synclines). This means or suggests for strong focus on identifying stratigraphic traps (as new opportunities for exploration or development wells) more if the structural closures have all been penetrated. However, there was partly closed structural feature in the NW part the depth map shown. One might argue that, given the availability of more data to the north, this might be a potential opportunity if we can figure out whether the contours close-up on the northern part. On this new area however, it will also be good to support it with sand presence verification (from the amplitude map as meaningful observation was not rich possibly due to poor data quality). Clear key concerns must be addressed to make better understanding of the uncertainties with the data and interpretations to enable accurate interpretations/inferences.

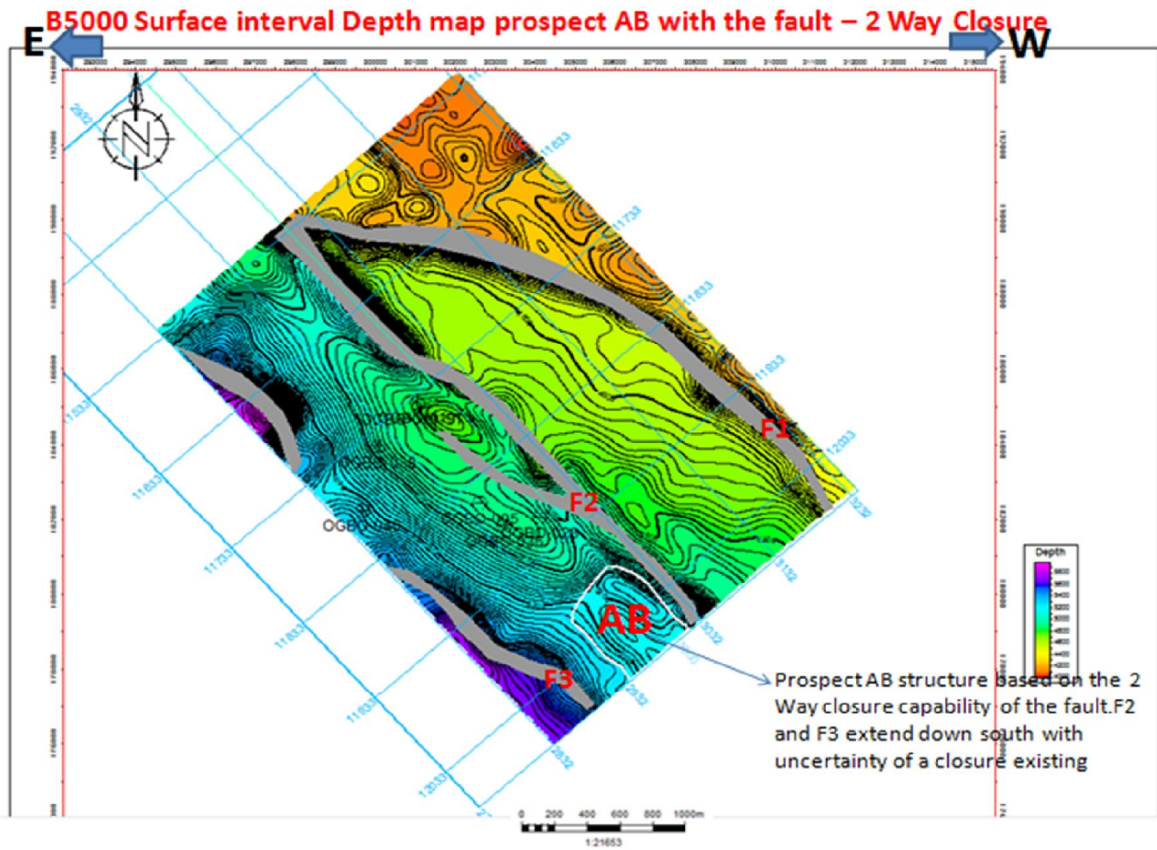


Figure 58: B5000 AB Prospect

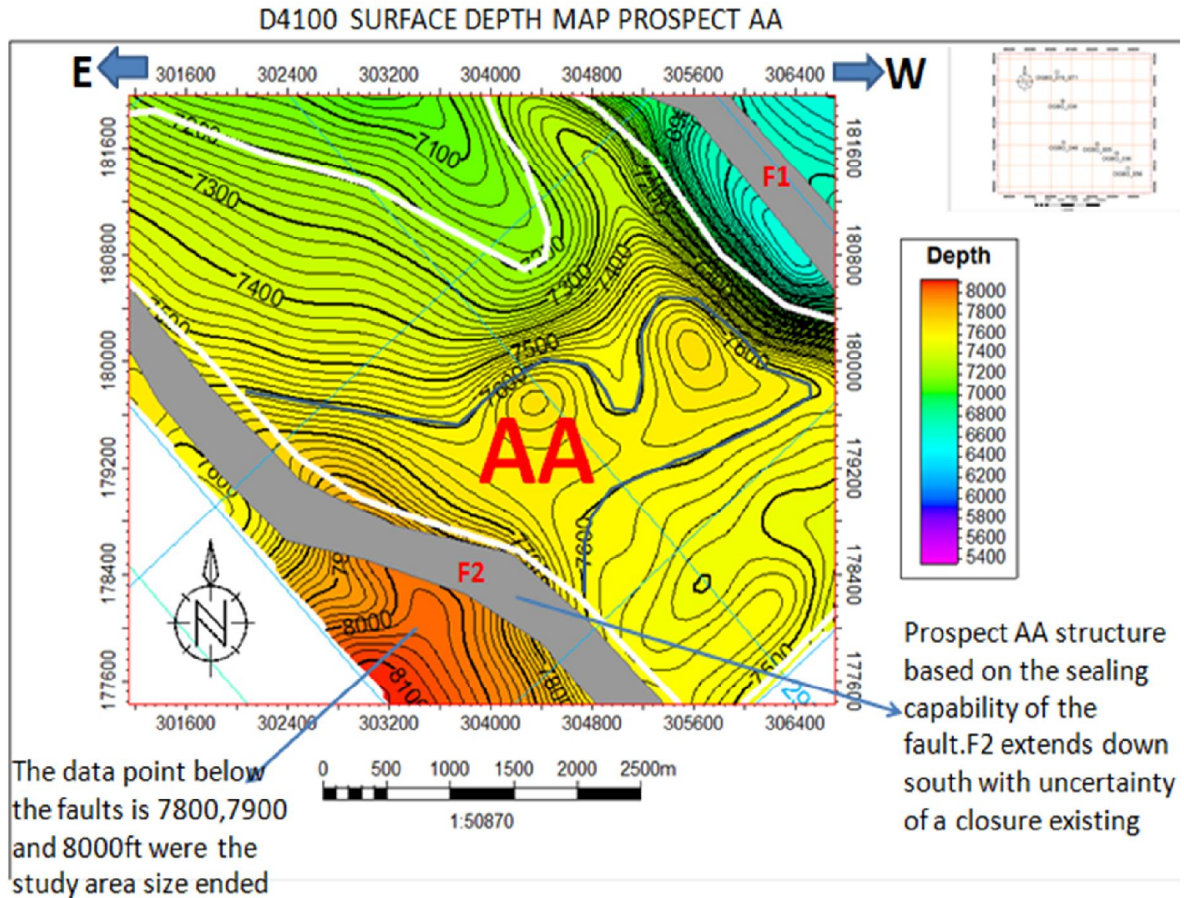
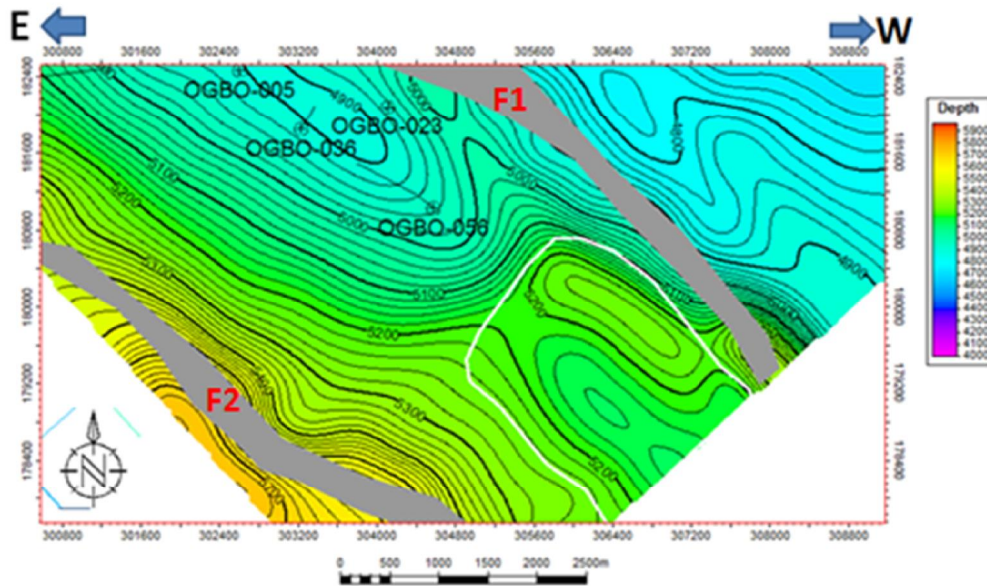


Figure 59: D4100 AA Prospect

The structural maps shown for D4100 surface interval (Figure 59), the contoured map has values ranging from 4600ft to 8000ft. Structural highs were observed at North-western and the central part of the field. This area formed a good trapping system thereby increasing retentive capacity for hydrocarbon. The hydrocarbon trapping system in the central part of the field where the wells were located is a faulted rollover anticlines. The low faults throw in the area is responsible for excellent retentive capacity of hydrocarbons. Structural lows were seen in the south-western region and the area was marked with low confidence prospect.

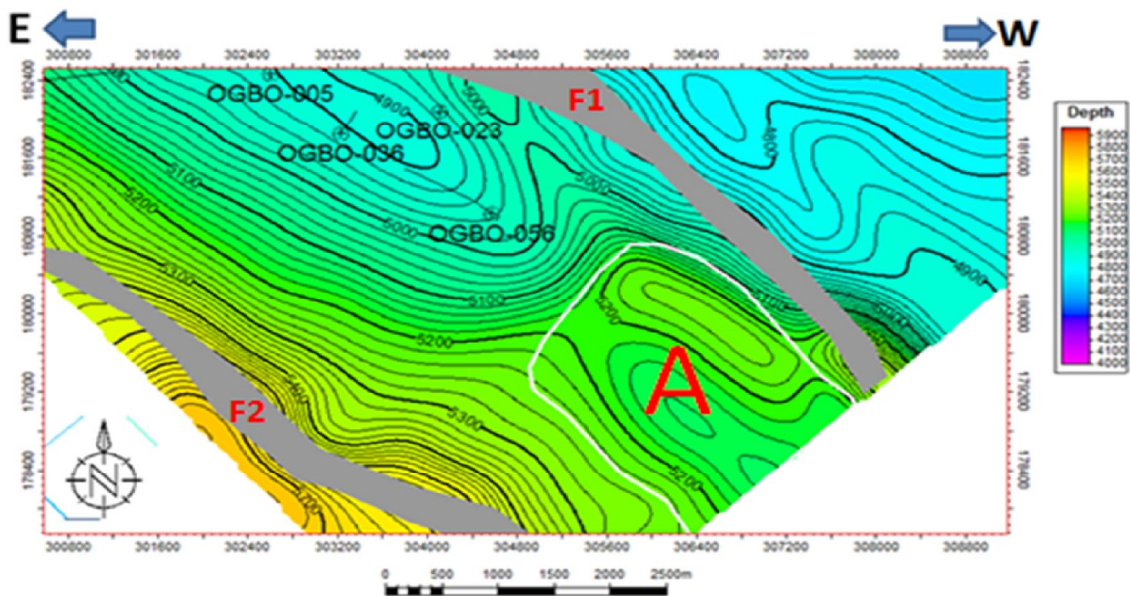
D4100 SURFACE DEPTH MAP PROSPECT



The drilled wells are on the north west section. The area (structure) in white could contain hydrocarbon. The 5200ft contour could be a spill point which may have caused the hydrocarbon to migrate to the areas that have been drilled above

Figure 60: D4100 Prospect A (in white indication) Nameless

D4100 SURFACE DEPTH MAP PROSPECT A



The drilled wells are on the north west section. The area (structure) in white could contain hydrocarbon. The 5200ft contour could be a spill point which may have caused the hydrocarbon to migrate to the areas that have been drilled above

Figure 61: D4100 Prospect A (in white indication) Named A

The depth structural map for D4100 horizon surface showing a prospect (Figure 60 and 61). The contoured interval value ranges from 5200ft Structural highs were observed in the North Western part and the central part served as good traps for the hydrocarbon accumulation. The hydrocarbon trapping system is still faulted rollover anticlines. In the South-Eastern portion of the field, structural lows were observed. The depth structure map of D4100 horizon surface is similar in characteristics to the C4000 horizon surface but is located at a considerable deeper depth. They have the same structural style. (Figures 22, 24, 26, 51, 52, 55, 53, 54 and 56) showed the RMS amplitude and time maps of the interpreted horizons. The amplitude map was used to know the distribution of high and low amplitude across each horizon and characterized the study area, such as lithology and fluid content. The high amplitude zones (red, yellow and green colour) at the E-W part of the map indicate the presence of hydrocarbon and correspond to the structural high of the map. The amplitude map for D4100 sand did not fully correspond to the lithology and this could be due to the technical error from the software used or poor quality data at the deeper zone of the field.

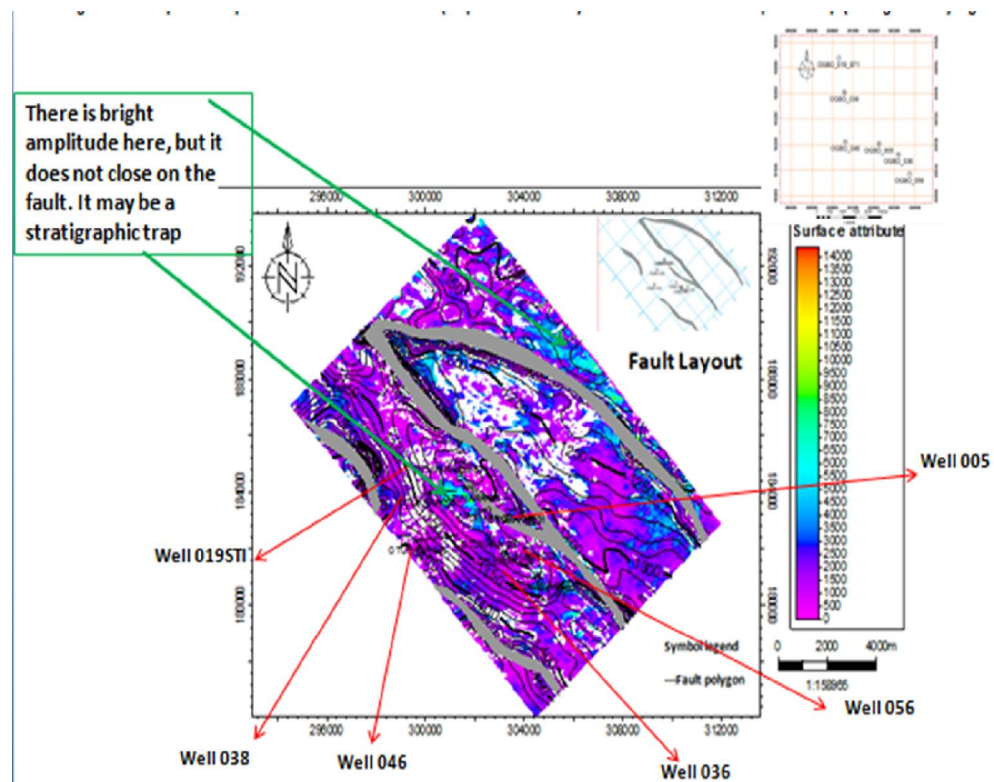


Figure 62: RMS amplitude map for B5000 prospect (stratigraphic trap prospect indication)

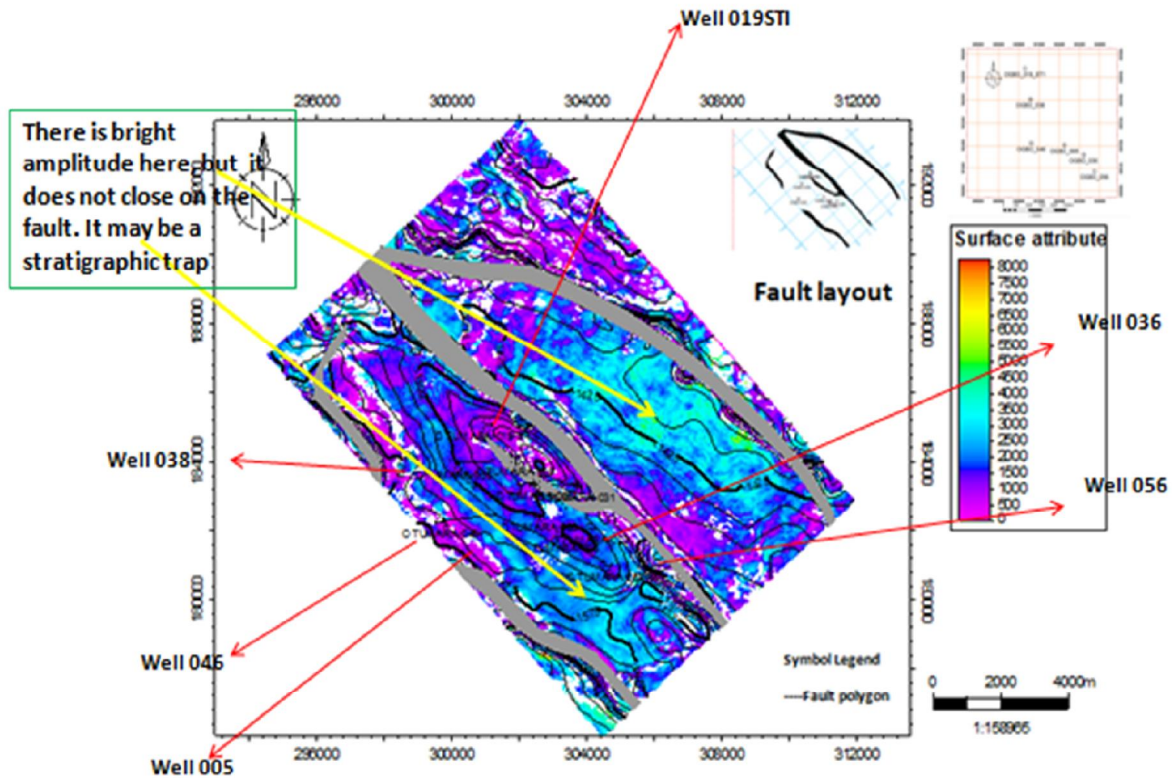


Figure 63: RMS amplitude map for C4000 prospect (stratigraphic trap prospect indication)

(Figures 62, 63 and 64) there is a bright amplitude (bright spot) in the North Eastern and North Western (indicated with a green arrow) portion of the B5000 sand horizon RMS amplitude map. It is not close on the fault and may be a stratigraphic trap, prospect in view to explore. There is a bright amplitude (bright spot) in the Southern and South Eastern (indicated with a yellow arrow) portion of the C4000 sand horizon RMS amplitude map. It is not close on the fault and may be a stratigraphic trap, prospect in view to explore. There is a bright amplitude (bright spot) in the Western (indicated with a green arrow) portion of the D4100 sand horizon RMS amplitude map. It is not close on the fault and may be a stratigraphic trap, prospect in view to explore. Bright spots may be seen as an indication of hydrocarbon presence Beka and Oti (1995). The observed bright spots (high negative anomaly) correspond to good sign for prospect with the rollover structure of the field. Not all of these have anticlinal structures that support hydrocarbon accumulation. (Figures 46, 47, 48 and 49) the 3D structural analysis of the OGBO field have provided a better understanding of the structural styles and hydrocarbon trapping systems of the field. From the seismic and well logs analysis, three hydrocarbon bearing reservoirs (B5000, C4000 and D4100) were

delineated. The net thickness of the reservoir varies between 5ft, 25ft, 31ft, 40ft, 45ft, 55ft, 86ft, 123ft, 139ft and 306 ft. A network of faults and three horizons were interpreted to generate the structure maps. The main faults in the field are growth faults which are listric in nature. The structure maps, indicates that hydrocarbon accumulations in the field are associated with the structural highs and closures that are faults dependent. These structures correspond to the crest of rollover structure in the field. The amplitude maps revealed bright spots on these regions thereby suggesting economic explorable hydrocarbon accumulations. (Figures 65, 66 and 67, also Figure 34) C4000 prospect has a 4-way closure, a rollover anticlinal structure. D4100A and D4100AA prospects have a 2-way closure, which was fault dependent. B5000AB prospect has a 2-way closure, supported by a major fault F2. The prospects have not been tested as 6 wells have been drilled in the field and the wells are producing since over two decades ago.

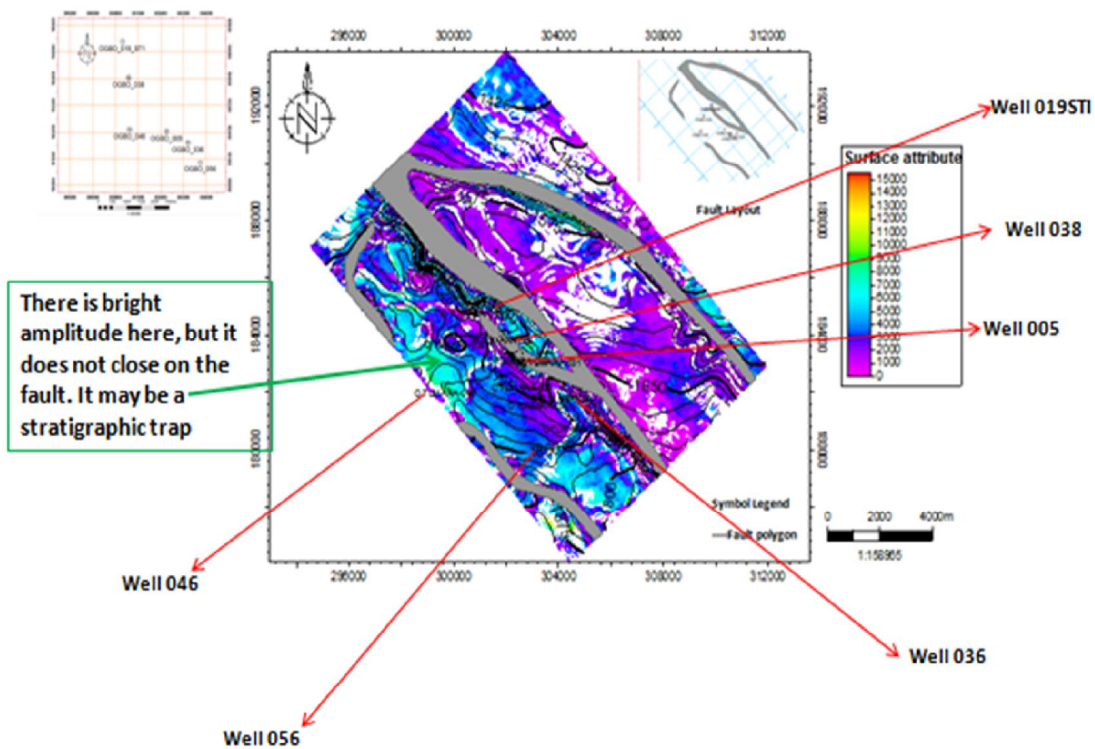
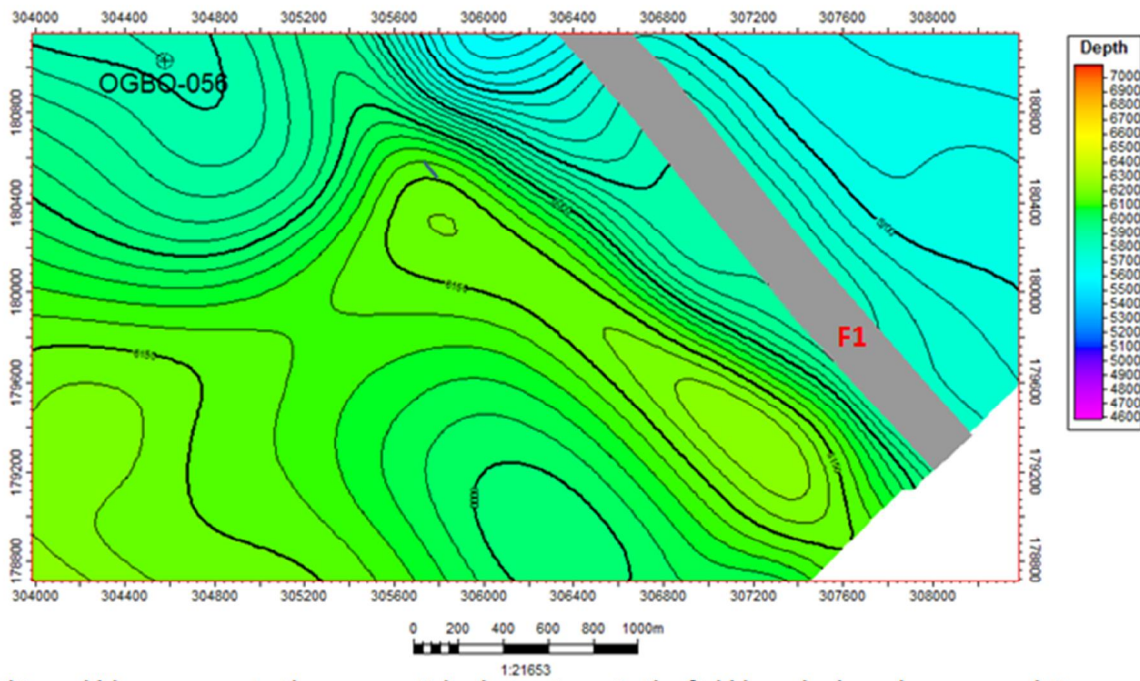


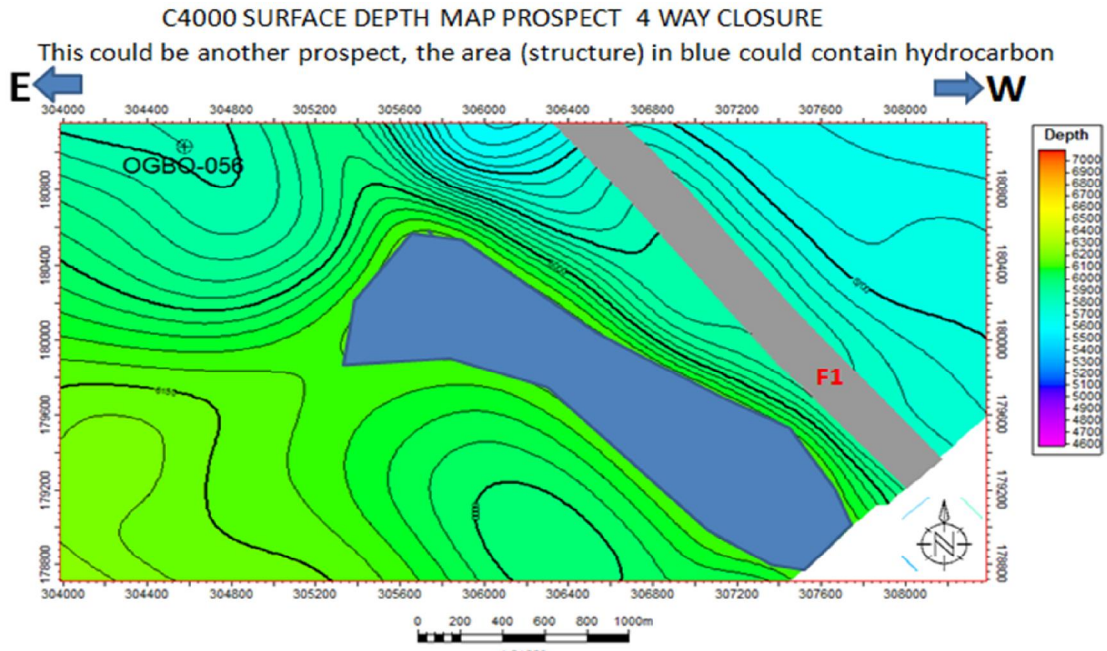
Figure 64: RMS amplitude map for D4100 prospects (stratigraphic trap prospect indication)

C4000 SURFACE DEPTH MAP PROSPECT 4 WAY CLOSURE



This could be a prospect, there are anticlinal structures in the field have hydrocarbon accumulations because of their structural closures. The prospects are anticlinal structure, but most probably unconnected because of the presence of a saddle, an effective saddle

Figure 65: C4000 Prospect



This could be the only prospect, there are anticlinal structures in the field have hydrocarbon accumulations because of their structural closures. The prospects are anticlinal structure, but most probably unconnected because of the presence of a saddle, an effective saddle

Figure 66: C4000 Prospect (blue blanket highlights the saddle structure)

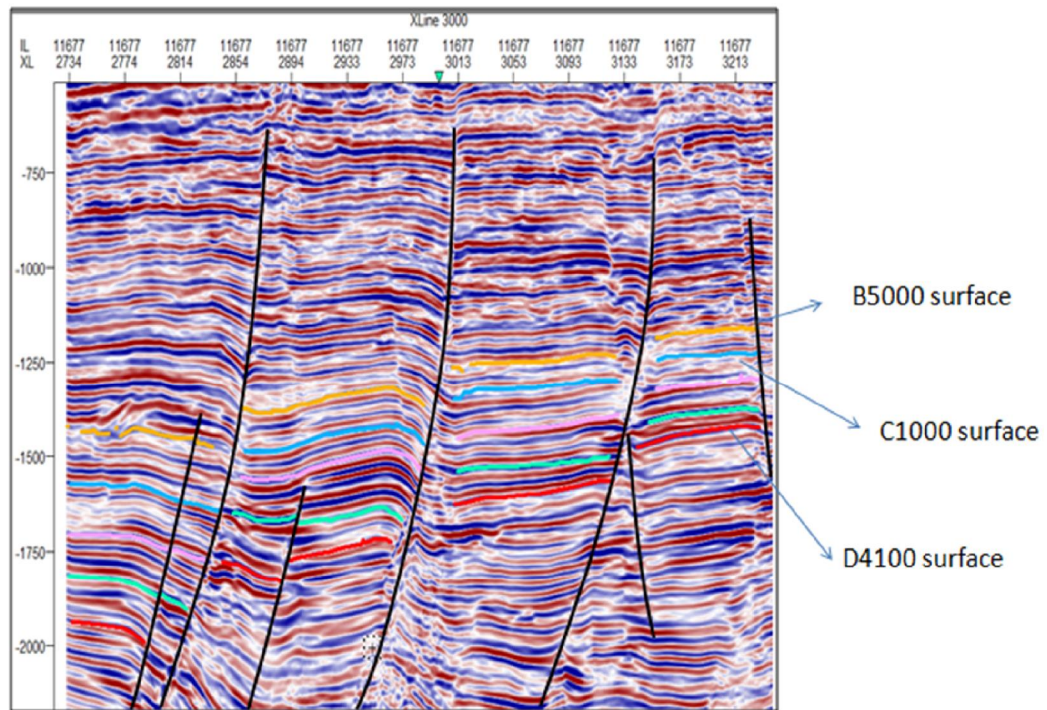


Figure 67: Seismic section and the sand surfaces studied

4.5 OGBO FIELD PETROLEUM SYSTEM POTENTIAL AND EVALUATION

Reservoir Potential of the OGBO field

Eight potential reservoirs (RS1,RS2, RS3, RS4, RS5, RS6, RS7 and RS8) outlined in the OGBO field for the most part were the tidal inlet and shoreface sands of LST/HST, HSTs and LSTs, respectively, that displayed low Gamma ray and high Resistivity values (Figures 68 - 74).

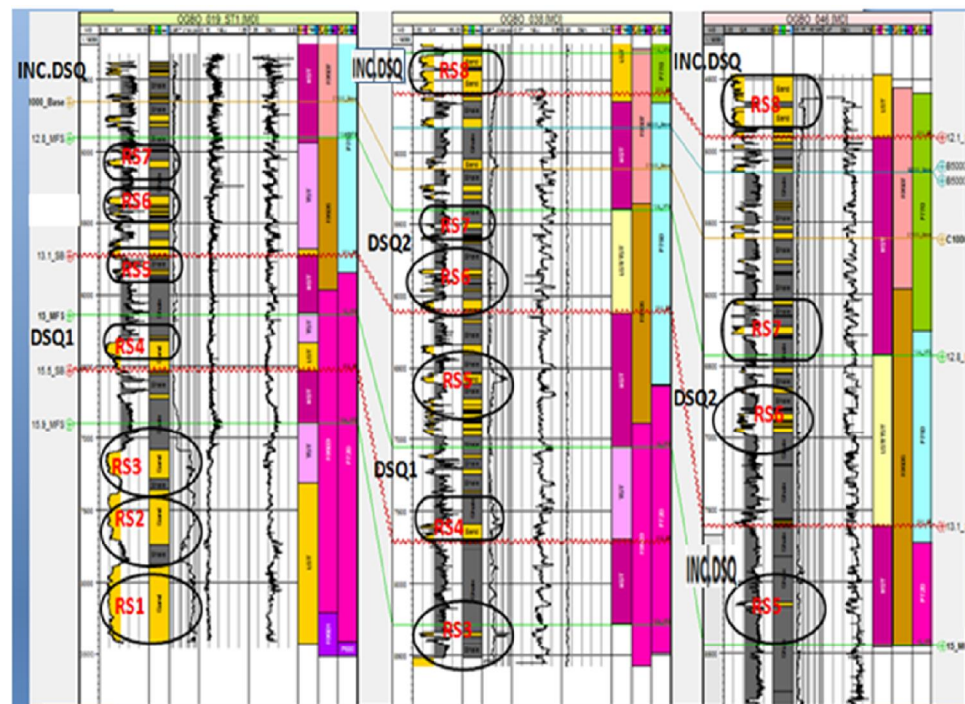


Figure 68: Low Gamma Ray and high resistivity values of potential reservoirs for wells in Strike direction

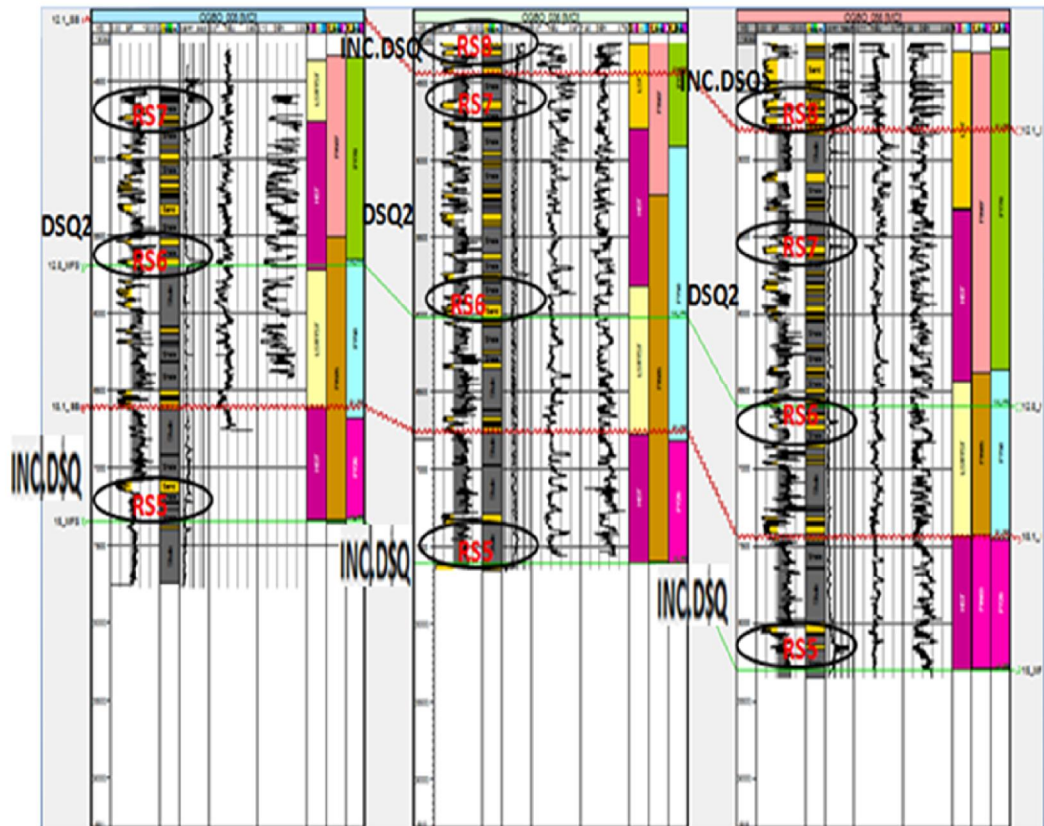


Figure 69: Low Gamma Ray and high resistivity values of potential reservoirs for wells in Dip direction

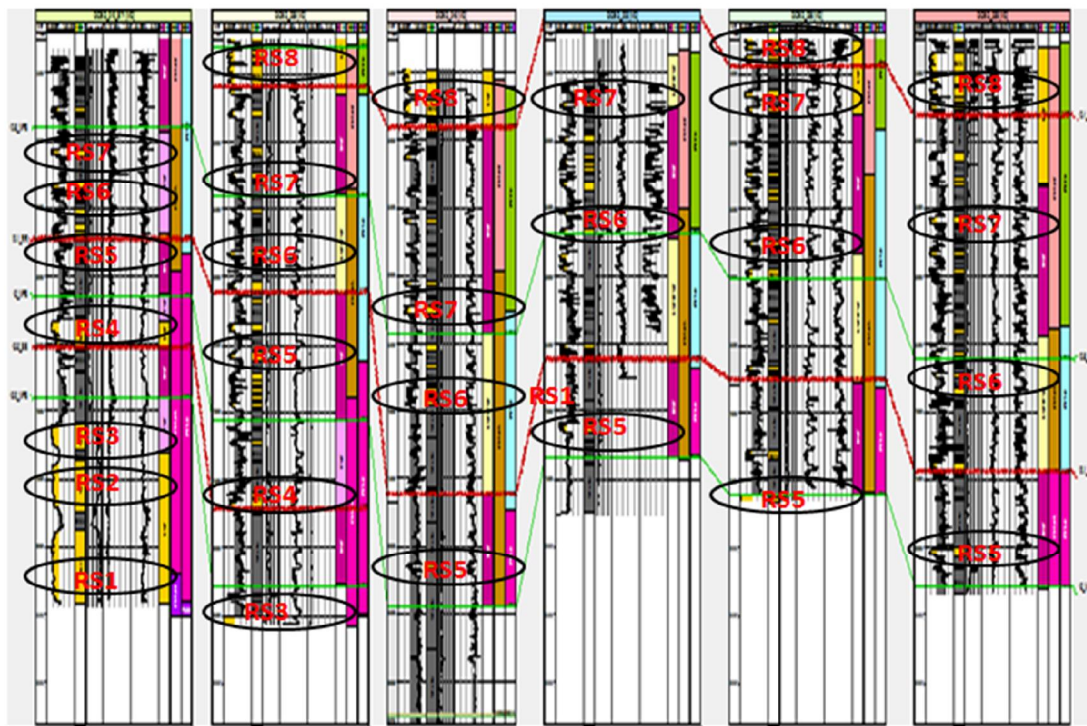
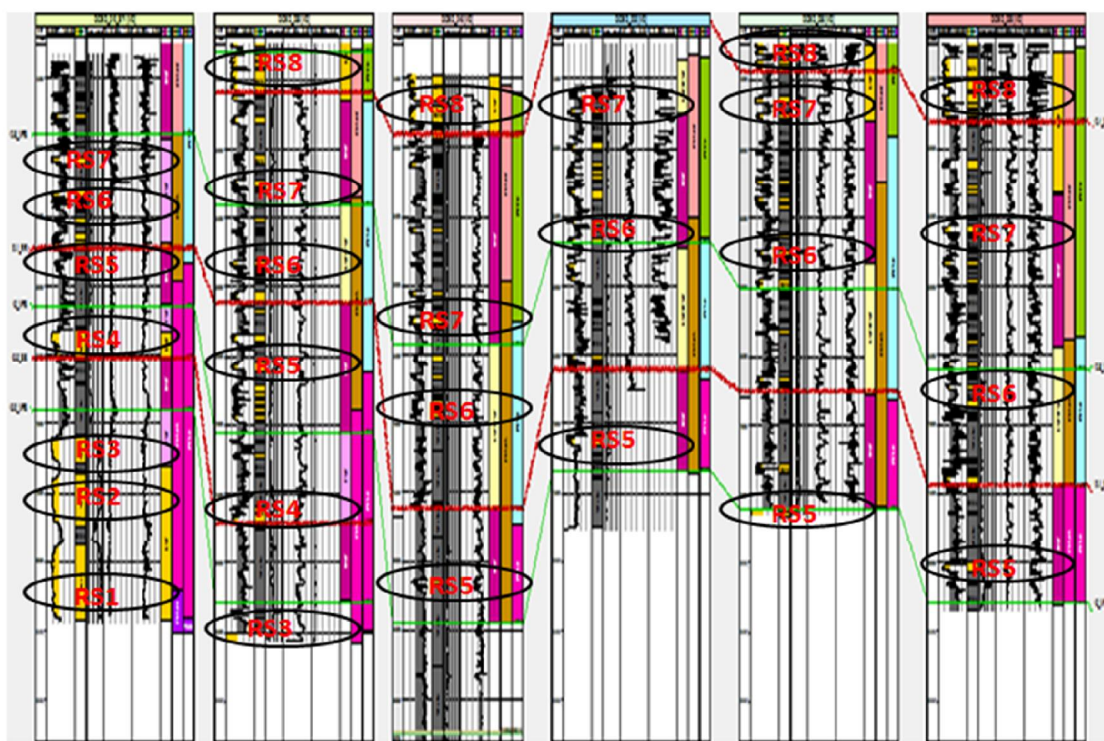


Figure 70: Low Gamma Ray and high resistivity values of potential reservoirs for wells in both Strike and Dip direction



Low Gamma Ray and high resistivity values of potential reservoirs for wells in both Strike and Dip direction from OGBO 019STI, 038, 046, 005, 036 and 056

Figure 71: Low Gamma Ray and high resistivity values of potential reservoirs for wells in both strike and Dip direction from OGBO 019STI, 038, 046, 005, 036 and 056

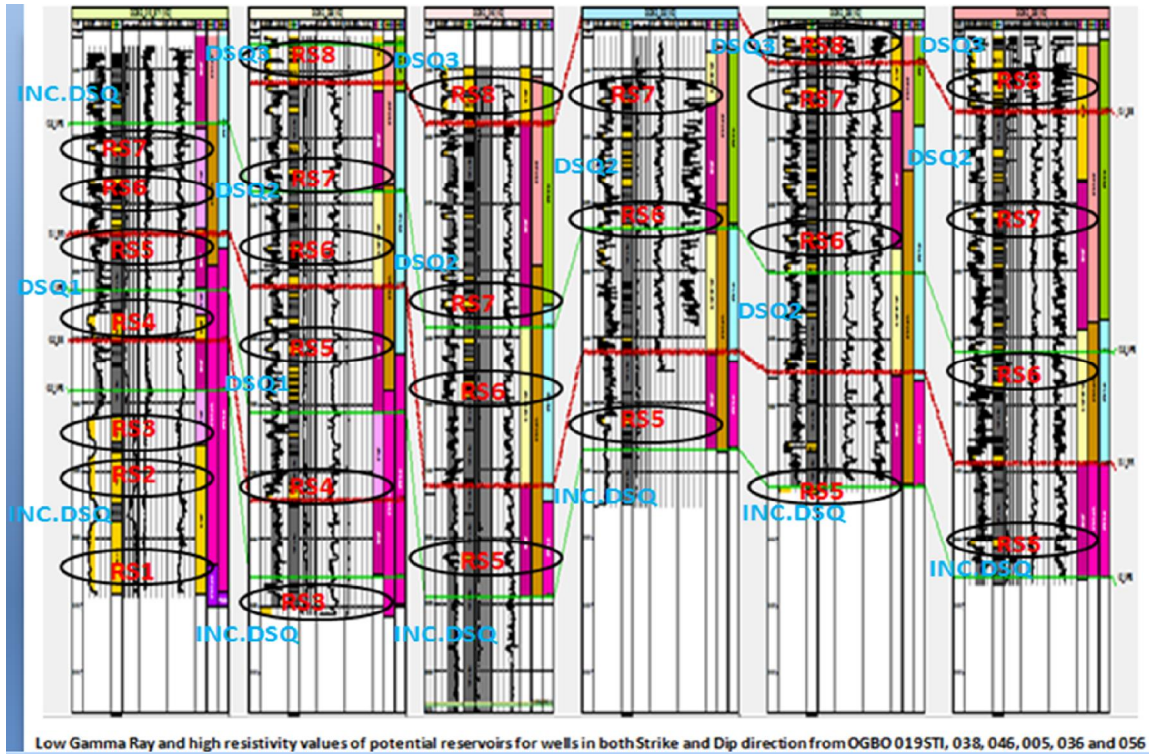


Figure 72: Depositional sequence analysis across the six OGBO wells in both strike and dip direction

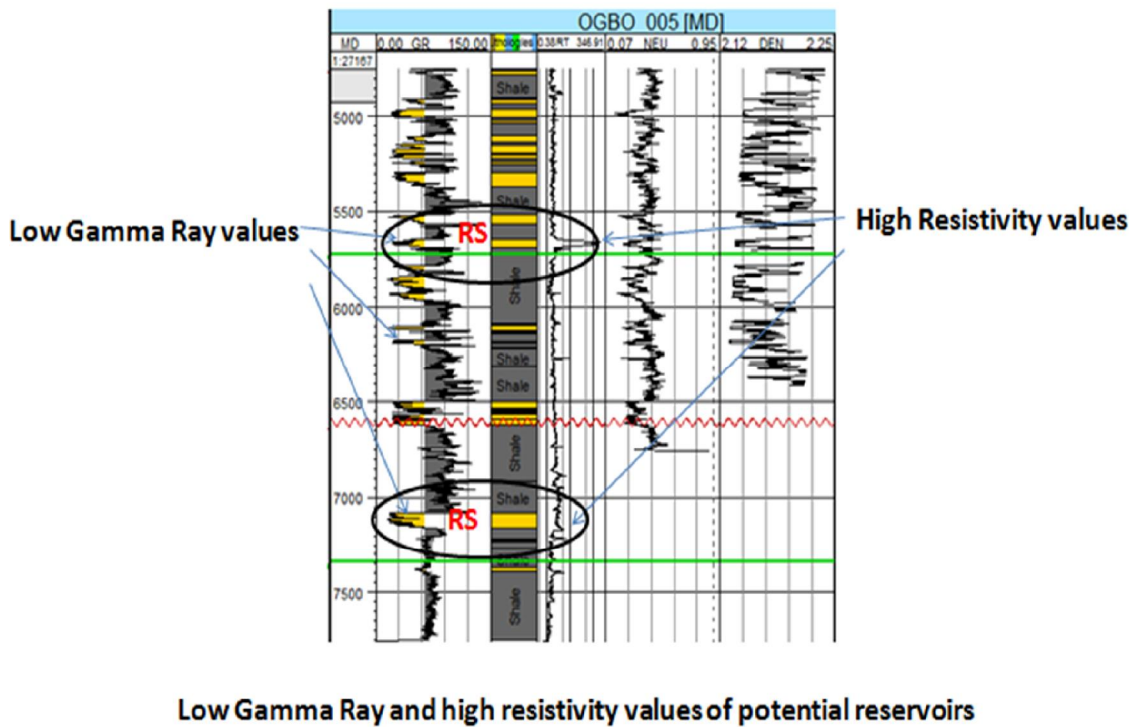
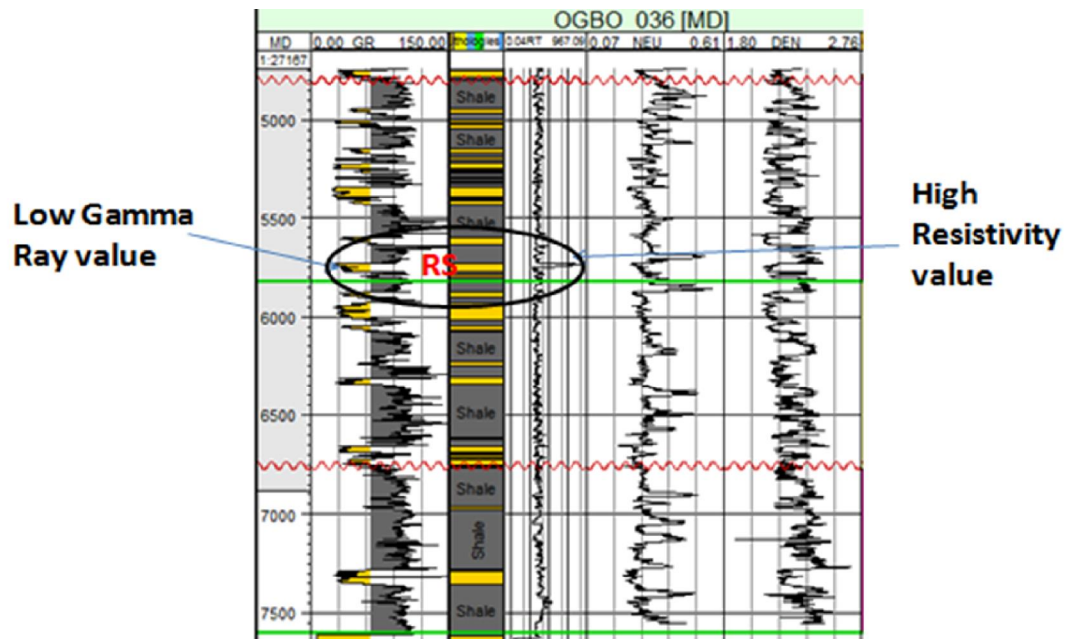


Figure 73: Delineated reservoir from OGBO 005 well



Low Gamma Ray and high resistivity value of potential reservoir

Figure 74: Delineated reservoir from OGBO 036 well

Reservoir Geometry

The variety of reservoirs in the field (Figures 68 - 74) which may likely be stacked lower and upper shoreface sands and tidal inlet, range above 5feet to about 306 feet thick. Based on reservoir quality and geometry in the OGBO field, the most important reservoir types range above 50ft.

Source Rock Potential

Considering individually dense shale units of the TST recognized in the studied wells were considered as likely potential source rocks for the hydrocarbons found in the reservoirs in OGBO field. In the absence/ non provision of TOC data of the field, literature revealed that the petroleum of this basin is sourced from the Akata Formation, with smaller amounts generated from the mature shale beds in the lower Agbada Formation. The total organic-carbon (TOC) content of sandstone, siltstone, and shale in his study is essentially the same (average of 1.4 to 1.6% TOC). The content, however, seemed to vary with age of the strata a trend of decreasing content with decreasing age (average of 2.2% in the late Eocene

compared to 0.9% in Pliocene strata). Bustin's Eocene TOC average compares well with the averages of 2.5% and 2.3% obtained for Agbada-Akata shales in two wells Udo and Ekweozor (1988). Ekweozor and Okoye (1980) reported TOC values from 0.4 to 14.4% in the both onshore and offshore paralic sediments. Nwachukwu and Chukwura (1986) report values as high as 5.2% in paralic shales from the western part of the delta. The higher TOC contents are limited to thin beds and are only easily recognized in conventional cores Doust and Omatsola (1990). The organic matter consists of mixed maceral components (85-98% vitrinite with some liptinites and amorphous organic matter) Bustin (1988). There is no evidence of algal matter and the shales are low in sulfur (.02 to .1 %). Hydrogen indices (HI) are low and range from 160 to less than 50 mg HC/g TOC. Ekweozor and Daukoru (1994) believed that Bustin's average of 90 mg HC/g TOC underestimated the true source-rock potential because of matrix effects on whole-rock pyrolysis of deltaic rocks. Udo and others (1988) report HI values of 232 for immature kerogen isolates from Agbada-Akata shales.

Seal/Trapping Mechanisms

The primary seal rock in the Niger Delta is the interbedded shale within the Agbada Formation. The shale provides three types of seals- vertical seals, clay smears along faults and interbedded sealing units in a direction opposite which reservoir sands are juxtaposed due to faulting, Doust and Omatsola (1990). Residue of well correlation showed that delineated constrained surfaces were not laterally continuous. These truncations were concluded by reasoning to be as a result of the sydepositional faults in the area. These faults laid the ground work of the major traps for hydrocarbon accumulation in this field. In this study, the shale of HST and shale units on the inside of the TST are able to form bottom and top seals for hydrocarbons in the reservoir sand was inferred. The reservoir rocks of the LST and HST and the seals out of the prodelta shales of the TST can combined to represent stratigraphic traps for hydrocarbon addition (accumulation) in the field. Known traps in the Niger Delta basin are structural, even though stratigraphic traps are not remarkable as stratigraphic traps. The structural traps worked out during synsedimentary deformation of Agbada paralic sequences Evamy et al, (1978); Stacher (1995). A collection of structural trapping elements, having those featured with simple rollover structures, clay/mud filled channels, structures having multiple growth faults, structures with antithetic faults, and collapsed crest structures, have been described by Doust and Omatsola (1990). On the flanks of the delta, stratigraphic traps are likely as important as structural traps Galloway (1989).

Furthermore, the sand units of the HST and LST formed the tidal inlet, lower shoreface sands and upper shoreface sands of the delta. The high resistivity log values suggested that they are potential good hydrocarbon reservoirs. The shales of the TST in which most of the MFS were delineated, could form seals to the reservoir units in the field. A combination of the reservoir sands of the LST and HST and the shale units of the TST can form good stratigraphic traps for hydrocarbon and as a result should also be targeted during hydrocarbon exploration.

4.6 FORMATION EVALUATION

Definition of terms:

Gross thickness: It is the thickness of the stratigraphically defined interval in which the reservoir beds occurred; including such non-productive intervals as may be interbedded between the productive intervals.

Net pay (net productive) thickness: It is the thickness of those intervals in which porosity and permeability are known or supposed to be high enough for the interval to be able to produce oil or gas.

Net oil-bearing thickness: It includes those intervals in which oil is present in such saturation that the interval may be expected to produce oil, if penetrated by a properly completed well.

4.6.1 PETROPHYSICAL ANALYSIS SUMMARY

The different petrophysical parameters computed for the D4100, C4000 and

B5000 reservoirs are tabulated below:

Table 7: Formation Evaluation (Petrophysical analysis summary)

Reservoir	Formation	Thickness s (ft)	GR	Gross s	Net (ft)	NTG (ft)	ICR	Vsh	Bulk Den	ϕ frac	ϕ_{den} frac	ϕ_{sh} frac	BWV	ϕ_{eff} frac	Rt	Sh	Sw	FRF	Smitr	K(MD)	Well no.
C4000	Aghbala	5010	73.23	97	45	0.43	0.46	0.20	2.21	0.28	0.27	0.06	0.22	0.22	2.19	0.21	0.79	10.96	0.07	245691	005
D4100	Aghbala	6192	64.17	6	5	0.83	0.40	0.23	2.16	0.30	0.30	0.04	0.27	0.24	1.90	0.15	0.90	9.21	0.07	648427	005
B5000	Aghbala	4905.5	77.92	97	86	0.83	0.49	0.18	2.09	0.33	0.33	0.01	0.26	0.26	2.28	0.22	0.81	7.35	0.06	6081398	046
C4000	Aghbala	5103.5	87.13	106	45	0.42	0.62	0.33	2.13	0.33	0.33	0.01	0.33	0.26	1.75	0.01	0.99	9.30	0.13	1090805	0195II
B5000	Aghbala	4726.5	96.69	221	123	0.53	0.80	0.58	2.19	0.15	0.25	0.01	0.01	0.10	2.31	0.99	0.01	18.54	0.09	2173	038
C4000	Aghbala	5631	65.40	96	40	0.41	0.32	0.21	2.16	0.30	0.30	0.01	0.01	0.24	1.50	0.99	0.01	9.89	0.07	537459	038
B5000	Aghbala	4890	98.29	476	306	0.64	0.44	0.18	2.26	0.24	0.24	0.01	0.01	0.20	1.16	0.99	0.01	14.96	0.08	94891	056
C4000	Aghbala	5637.5	58.33	57	55	0.96	0.22	0.09	2.20	0.28	0.28	0.01	0.01	0.26	1.43	0.99	0.01	11.83	0.08	714760	056
B5000	Aghbala	4108	10.85	334	139	0.41	0.17	0.04	2.16	0.30	0.30	0.01	0.02	0.26	2.40	0.05	0.05	9.23	0.06	711639	026
C4000	Aghbala	5039.5	33.60	71	25	0.35	0.10	0.03	2.17	0.30	0.30	0.03	0.26	0.25	3.46	0.15	0.85	9.43	0.07	787311	036
D4100	Aghbala	6315	48.47	56	21	0.62	0.29	0.11	2.20	0.26	0.26	0.01	0.01	0.21	1.91	0.90	0.02	12.31	0.00	220351	026

Table 8: Reservoir Delineation and petrophysical parameters summary

OCBO Well	Reservoir Sands	Thickness (Ft)	NTC (%)	Vshale (%)	Sw	Sh	Bulk Den	BVW	Φ_{den}	K (Md)	Φ_{eff}	Fm
005	C4000	92	48	10	0.99	0.01	2.18	0.28	0.28	3795.90	0.25	Agbada
005	D4100	6	83	2	0.89	0.11	2.12	0.28	0.31	12448.05	0.30	Agbada
046	D5000	97	88	1	0.86	0.17	2.08	0.29	0.33	18903.38	0.33	Agbada
019STI	C4000	106	42	41	0.32	0.68	2.28	0.08	0.24	213.75	0.14	Agbada
038	B5000	231	53	40	0.24	0.76	2.08	0.04	0.16	19.49	0.09	Agbada
038	C4000	95	41	10	0.93	0.07	2.07	0.31	0.33	11166.78	0.29	Agbada
056	B5000	476	64	10	0.21	0.79	2.25	0.05	0.23	948.91	0.19	Agbada
056	C4000	57	96	1	0.11	0.89	2.12	0.04	0.31	14350.63	0.31	Agbada
036	B5000	41	41	4	0.05	0.95	2.15	0.01	0.29	7416.39	0.28	Agbada
036	C4000	35	35	3	0.85	0.15	2.15	0.26	0.30	8375.40	0.28	Agbada
036	D4100	50	62	18	0.02	0.98	2.15	0.01	0.26	1844.37	0.21	Agbada

From the well logs analysis in the six wells, three hydrocarbon bearing reservoirs (B5000, C4000 and D4100) were delineated. The net thickness of the reservoir varies between 5ft, 25ft, 31ft, 40ft, 45ft, 55ft, 86ft, 123ft, 139ft and 306 ft.

DISCUSSION AND INTERPRETATION OF PETROPHYSICAL PARAMETERS

Abnormally lower porosity values possibly may be due to secondary compaction caused by the shale diapir. Permeability decreases may be attributed to secondary compaction also. Net to gross ratio had similar trend as effective porosity with localized lower values around OGBO wells 036, 046, 019STI and 056 were at the higher side whereas wells 038 and 005 were on the lower side. This also indicated that the reservoir sand was thicker in the western portion than in the eastern portion. The total shale volume followed a reversed trend with the higher values at OGBO wells 038, 019STI and 005 while 036,046 and 056 have lower values. This indicated a deeper marine setting as you go further Eastward which depicted the distal portion of the slope channel. The field generally showed decrease in the reservoir apparent thickness from West to East. The Irreducible water saturation in the entire field is dominantly between 6 to 8% and there is every tendency of producing water alongside the hydrocarbon. To produce less water therefore, the production well must be sited on the crest of the dome. The central portion also have higher tendency to store hydrocarbon. This is so because of the 4-way closure provided by the sedimentary dome as inferred in this study.

4.7 PROSPECT EVALUATION

A prospect is a potential trap which geologists believe may contain hydrocarbons. A significant amount of geological, structural (analysis and evaluation of the generated attribute maps) and seismic investigation must first be completed to redefine the potential hydrocarbon drill location from a lead to a prospect. Five geological factors have to be present for a prospect to work and if any of them fail neither oil nor gas will be present. They are ;

A source rock - When organic-rich rock such as oil shale or coal is subjected to high pressure and temperature over an extended period of time, hydrocarbons form.

Migration - The hydrocarbons are expelled from source rock by three density-related mechanisms: the newly matured hydrocarbons are less dense than their precursors, which cause over-pressure; the hydrocarbons are lighter, and so migrate upwards due to buoyancy,

and the fluids expand as further burial causes increased heating. Most hydrocarbons migrate to the surface as oil seeps, but some will get trapped.

Reservoir - The hydrocarbons are contained in a reservoir rock. This is commonly a porous sandstone or limestone. The oil collects in the pores within the rock although open fractures within non-porous rocks (e.g. fractured granite) may also store hydrocarbons. The reservoir must also be permeable so that the hydrocarbons will flow to surface during production.

Trap - The hydrocarbons are buoyant and have to be trapped within a structural (e.g. Anticline, fault block) or stratigraphic trap. The hydrocarbon trap has to be covered by an impermeable rock known as a seal or cap-rock in order to prevent hydrocarbons escaping to the surface. (Figure 67) seismic section showing the three studied sands and (Figures 60 ó 65 and 75- 79) Three reservoirs B5000 surface interval, C4000 surface interval and D4100 surface interval were delineated and properly evaluated in the study.

B5000 horizon surface interval

The structural maps shown for B5000 surface interval with B5000AB prospect, the wells have been drilled into the structural highs (2-way and 3-way fault dependent closures). The areas circled in white (prospect) may not hold with high confidence because it appeared to be on the structural lows (i.e. synclines). This means or suggests for strong focus on identifying stratigraphic traps (as new opportunities for exploration or development wells) more if the structural closures have all been penetrated. However, there was partly closed structural feature in the NW part the depth map shown. One might argue that, given the availability of more data to the north, this might be a potential opportunity if we can figure out whether the contours close-up on the northern part. On this new area however, it will also be good to support it with sand presence verification (from the amplitude map as meaningful observation was not rich possibly due to poor data quality). Clear key concerns must be addressed to make better understanding of the uncertainties with the data and interpretations to enable accurate interpretations/inferences (Figures 58, 59, 60, 61, 62, 63, 64, 65, 66 and 67).

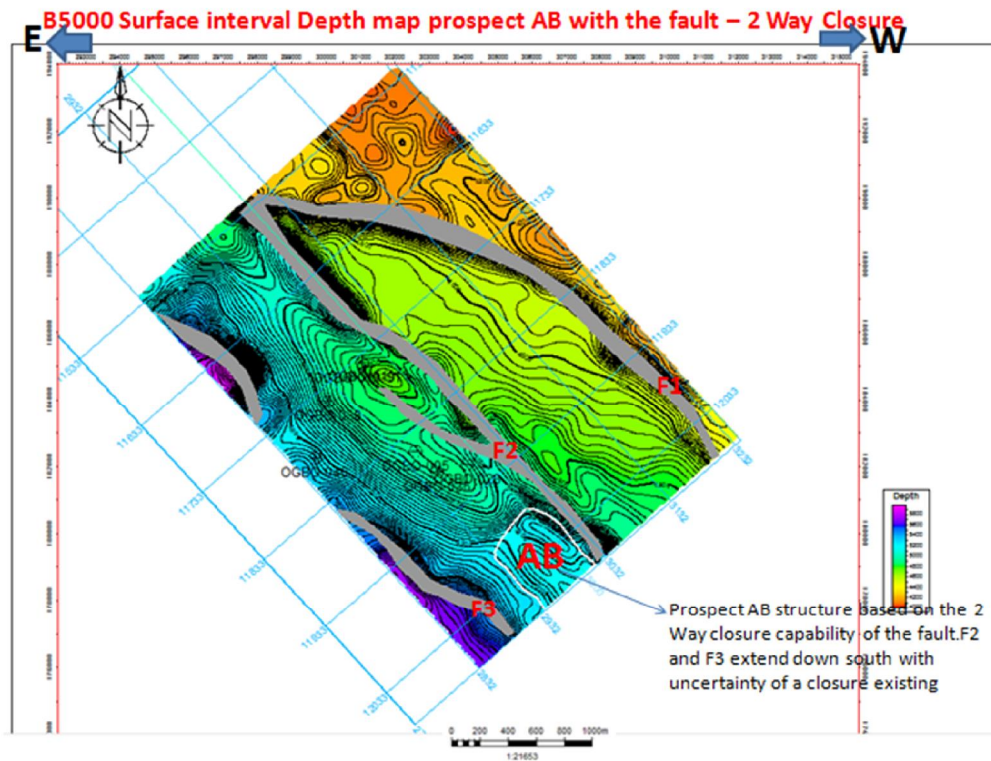


Figure 75 : Depth Structural map for horizon B5000 surface with B5000AB prospect

There is bright amplitude indication (indicated with green arrow) (Figure 62) at the North Eastern portion of the field between well 038 and 046 but it does not close on the fault and the second one at the North Western portion in the study area, which is close on the fault. Both may be a stratigraphic trap and also an interesting prospect while the NW portion prospect is more promising because of fault closure presence.

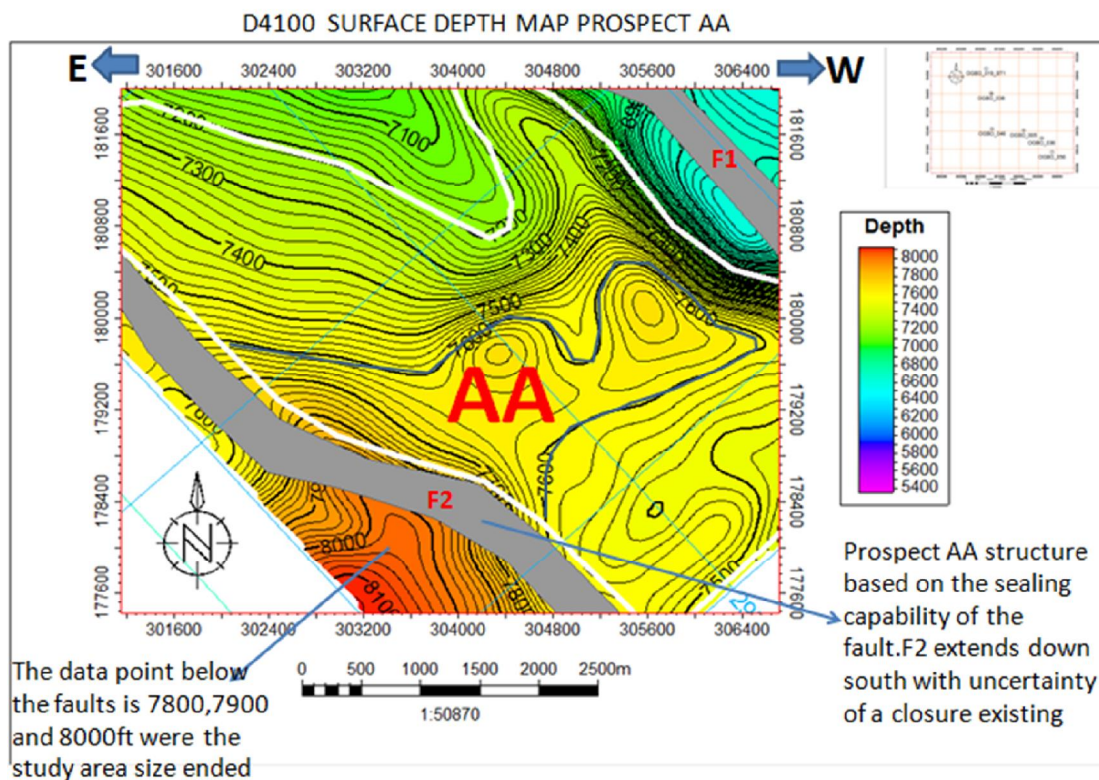


Figure 76: D4100 horizon surface interval depth map with prospect AA

D4100 horizon surface interval

The structural maps shown for D4100 horizon surface interval with D4100 A and D4100AA prospects (Figures 59, 60, 61, 74,75 and 76), the contoured map has values ranging from 4600ft to 8000ft Structural highs were observed at North-western and the central part of the field. This area formed a good trapping system thereby increasing retentive capacity for hydrocarbon. The hydrocarbon trapping system in the central part of the field where the wells were located is a faulted rollover anticlines. The low faults throw in the area is responsible for excellent retentive capacity of hydrocarbons. Structural lows were seen in the south-western region and the area was marked with low confidence prospect. (Figures 60 and 61) the depth structural map for D4100 horizon surface interval. The contoured interval value ranges from 5200ft Structural highs were observed in the North Western part and the central part served as good traps for the hydrocarbon accumulation. The hydrocarbon trapping system is still faulted rollover anticlines. In the South-Eastern portion of the field, structural lows are observed. There is bright amplitude indication (indicated with green arrow) (Figure

64) close to well 046 at the North Eastern portion in the study area, but it does not so close on the fault. It may be a stratigraphic trap and also an interesting prospect.

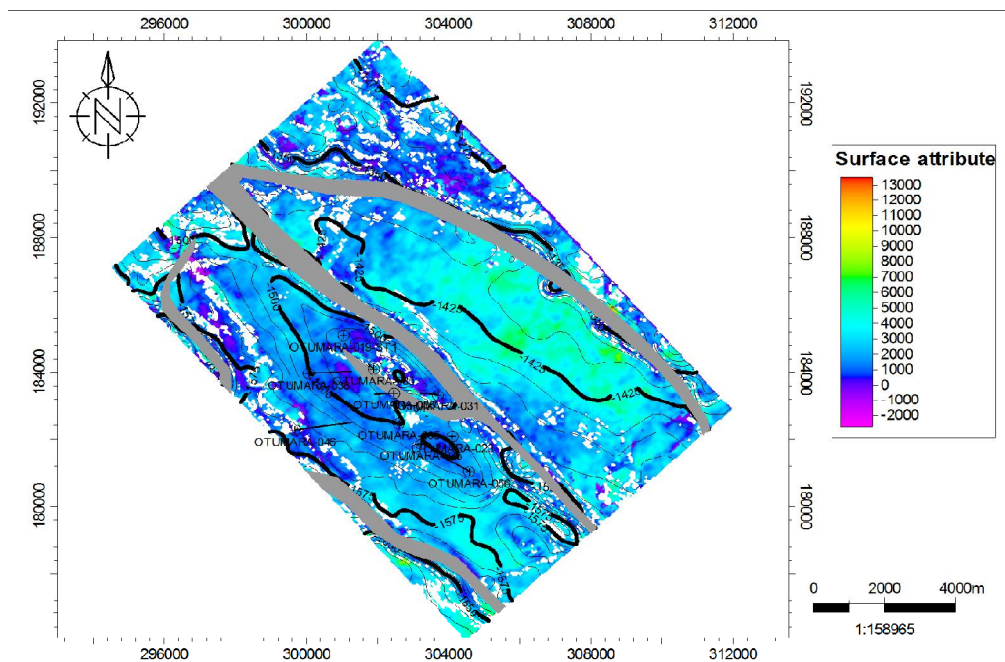


Figure 78: C4000 Surface Maximum Amplitude map

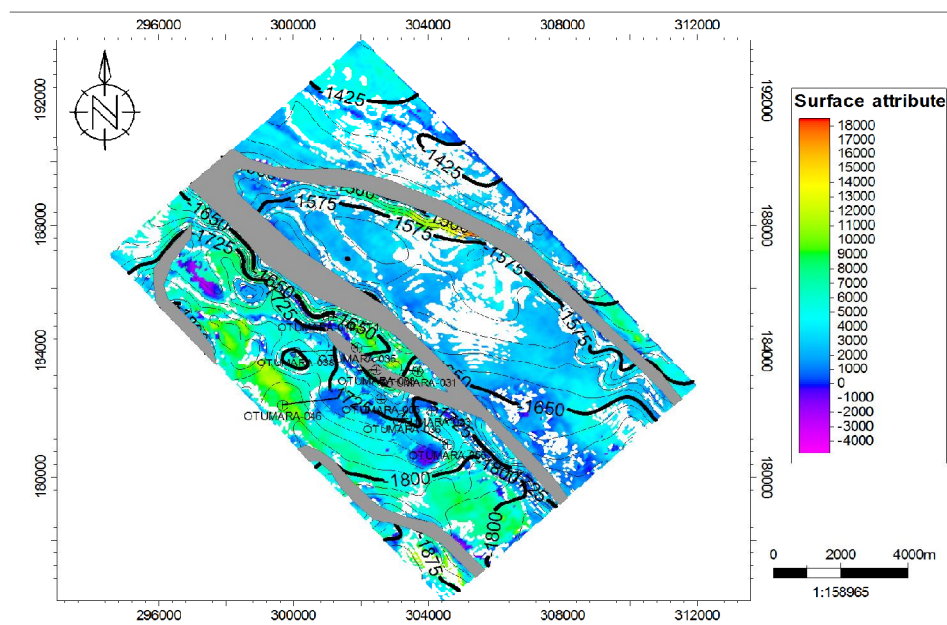


Figure 77: D4100 surface Maximum Amplitude map

C4000 horizon surface interval

The structural maps shown for C4000 horizon surface interval with C4000 prospect, the contoured map has values ranging from 4600ft to 7000ft Structural highs were observed at North-western and the central part of the field. C4000 horizon surface has a 4-way closure, a rollover anticlinal structure and this area formed a good trapping system thereby increasing retentive capacity for hydrocarbon. The hydrocarbon trapping system in the central part of the field where the wells were located is a faulted rollover anticlines. The depth structure map of D4100 horizon surface is similar in characteristics to the C4000 horizon surface but is located at a considerable deeper depth. They have the same structural style. (Figure 63) showed the RMS amplitude map of the interpreted horizons. The amplitude map was used to know the distribution of high and low amplitude across each horizon and characterized the study area, such as lithology and fluid content. The high amplitude zones (red, yellow and green colour) at the E-W part of the map indicate the presence of hydrocarbon and correspond to the structural high of the map. The amplitude map for D4100 sand did not fully correspond to the lithology and this could be due to the technical error from the software used or poor quality data at the deeper zone of the field. A greater part of the central part shows bright spot. Bright spots may be seen as an indication of hydrocarbon presence Beka and Oti (1995), the observed bright spots (high negative anomaly) correspond to good sign for prospect with the rollover structure of the field. Not all of these have anticlinal structures that support hydrocarbon accumulation. There is bright amplitude indication (indicated with yellow arrow) (Figure 63) very close to well 056 South Eastern portion and another location towards South Western portion of the study area, but both are not so close on the faults. It may be a stratigraphic trap and also an interesting prospect. However, the 3D structural analysis of the OGBO field provided a better understanding of the structural styles and hydrocarbon trapping systems of the field. From the seismic and well logs analysis, three hydrocarbon bearing reservoirs (B5000, C4000 and D4100) were delineated. The net thickness of the reservoir varies between 5ft, 25ft, 31ft, 40ft, 45ft, 55ft, 86ft, 123ft, 139ft and 306 ft. A network of faults and three horizons were interpreted to generate the structure maps. The main faults in the field are growth faults which are listric in nature. The structure maps, indicates that hydrocarbon accumulations in the field are associated with the structural highs and closures that are faults dependent. These structures correspond to the crest of rollover structure in the field. The amplitude maps revealed bright spots on these regions thereby suggesting economic explorable hydrocarbon accumulations. C4000 horizon surface has a 4-way closure

(Figures 65 - 66), a rollover anticlinal structure. D4100 has a 2-way closure, which was fault dependent. B5000AB Prospect has a 2-way closure, supported by a major fault F2. The prospects have not been tested as 6 wells have been drilled in the field and the wells are producing.

4.8 VOLUMETRICS , PROSPECT RANKING, RISK AND UNCERTAINTY ASSESSMENT

4.8.1 VOLUMETRICS

This is a broad category process of reserves estimation with the goal of meeting the certainty criteria in the definition of reserves. Volumetric method involved the calculation of reservoir rock volume, the hydrocarbons in place in that rock volume and the estimation of the portion of the hydrocarbons in place that ultimately will be recovered. For various reservoir types at varied stages of development and depletion, the key unknown in volumetric reserves determinations may be rock volume, porosity and fluid saturation.

Rock volume may simply be determined as the product of a single well drainage area and wellbore net pay or by more complex geological mapping. Estimates must take into account geological characteristics, reservoir fluid properties and the drainage area that could be expected for the well or wells. Consideration must be given to any limitations indicated by geological, geophysical data or interpretations as well as pressure depletion or boundary conditions exhibited by test data. Recovery factor based on analysis of production behavior from the subject reservoir, by analogy with other producing reservoirs and/or by engineering analysis. In estimating recovery factors, the evaluator must consider factors that influence recoveries such as rock and fluid properties, hydrocarbons-in-place, drilling density, future changes in operating conditions, depletion mechanisms and economic factors. Porosity and fluid saturation and other reservoir parameters determined from logs and core and well test data. The lower the water saturation, the higher the hydrocarbon saturation in the reservoir sand, also the higher the net to gross value, the higher the hydrocarbon saturation. During this study, a volumetric method is adopted to attempt the determination of the amount of oil in place by using the size of the reservoir as well as the physical properties of its rocks and fluids. Then a recovery factor is assumed, using assumptions from fields with similar characteristics. STOOIP is multiplied by the recovery factor to arrive at a reserve estimate.

The recovery factors for gas cap fields (typical of OGBO field) is usually in the range from 0.15 - 0.25 Ivan Sandra and Rafael Sandra (2007) for solution gas drive, gas cap drive and water drive saturated reservoirs and is usually the first estimate for a new discovery until other production mechanisms have been observed in the field. A simple weighted average among the major oil provinces gives an average recovery factor of 0.22 which is well within the range of the solution gas drive reservoirs. By analogy, the overall recovery factor for the bulk of the world's conventional oil reserves would at best be about 0.20 Ivan Sandra and Rafael Sandra (2007). For the sake of this work however, a recovery factor of 0.20 is employed.

STOIP = Stock tank oil-initially-in-place

STOGIP = Stock tank of gas-initially-in-place

Volumetric Equation = $GRV * \emptyset * NTG * Sh * 1/Bo$

GRV= Gross Roc Volume, \emptyset = Porosity

NTG = Net-to-Gross, (NTG is i.e. percentage ratio of reservoir sand to the total rock volume)

Sh = Oil Saturation, $1/Bo$ = Formation Volume Factor

(Tables 9 and 10) The prospects have relatively low irreducible water saturation. The porosity and effective porosity values across the reservoir have very close similarities. The net to gross ratio is also relatively high. These are direct indications that the reservoir has very good interconnected pore spaces and is symptomatic of the locally high permeability values as against the 1 ó 2 Darcies of the Niger Delta permeability range. They have good hydrocarbon saturation and therefore huge prospect for hydrocarbon production. The low irreducible water saturation would account for a low water saturation cut-off to be employed when considering production well siting. There is every tendency to produce water alongside the hydrocarbon and thus measures for separation must be put in place unless the water saturation cut-off is less than or equal to the irreducible water saturation. The oil reserve was estimated as STOOIP to be about 510953.13 million barrels for B5000 AB prospect, 868124.44 million barrels for C4000 prospect, 2089267.28 million barrels for D4100A prospect and 300405.58 million barrels for D4100AA prospect while the gas reserve was estimated as STOGIP to be

about 6423191.79 MMscf for B5000 prospect, 10913192.34 MMscf for C4000 prospect, 26264178.98 MMscf for D4100A prospect and 3776398.55 MMscf for D4100AA prospect. If the field is produced at the rate of 10,000 barrels per day, it would yield production for approximately 4 years before subsequent secondary and tertiary recovery measures would be employed.

Table 9: Prospects Volumetric analytical studies

ITEM	B5000(046)	B5000(038)	E5000 (040)	B5000(036)	C4000(005)	C4000 (0195II)	C4000 (038)	C4000(016)	C4000(036)	D4100(A003)	D4100(A036)	D4100(AA003)	D4100(AA036)
GROSS ROCK VOLUME (GRV) M ³	4856775	4856775	4856775	4856775	1635625	1635625	1635625	1635625	1635625	16583425	16583425	2387425	233342
NFT-G-GROSS POTENTIAL	0.33	0.53	0.64	0.41	0.48	0.42	0.41	0.96	0.35	0.83	0.62	0.83	0.62
POROSITY Fac.	0.33	0.74	0.74	0.30	0.78	0.33	0.30	0.37	0.30	0.30	0.76	0.30	0.76
HYDROCARBON SATURATION (%) Fac.	0.12	0.95	0.99	0.95	0.21	0.01	0.99	0.99	0.15	0.15	0.98	0.15	0.98
FORMATION VOLUME FACTOR (GVF)	1.29	1.25	1.29	1.29	1.29	1.29	1.29	1.29	1.29	1.29	1.29	1.29	1.29
STOIP (A/B/O/E)	40073.64	821842.32	896021.15	752093.92	39551.41	2924.40	256929.37	641696.77	3379520.26	799014.10	3379520.26	114586.38	485924.78

4.8.2 PROSPECT RANKING

Generating many prospects is one thing, but analyzing each one of them is another and is near impossible. It is therefore necessary to be able to select representative prospect for a more in-depth analysis and understanding of the possible dynamic responses of the reservoirs. However, the rank of a particular prospect is, of course, dependent on the criteria chosen to perform the ranking. This means that a model is representative to serve as a basis of a given decision only if the ranking criterion is representative of the decision that needs to be made. The ranking of all prospects given the displayed criteria, e.g., the highlighted realization with respect to the original Oil in Place. It must capture and integrate structural, reservoir, and flow uncertainty. In this study, considering the above criteria and analysis of both stratigraphic and structural trap and key other elements rank the prospect C4000 as top most prospect followed by D4100AA prospect, D4100A prospect and B5000AB prospect as the least interest.

4.8.3 RISK ASSESSMENT

Hydrocarbon exploration is a high risk investment and risk assessment is paramount for successful project portfolio management. The aim of such procedures is to force the geologist to objectively assess all different geological factors. Exploration risk is a difficult concept and is usually defined by assigning confidence to the presence of imperative geological factors, as discussed in this study. This confidence is based on data and/or models adopted in the study/analysis (Play Fairway Analysis).

Table10: Summary of Prospects Volumetric analytical studies

ITEM	B5000 PROSPECT	C4000 PROSPECT	D4100 PROSPECT A	D4100 PROSPECT AA
BULK ROCK VOLUME (BRV) M ³	4856775	1635625	16583425	2383425
NET-TO-GROSS (NTG) Frac	0.60	0.52	0.72	0.72
POROSITY Frac	0.28	0.31	0.28	0.28
HYDROCARBON SATURATION (Sh) Frac	0.79	0.47	0.57	0.57
FORMATION VOLUME FACTOR (FVF)	1.29	1.29	1.29	1.29
STOIIP (MMBOE)	510953.13	868124.44	2089267.28	300405.58
STOGIP (MMSCF)	6423191.79	10913192.34	26264178.98	3776398.55

There are different kinds of risk: geologic risks govern the existence of oil and gas; finding risks dictate whether or not any existent hydrocarbons will be found; and economic risks determine whether the discoveries can be produced. Industry has many reasons for making quantitative assessments of undiscovered oil and gas. First and foremost, assessments can guide exploration by ranking the opportunities and potential rewards in terms of barrel or cubic meters. Economic analyses may convert these amounts into monetary expectations, which strongly influence selective acreage acquisition, bidding strategy, and choice of well locations. The evaluation of geologic risk lies at the foundation of every one of these assessment applications. This study evaluates risks for a group of related prospects having basically the same geologic controls of trap, reservoir, and source for hydrocarbons. The best way to illustrate risking principles, however, is to consider the assessment of a single potential reservoir at a single prospect as a strategy. The method described here is a systematic assessment of potential exploration rewards in terms of barrels or cubic meters, and of the associated geology risks that may deny these rewards. All basic geologic data and interpretations in the oil/gas industries were laid out for use in comparing prospects realistically and for judging the reliability of the estimates. The total trap volume available for oil is the product of the area of closure at the spill point, the average reservoir thickness, and the average effective porosity. This volume multiplied by an estimate of the degree of

oil-fill in the trap gives the amount of oil in place. Multiplying the oil in place by the last factor, recovery efficiency, gives the final answer in terms of potentially recoverable oil. The estimate for average net reservoir thickness requires inclusion of a net ϕ to ϕ gross ratio and a geometry correction that accounts for any thinning at the edges of the oil column. The estimate for net effective porosity must allow for the irreducible water saturation and for the volume shrinkage of oil brought from the reservoir to the surface. All the volume factors must be multiplied together to determine the potential reward. Obviously, if any one of the factors is zero, there is no reward. This relation sets up the second assessment step, that of risk analysis. If any one of these controls or risk factors is inadequate, making the related volume factor zero or near zero, then the chance for the prospect's success is wiped out. The closure area depends on the actual existence of the postulated structural or stratigraphic feature. If the anticline turns out to be a velocity anomaly and there is no closure, there is no prospect. Cementation may destroy the porosity, or porosity development by solution or fracturing may not be present. The biggest question in any assessment is whether or not hydrocarbon is available and can be retained in the trap. The degree of trap fill is dependent on the amount and types of organic matter in the source rock, the maturation level, adequate migration, plumbing with respect to trap timing and seal, and preservation from flushing, overcooking, and biodegradation. If the prospect passes all these rugged tests and indeed contains hydrocarbons in place, the permeability, fluid viscosity, and drive must all be adequate for effective recovery. Since the postulated source bed is the same for all prospects. If the source bed is inadequate for one prospect, it is apt to be inadequate for all. On the other hand, if the source is good at one prospect it is likely to be good for all, so the maximum potential is much greater where the group risk is applied. Assessment is a tough job that has its inherent limitations. It has to deal with all poorly understanding variables in the generation, migration, and entrapment of petroleum. The all-important risking step is still quite subjective, even when guided by experience. We often are able to put prospects in a good relative order of risk, but the correct absolute values are sometimes elusive. We must usually be content if the real answer falls anywhere within our postulated range. Since we cannot know this real answer ahead of the drill, we are forced to play the average, in both the volume and risk factors. The end result is that our mean assessments of individual prospects (Table 10) tend to overestimate the failures and underestimate the successes. Only in the long run, if our risking levels are correct, will the sum of the risked mean assessments for many ventures come close to tracking reality.

Risk assessment: Chance of finding minimum amount of recoverable hydrocarbons estimated in the prospect assessment.

Key things to risk

Risking factors: Risk of Trap closure, Reservoir, Risk of Porosity, Risk of Source. Including, Migration, seal and timing presentation, Risk of Recovery.

Source Rock (SR): geologic unit where hydrocarbon were originally deposited, geologic unit in which hydrocarbons migrated into; permeable rock. SR risk is generally minimal in the Niger Delta because it is a proven, working petroleum system. Is there a top seal; (Seal: faults can provide potential seals for hydrocarbon plays; typically less permeable unit) thick shale above the reservoir. How thick and Is there possibility of much sand in the overlying top seal .We attached 0.1 to 0.2 to Source rock and seal risk.

Reservoir presence: what is the probability of not finding a reservoir (unit with hydrocarbons) when you drill that prospect. We attached 0.2 to 0.3 to chance you will not find any reservoir. It is your subjective judgment but the risk is generally high in exploration (where you have less data) than in production (where you have many data points).

Trap: (öany geometric arrangement of rock that permits significant accumulation of hydrocarbons in the subsurfaceö (Biddle and Wielchowsky, 1994)) what is the chance that the trap is breached, such that hydrocarbon has leaked out even if there was an initial accumulation. Ability to map the fault/trap clearly on seismic, analysing presence of sand-on-sand juxtaposition across the fault to make the trap leak, etc. Across the fault in this study, there may not be tight closure or, a different closure may exist in the three prospects except C4000 four way closure prospects. Depending on events in the study, we attached 0.2 to 0.3 to risk for trapping structure/mechanism (Tables 11a-d below).

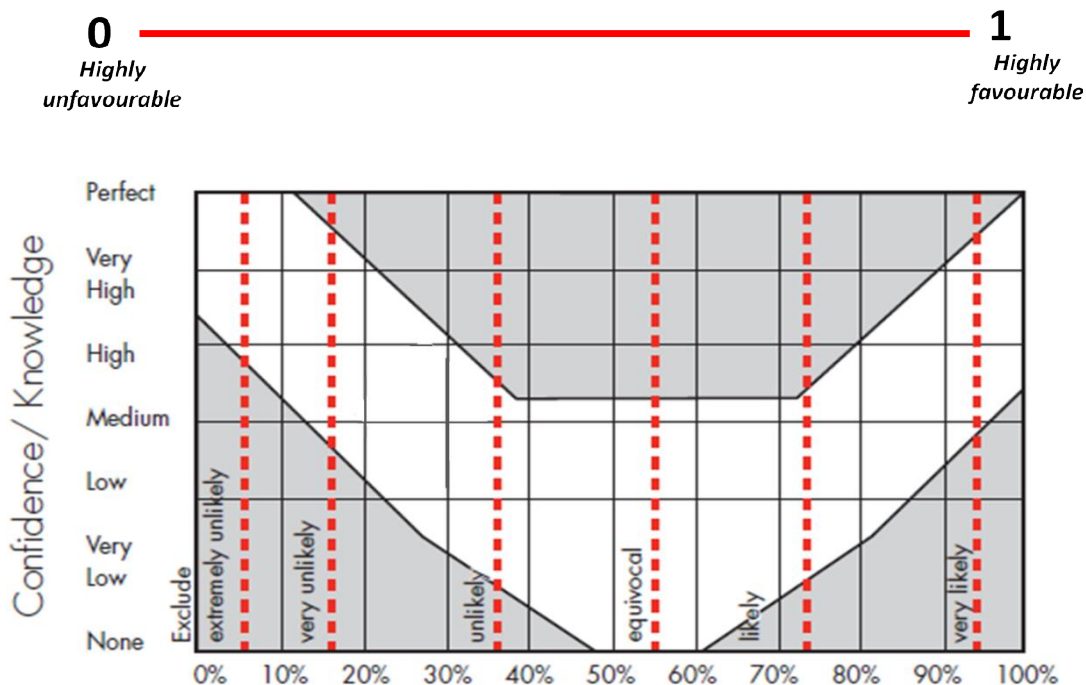


Figure 79: Maastricht Template (Shell, 2004)

Table 11a: Risk analysis for Prospect B5000 AB

GEOLOGICAL CONTROL	CHANCE OF ADEQUACYøS (1.0-RISK)
Trap closure	0.7
Reservoir	0.8
Porosity	1.0
Source. Including seal timing presentation	0.8
Recovery	1.0

Overall chance of exceeding minimum potential = 0.7 x 0.8 x 1.0 x 0.8 x 1.0 = 0.448

Risked Volume (Mean Success Volume) = 0.448 x 510953.1325 = 228907.00336MMSCF

Table 11b: Risk analysis for Prospect C4000

GEOLOGICAL CONTROL	CHANCE OF ADEQUACYøS (1.0-RISK)
Trap closure	0.9
Reservoir	0.8
Porosity	1.0
Source. Including seal timing presentation	0.8
Recovery	1.0

Overall chance of exceeding minimum potential = 0.9 x 0.8 x 1.0 x 0.8 x 1.0 = 0.576

Risked Volume (Mean Success Volume) = 0.576 x 868124.442 = 500039.678592MMSCF

Table 11c: Risk analysis for Prospect D4100 A

GEOLOGICAL CONTROL	CHANCE OF ADEQUACY (1.0-RISK)
Trap closure	0.7
Reservoir	0.8
Porosity	1.0
Source. Including seal timing presentation	0.8
Recovery	1.0

Overall chance of exceeding minimum potential = $0.7 \times 0.8 \times 1.0 \times 0.8 \times 1.0 = 0.448$

Risked Volume (Mean Success Volume) = $0.448 \times 2089267.28 = 419324.30016512 \text{ MMSCF}$

Table 11d: Risk analysis for Prospect D4100 AA

GEOLOGICAL CONTROL	CHANCE OF ADEQUACY (1.0-RISK)
Trap closure	0.8
Reservoir	0.8
Porosity	1.0
Source. Including seal timing presentation	0.8
Recovery	1.0

Overall chance of exceeding minimum potential = $0.8 \times 0.8 \times 1.0 \times 0.8 \times 1.0 = 0.512$

Risked Volume (Mean Success Volume) = $0.512 \times 300405.58 = 153807.65696 \text{ MMSCF}$

Table 11a ó d above showed the prospect risk analysis carried out the study.

4.8.4 UNCERTAINTY

Uncertainty analysis should be conducted for investigational analyses, and for decision analysis under uncertainty and risk. Constructing a realistic reservoir model, and reducing and quantifying the uncertainty is key to good business and investment. A reservoir is complex in its geometry as well as in the variability of its rock properties. Yet improving hydrocarbon recovery requires detailed and accurate descriptions of reservoir properties. Integrated modeling attempts to improve quantitative reservoir descriptions by incorporating geologic knowledge, well data and seismic data. Proper integration of diverse data can help build a more realistic geologic model and reduce the uncertainty in describing the reservoir properties. A reservoir is the result of geologic processes and is not randomly generated. However, many uncertainties exist in reservoir characterization because of subsurface complexity and limited data. Uncertainties can be mitigated by gaining more information and/or using better science and technology. How much uncertainties should be mitigated

depends on the needs of decision analysis for reservoir management and the cost of information. Uncertainty analysis should be conducted for investigational analyses and for decision analysis under uncertainty and risk. To know what needs to be known and what can be known should be the main focal points of uncertainty analysis in reservoir characterization and management. The range in the estimates includes the uncertainty in our seismic and facies maps and in our historical experience with porosity, hydrocarbon fill, and recovery efficiency. The range not only serves to record the relative uncertainty in each estimate but also allows for the possibility that the reward will be greater than indicated by the most likely values alone.

CHAPTER FIVE

SUMMARY AND CONCLUSION

5.1 SUMMARY AND CONCLUSION

Explanation of gamma ray logs results of the wells considered showed that the lithology is controlled by alternating shale and sand strata that were induced by fluvial, tidal and marine systems which are peculiarized by continental-marine facies of the Agbada Formation i.e. (Inner Neritic, Middle Inner Neritic and Shallow Inner Neritic). Sequence stratigraphic analysis was served out on six wells (OGBO-019STI, OGBO-038, OGBO-046, OGBO-005, OGBO-036 and OGBO-056) in OGBO field within the coastal swamp depobelt of the Niger Delta, which facilitated their subdivision into key surfaces, depositional sequences and their correlated systems tracts. Paleoenvironment interpretations were based on paleobathymetric sedimentary facies derived from biofacies data. This has established that the six wells within the western offshore Niger Delta fall within Early Miocene to Middle Miocene age, limited chronologically by third order 15.5 Ma SB, 13.1 Ma SB and 12.1 Ma SB (Reijers, 1996). Marker Shales recognized were 15.9 Ma, 15.0Ma, 12.8Ma and 11.5Ma. These marker shales have high faunal content and parallel to the recognized maximum flooding surfaces. The incorporation of the data sets has made easier the understanding of the form that generated the vertical stratigraphic succession of sediments and lateral facies changes, which are the distinctive feature of the systems tracts. Two (2) major depositional sequences were identified in majority of the wells studied. Depositional Sequence DSQ1 is the oldest sequence in the field and overlain by sequence boundary 15.5Ma. Depositional Sequence DSQ2 experienced transgressive episodes marked by faunal diversity and abundance which formed the 15.0 MFS (*Bolivina 25*). Incomplete Depositional Sequence INC DSQ experienced other transgressive episodes that formed the 12.8 MFS (*Cassidulina 7*) while also Incomplete Depositional Sequence INC DSQ, the topmost sequence is marked by the 11.5 MFS (*Dodo shale*). The systems tracts are the prograding wedge complexes of the lowstand systems tracts, transgressive systems tracts and highstand systems tracts with three sequence boundaries and three maximum flooding surfaces. Well log shapes of the sub-environments include Tidal inlet sands with thinly bedded shale; hemipelagic sediments with inter-bedded shoreface sands delineated from the EOD delineation integrated approach adopted in this study as lithostratigraphic and genetic unit analysis using log motif

and 3D Seismic data revealed that we have the dominance of three major environment of deposition; Tidal inlet, Lower and Upper Shoreface (shallow marine environment). The environments of deposition (EOD) influenced the properties of the rock units. The shale units serve both as source rocks and seals while the sand units have good quality properties as reservoir rocks. The shales of the TST in which most of the MFS were delineated could form seals to the reservoir units. An integration of the reservoir sands of the HST and LST can form good stratigraphic traps for hydrocarbon and hence should also be targeted during hydrocarbon exploration. The structural setting of the field signaled growth fault line depositional model and also the displacement of sediments across the fault planes by the rollover fault systems, where hanging walls were displaced during deposition which are characteristic of the Niger Delta. In addition to this, the up dip areas which seismically form continuous high-amplitude reflections with closure signify possible hydrocarbon deposits which can be exploited at profit. Formation evaluation indicated that there are three major hydrocarbon producing reservoirs. Also hydrocarbon traps within the study area are Structural (anticlines and faults) and Stratigraphic (likely Pinch-out, Wedge structures and Unconformities). Prospect evaluation indicated that there are four prospects with increased prospectivity at shallower and intermediate horizons. The deeper horizons look interesting with satisfactory amplitude response quality, relatively good structural entrapment marred by poor well data at most interval quality. Volumetric analysis carried out showed that the mapped out prospects maintain a hydrocarbon quantity of (2,089,267MMBOE and 26,264,179MMSCF ó D4100A, 300,406MMBOE and 3,776,399MMSCF -- D4100AA, 868,124MMBOE and 10,913,192MMSCF ó C4000 and 510,953MMBOE and 6,423,192 MMSCF -- B5000AB), which are economically beneficial.

5.2 RECOMMENDATION

The observations made in this study compelled the suggestion and recommendation that the existing wells (OGBO 019STI - 056) should be drilled deeper. Drilling of more detailed exploratory wells should be carried out with due logging aimed at providing enough data for the study of a well defined stratigraphic framework. This will help in the clear interpretations of downdip and updip facies variability and the controls on sediment supply in coastal swamp depositional environments, because Niger Delta depositional systems are more of supply driven than accommodation driven (Porbeski and Steel,2006) which can make sequence boundary more difficult to identify. This work could be used as an input tool for pre existing models to generate excellent dynamic simulations for optimum productivity. This work could also be incorporated into a number of multi-disciplinary projects that use integrated subsurface datasets (core, wireline log, 3D seismic and production data), insights from outcrop analogues and novel modeling techniques to characterize geology and fluid flow in hydrocarbon reservoirs. Water saturation, irreducible water saturation, porosity, permeability and hydrocarbon saturation combined could be used to give advice on possible locations to site water injection wells and drain holes for further field development. The volumetric reserve estimate could be used to evaluate reserve economics and producibility rate to ascertain possible duration before field abandonment. The volume of oil and gas resources contours could be used as a predictive model to estimate hydrocarbon reserve potentials for proper field management. For overall field management to be achieved, there is need for effective exploitation of these reserves and part of continuing research work in the studied field, acquisition of high-resolution biostratigraphic data should be done and made available in all the wells. Also, there should be an integrated study using input from petrophysical data, seismic data, production data, and core data analysis. Advance geologic information should be carried out in the study area in order to ensure confidence in the result obtained and thus reduce risk in exploration of hydrocarbon.

REFERENCE

- Adeogba, A. A., McHargue T. R., and Graham S. A., (2005). Transient fan architecture and depositional controls from near-surface 3-D seismic data, Niger Delta continental slope: AAPG Bulletin, v. 89, pp. 627-638.
- Adepelumi, A. A., Alao, O. A., & Kutemi, T. F. (2011). Reservoir characterization and evaluation of depositional trend of the Gombe sandstone, southern Chad basin Nigeria. *Journal of Petroleum and Gas Engineering* Vol. 2(6). pp. 118-131.
- Allen, G. P., and Posamentier, H. W., (1993). Sequence stratigraphy and facies model of an incised valley fill: The Gironde estuary, France: *Journal of Sedimentary Petrology*, v. 63, No. 3, p. 378-391.
- Anyiam, A. O. and Mode A.W., (2008). Sequence stratigraphic framework of the Paradise-Field Niger Delta, Nigeria. *The Pacific Journal of Science and Technology*, vol. 9 No 1 pp 227-236.
- Archie, G. E. (1942). The electrical resistivity log as an aid in determining some reservoir characteristics. *J. Petroleum Technol.*, 5: 54-62.
- Asquith, G., & Krygowski, D. (2004). *Basic Well Log Analysis: AAPG Methods in Exploration Series*. 6- 16p.
- Balogun, A. O. (2003). Sequence Stratigraphy of "X" Field in the Coastal Swamp Depobelt of the Niger Delta, Nigeria. AAPG Search and Discovery Article #90017©2003.
- Beka, F. T. & Oti, M. N. (1995). The distal offshore Niger Delta: frontier prospects of a mature petroleum province, in, Oti, M.N and Postma, G., eds., *Geology of Deltas: Rotterdam, A.A. Balkema*, 237-241.
- Bevis, K.A. (2014). Report PDF- USGS. Scientific investigations report 2014. [web.www.pubs.usgs.gov/sir/pdf/sir2014-5208](http://www.pubs.usgs.gov/sir/pdf/sir2014-5208)
- Biddle K.T.C and Wielchowsky (1994). Hydrocarbon Traps: in Magoon and Dow, eds., *The petroleum system from source to trap: AAPG memoir* 60.
- Boggs, S. (1995). *Principles of Sedimentology and Stratigraphy*, 2nd Edition, Prentice Hall, Englewood Cliffs, 1995.
- Burke, K., (1972). Longshore drift, submarine canyons, and submarine fans in development of Niger Delta: *American Association of Petroleum Geologists*, v. 56, p. 1975-1983.
- Burke, K., Dessauvage, T. F. J. and Whiteman, A. J., (1972). Geological history of the Benue Valley and adjacent areas, in 1st Conference on African geology, Ibadan, 1970, *Proceedings: Ibadan, Nigeria, Ibadan Univ. Press*, p. 287-305.

- Bustin, R. M., (1988). Sedimentology and characteristics of dispersed organic matter in Tertiary Niger Delta: origin of source rocks in a deltaic environment: American Association of Petroleum Geologists Bulletin, v. 72, p. 277-298.
- Cant, D. J., (1992). Subsurface facies analysis, Facies Models: Response to Sea level Change, in Walker, R.G., and James, N.P.; eds: Geological Association of Canada, p. 195-218.
- Cathles, L. M., Colling E. L., Erendi A., Wach G. D., Hoffman M. W., and Manhardt P. D., (2003). 3-D flow modeling in complex fault networks: Illustration of new methods with an exploration application in offshore Nigeria, in S. Duppenbecker and R. Marzi, eds., Multidimensional basin modeling: AAPG Datapages Discovery Series no. 7, pp. 177-195.
- Corredor, F., Shaw J. H., and Billoti F., (2005) Structural styles in the deep-water fold and thrust belts of the Niger Delta: AAPG Bulletin, v. 89, pp. 753-780.
- De Angelo, M. V., and Wood, L. J., (2001). 3-D seismic detection of undrilled prospective areas in a mature province, South Marsh Island, Gulf of Mexico: The Leading Edge, p. 1282-1292.
- Doust, H., (1990). Petroleum Geology of the Niger Delta. Geochemical Society, London, Special Publications. 50: 365.
- Doust, H., and Omatsola, E. (1990). Niger Delta, *in*, Edwards, J. D., and Santogrossi, P.A., eds., Divergent/passive Margin Basins, AAPG Memoir 48: Tulsa, American Association of Petroleum Geologists, 239-248.
- Ekweozor, C. M., and Daukoru, E.M, (1994) Northern delta depobelt portion of the Akata Agbada(!) petroleum system, Niger Delta, Nigeria, *in*, Magoon, L.B., and Dow, W.G., eds., The Petroleum System: From Source to Trap, AAPG Memoir 60: Tulsa, American Association of Petroleum Geologists, p. 599-614.
- Ekweozor, C.M., and Okoye, N.V., (1980) Petroleum source-bed evaluation of Tertiary Niger Delta: American Association of Petroleum Geologists Bulletin, v. 64, p 1251-1259.
- Emery, D., and Myers, K., (1996). *Sequence Stratigraphy*, Blackwell Science Ltd., Oxford.
- Etu-Efeotor, J. O., (1997). Fundamentals of Petroleum Geology. Paragraphics Pub. Nigeria, Port Harcourt, pp 30 - 130.
- Evamy, B.D., Haremboure, J., Kamerling, P., Knaap, W.A., Molloy F.A., & Rowlands P.H. (1978). Hydrocarbon habitat of Tertiary Niger Delta: American Association of Petroleum Geologists Bulletin, 62, 277- 298.

- Galloway, W. E., (1989). Genetic stratigraphic sequences in basin analysis: I. Architecture and genesis of flooding surface bounded depositional units: AAPG Bulletin, v. 73, pp. 125-142.
- Gonzalez, A. P., (2003). Stratigraphic framework of the Fox Hills Sandstone and Lewis Shale, Great Divide basin, Wyoming: Unpublished M.Sc. Thesis, Colorado School of Mines, Golden, CO, 189 p.
- Haack, R.C., Sundararaman, P., and Dahl, J., (1997). Niger Delta petroleum System, *in*, Extended Abstracts, AAPG/ABGP Hedberg Research Symposium, Petroleum Systems of the South Atlantic Margin, November 16-19, 1997, Rio de Janeiro, Brazil.
- Haq, B. U., Hardenbol, J., and Vail, P. R. (1988). Mesozoic and Cenozoic chronostratigraphy and cycles of sea-level change. *In Sea Level Changes—An Integrated Approach* (C. K. Wilgus, B. S. Hastings, C. G. St. C. Kendall, H. W. Posamentier, C. A. Ross and J. C. Van Wagoner, Eds.), pp. 71-108. SEPM Special Publication 42.
- Hospers, J., (1965). Gravity field and structure of the Niger Delta, Nigeria, West Africa: Geological Society of American Bulletin, v. 76, p. 407-422.
- Hunt, J.M., (1990). Generation and migration of petroleum from abnormally pressured fluid compartments: American Association of Petroleum Geologists Bulletin, v. 74, p. 1-12.
- Ivan Sandra and Rafael Sandra, (2007). Global Oil Reserves & Recovery Factors Leave Vast Target for EOR Technologies. Oil and Gas Journal. Part 1 and 2.
- Kaplan, A., Lusser, C.U., Norton, I.O., (1994). Tectonic map of the world, panel 10: Tulsa, American Association of Petroleum Geologists, scale 1:10,000,000.
- Kendall, C., (2003). Use of well logs for sequence stratigraphic interpretation of the subsurface. USC Sequence Stratigraphy Web. <http://strata.geol.sc.edu/index.html>, University of South Carolina.
- Kendall, C.G. St. C., (2004). Critical accidents in paleo-geography and oceanography induced by abrupt changes in base level, signaled by hard or firm grounds in shallow water clastics and carbonates: American Association of Petroleum Geologists Bulletin, Vol. 13, p. 75.
- Kendall, C. G., (2008). Template for conceptual models used to interpret depositional systems USC Sequence Stratigraphy Web. <http://strata.geol.sc.edu/index.html>, University of South Carolina.
- Klett, T.R., Ahlbrandt, T.S., Schmoker, J.W., and Dolton, J.L., (1997). Ranking of the world's oil and gas provinces by known petroleum volumes: U.S. Geological Survey Open-file Report-97-463, CD-ROM.
- Kogbe, C. A. 1989. The Cretaceous Paleocene Sediments of Southern Nigeria. In C. A. Kogbe (Ed.), Geology of Nigeria (pp. 320-325). Jos: Rock View Ltd.

- Kulke, H. (1995): Nigeria, *in*, Kulke, H., ed., Regional Petroleum Geology of the World. Part II: Africa, America, Australia and Antarctica: Berlin, Gebruder Borntraeger, 143-172.
- Larionov, V. (1969). Borehole Radiometry: Moscow, U.S.S.R., Nedra.
- Lehner, P., and De Ruiter, P.A.C., (1977). Structural history of Atlantic Margin of Africa: American Association of Petroleum Geologists Bulletin, v.61, p. 961-981.
- Maastricht Template (Shell, 2004).
- McCabe. A.M., Dardis. G.F. and Hanvey. P.M (1992). "Glacial Sedimentology in Northern and Western Ireland, In: *Pre- and Post-Symposium Field Excursion Guide Book*, Anglia Polytechnic, Cambridge, 1992.p.1-25
- Merki, P. J. (1972). Structural geology of the Cenozoic Niger Delta: 1st Conference on African Geology Proceedings, Ibadan University Press, 635-646.
- Mitchell, P., Kieckhefer, B., and Rieth, A., (2004). Synthetic seismogram school manual: Reservoir Properties from Seismic: Unpublished report, Chevron EnergyTechnology Company.
- Morris, R. L., & Biggs, W. P. (1967). "Using log-derived values of water saturation and porosity". Trans. SPWLA Ann. Logging Symp. Paper, 10, 26.
- Nwachukwu, J.I., and Chukwurah, P. I., (1986). Organic matter of Agbada Formation, Niger Delta, Nigeria: American Association of Petroleum Geologists Bulletin, v. 70, p. 48-55.
- Onyekuru S. O., Ibelegbu E. C, Iwuagwu J. C., Essien A. G., Akaolisa A. Z., (2012). Sequence Stratigraphic Analysis of "XB Field", Central Swamp Depobelt, Niger Delta Basin, Southern Nigeria *International Journal of Geosciences*, 2012, v 3, pp 237-257
- Oomkens, E., (1974). Lithofacies relations in late Quaternary Niger Delta complex: Sedimentology, v.21, pp.195-222.
- Owoyemi, A. O., (2004). The sequence stratigraphy of Niger Delta, Delta Field, Offshore Nigeria A thesis submitted to the Office of Graduate Studies of Texas A&M University.
- Ozumba, B.M., (1999). Middle to Late Miocene sequence stratigraphy of the Western Niger Delta. NAPE Bulletin, 13 & 14(2), pp. 176-192.

- Posamentier, H.W and Kolla V., (2003). Processes and reservoir architecture of deepwater sinuous channels from the shelf edge to the basin floor, based on analyses of 3D seismic and side scan imagery , *in* D. Hodgson, C. Edwards, R. Smith, eds., submarine slope systems: processes, products and prediction: Presented at the 2003 Slope Conference, Liverpool, UK., abstract volume, . 67.
- Porbski, S. J., Steel, R. J. (2006). Deltas and Sea-Level Change, *Journal of Sedimentary Research*. Vol. 76, pp 390 ó 403.
- Reijers, T.J.A., (2011). Stratigraphy and sedimentology of the Niger Delta. *Geologos* 17 vol 3, pp 133ó162.
- Sangree, J.B and J.M. Widmier, (1979). Seismic stratigraphy and global changes in sea level Part 9: seismic interpretation of clastic depositional facies. In: Payton (Ed.), *Seismic Stratigraphy: Application to Hydrocarbon Exploration*, AAPG-Memoir No. 26, AAPG, Tulsa, p. 165ó184.
- Schlumberger ,(1985). *Log Interpretation Charts*, Schlumberger Educational Services, New York, 83p.
- Selley, R.C., (1985). *Elements of petroleum geology*. W. H. Freeman and company, New York. P.423.
- Short, K.C., & Stauble A.J. (1967).Outline of Geology of the Niger delta. *Am. Assoc. Petrol. Geol. Bull.*, 51,p.761-779.
- Stacher, P., (1995). Present understanding of the Niger Delta hydrocarbon habitat, *in*, Oti, M.N., and Postma, G., eds., *Geology of Deltas*: Rotterdam, A.A. Balkema, p. 257-267. Thomas, 1995, Niger delta oil production, reserves, field sizes assessed: *Oil & Gas Journal*, November 13, 1995, p. 101-103.
- Stacher, P. (1994). ðNiger Delta Hydrocarbon Habitatö. *Nigerian Association of Petroleum Explorationists Bull.* 9(10): pp. 67-75.
- Stoneley, R., (1966). The Niger Delta region in the light of the continental drift. *Geol. Magazine*. 103, pp. 385-397.
- Timur A., June, (1968). An investigation of permeability, porosity and residual water saturation relationship for sandstone reservoirs. *SPWLA Transaction*.
- Udo, O.T. and Ekweozor C.M., (1988). Comparative source rock evaluation of Opuama Channel Complex and adjacent producing areas of Niger delta:Nigerian Association of Petroleum Explorationists Bulletin, v. 3, no. 2, p.10-27.

- Udo, O.T., Ekweozor, C.M., and Okogun, J.I., (1988). Petroleum geochemistry of an ancient clay-filled canyon in the western Niger delta, Nigeria: Nigerian Association of Petroleum Explorationists Bulletin, v. 3, p. 8-25.
- Walker, R.D and Plint, A.G (1992). "Wave- and Storm-Dominated Shallow Marine Systems," In: R. G. Walker and N. P. James, Eds., *Facies Models-Response to Sea-Level Changes*, Geological Association of Canada, Newfoundland, pp. 219-238.
- Weber, K. J. (1971). Sedimentological aspect of oil fielding the Niger Delta. *Geol. Minjbouw*, 50, 559-576.
- Weber, K. J., & Daukoru, E. D. (1975). Petroleum Geology of the Niger Delta. *Tokyo*, 9th World Petroleum Congress Proceedings, 2, 209-221.
- Weber, K. J., Mandi, J., Pilaar, W. F., Lehner, E., & Precious, R. G (1978). The role of faults in hydrocarbon migration and trapping in Nigeria growth fault structures. 10th Annual Offshore Technology Conference Proceedings, 4, 2643-2653.
- Weimer, R. J., Rebne, C. A., and Davis, T. L., (1988). Geologic and seismic models, Muddy Sandstone, Lower Cretaceous, Bell Creek--Rocky Point area, Powder River basin, Montana and Wyoming, in Diedrich, R., Dyka, M., and Miller, W. (Eds.), *Eastern Powder River basin--Black Hills: Wyoming Geological Association 39th Field Conference Guidebook*, p. 147-160.
- Winker, C.D (1982). "Cenozoic Shelf Margins, Northwestern Gulf of Mexico," *Gulf Coast Association of Geological Societies*, Vol. 32, 1982, pp. 427-448.
- Wornardt, W.W.,(1994). Subsalt Risk Reduction Using Seismic Sequence Stratigraphic Analysis. GCAGS and Gulf Coast SEPM 44th Annual Meeting Proceedings, pp. 272-281.
- www.dpr.gov.ng
- Xiao, H., and Suppe, J.,(1992). Origin of rollover: American Association of Petroleum Geologists Bulletin, v. 76, p. 509-229.
- Ziolkowski, A., Underhill, J.R., and Johnston, R.G.K., (1998). Wavelets, well ties and the search for subtle stratigraphic traps. *Geophysics*, Vol.63. No.1, pp. 297-313.

SEQUENCE STRATIGRAPHIC CORRELATION

